The Role of Actin and Twisted Dwarf 1 in the Regulation of Auxin Transport

Dissertation
zur
Erlangung der naturwissenschaftlichen Doktorwürde
(Dr. sc. nat.)

vorgelegt der
Mathematisch-Naturwissenschaftlichen Fakultät
der
Universität Zürich

von
Hanna Valpuri Sovero
aus
Finnland

Promotionskomitee
Prof. Dr. Enrico Martinoia (Vorsitz)
PD Dr. Markus Geisler (Leitung der Dissertation)
Prof. Ueli Grossniklaus

Zürich, 2010

Oats, peas, beans and barley grow,
Oats, peas, beans and barley grow,
Can you, or I, or anyone know
How oats, peas, beans and barley grow?

-Old English Nursery Rhyme
(Used as epigraph in *Phytohormones*
by F.W. Went and K.V. Thimann, 1937)

Table of Contents

Summary

How do plants grow? A significant part of this question could be answered by studying the mechanisms of auxin transport. Auxin is the most important of the plant hormones, affecting nearly every part of development, from early embryo patterning to apical dominance patterns, and environmental responses such as photo- and gravitropisms. A key feature of auxin activity is its polar transport through the plant (Polar Auxin Transport, or PAT), so understanding the regulation of this transport is a major component of understanding auxin activity. Auxin Transport Inhibitors (ATIs) are important to auxin research, helping to define and delineate the roles of the various parts of the auxin efflux complex.

In this work, an attempt is made to discover the mechanism of regulation of one family of auxin transporters, the ABCBs, specifically, ABCB1 and ABCB19. Earlier work had shown their activity to be modulated by interaction with a 42 kD immunophilin, TWisted Dwarf 1 (TWD1). Here, it is shown that this modulation is affected by the ATI, NPA, and conversely, that TWD1 regulates the activity of NPA on the ABCBs. Using yeast-based bioluminescence resonance energy transfer (BRET) and auxin transport and drug binding assays, it was shown that NPA binding to both TWD1 and ABCB1 disrupts the protein-protein interaction, and that this disruption of interaction is the cause of reduction of transport by ABCB1 on NPA.

In another part of this work, a new ATI, BUM, is described. BUM has a similar activity to NPA, directly interacting with ABCBs, while having no significant effect on PIN protein activity, and works at a far lower concentration. The specific activity of this chemical, especially when compared with that of the well-established ATI NPA, could be very beneficial to understanding the fine details of ABCB-mediated auxin transport.

The main bulk of my work has been focused on the role of TWD1, and especially its interaction with the actin cytoskeleton. Actin was identified as a TWD1-interacting protein via pull-down assays. Although in vitro assays rather suggest an indirect mode of interaction, similarities like trichome shape

and responses to ATIs, as well as the altered actin formation in *twd1* roots show a clear functional link between the two. Along with the altered auxin transport profile in *act7-4* plants, these are evidence of a model in which TWD1 integrates ATI activity and, possibly indirectly, coordinates stable actin interactivity with the auxin transport complex.

Overall, this work contributes valuable information about the regulation of auxin transport by ABCB proteins to the body of knowledge about the complex network of auxin transport as a whole.

Zusammenfassung

Wie wachsen Pflanzen? Ein wesentlicher Teil dieser Frage konnte durch das Studium des Auxintransportes beantwortet werden. Auxin ist das wichtigste Pflanzenhormon, bestimmt es doch beinahe alle Aspekte der pflanzlichen Entwicklung: von der Musterbildung des frühen Embryos bis zur Apikaldominanz, als auch Reaktionen auf Umwelteinflüsse, wie dem Photo- and Gravitropismus. Ein wesentliches Merkmal der Auxinwirkung ist sein polarer Transport durch die Pflanze, genannt der Polare Auxin Transport oder auch PAT. Daher ist das Verständnis der Regulation des Auxintransportes Bedingung für das Verständnis seiner Wirkungsweise. Auxintransport-Inhibitoren (ATIs) sind eminent wichtig für die Auxinforschung, weil sie uns helfen können die Komponenten des Auxintransport-Komplexes zu entschlüsseln und zuzuordnen.

In dieser Arbeit wurde der Versuch unternommen, den Regulationsmechanismus einer Auxintransporter-Familie, den ABCBs (insbesondere ABCB1 and ABCB19), zu untersuchen. Die bisherige Arbeit hatte gezeigt, dass deren Aktivität von der Interaktion mit einem Immunophilin von 42 kD, TWisted Dwarf 1 (TWD1), abhängt. Hier zeigen wir, dass diese Interaktion durch den ATI, NPA, beeinflusst wird und, dass TWD1 die Komponente ist, die den inhibitorischen Effekt auf die ABCBs überträgt. Mittels Bioluminescence Resonance Energy Transfer (BRET)-, Auxintransport-Assays und ATI-Bindungstest konnten wir zeigen, dass NPA durch Bindung an TWD1 and ABCB1 diese Protein-Protein-Interaktion zerstört, und dass diese Zerstörung die Ursache für den Block des Auxintransportes darstellt.

Im zweiten Tei dieser Arbeit gelang es uns einen neuen ATI namens BUM zu charakterisieren. BUM hat eine ähnliche Wirkung wie NPA, interagiert direkt mit ABCBs, während es keinen direkten Effekt auf PIN-Proteine hat, benötigt dazu aber wesentlich geringere Konzentrationen. Die spezifische Aktivität dieses Inhibitors könnte im direkten Vergleich mit dem

etablierten Inhibitor NPA sehr nützlich für das weitere Verständnis der Rolle des ABCB-vermittelten Auxintransportes werden.

Der Hauptteil meiner Arbeit betraf die Rolle von TWD1 insbesondere im Hinblick auf eine Interaktion mit dem Zytoskelett. Die Isoform Actin7 konnte durch Co-Immunoprezipitation als TWD1–interagierendes Protein identifiziert werden. Obwohl in vitro-Assays eher einen indirekten Interaktionsmodus suggerieren, belegen überlappende Phänotypen, wie Trichomarchitektur, und Inhibitorsensitivitäten, als auch eine gestörte Aktinformation in *twd1* Wurzeln einen klaren funktionellen Zusammenhang zwischen beiden Partnern. In Übereinstimmung mit gestörten Auxintransportkapazitäten in *act7-4* unterstützen diese Daten ein Model, in dem TWD1 als Integrator der NPA-Funktionalität agiert, und, möglicherweise indirekt, die Interaktion des Zytoskelettes mit dem Auxinefflux-Komplex koordiniert.

Zusammenfassend bietet diese Arbeit einen neuen Einblick in die Regulation des ABCB-vermittelten Auxintransportes und damit auch darüber hinaus in das komplexe Netzwerk des Auxintransportes.

Chapter 1:

Introduction

1: Auxin

Historical beginnings

How does a plant know how to grow? This is a question that scientists have been asking for hundreds of years. Julius von Sachs was the first to suggest in 1865, that chemical messengers, or "organ-forming substances", could influence plant growth. The history of research into auxin really begins, however, with Charles Darwin. In 1880, Darwin and his son Francis published *The Power of Movement in Plants*, in which was described for the first time the existence of an "influence" that moved from the tip of a coleoptile to a region somewhat below this, causing the tip to bend toward a unilateral light source (Darwin, 1880). Frits Went showed in 1926 that this compound could be isolated into agar blocks, which would then have the same effect as the excised coleoptile tips, and that blocks with a higher concentration would have a stronger effect. Later, independent experiments by Nicolaj Cholodny and Went led to the development of the Cholodny-Went theory, stating that this "influence" is differentially

Figure 1: Darwin's drawing of cotyledons bending toward light.

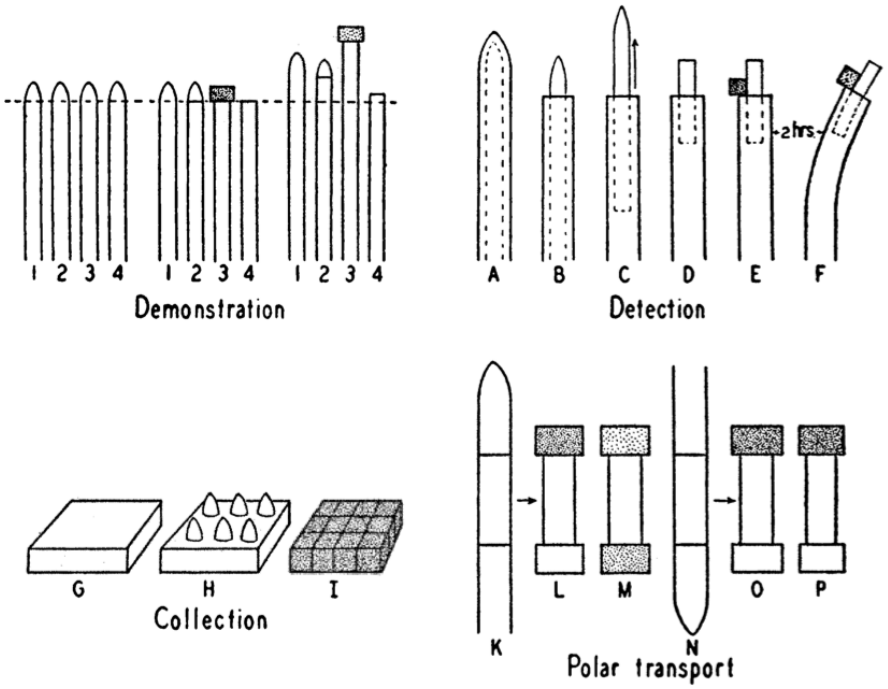

Figure 2: Early experiments in collecting and demonstrating auxin function and polar transport (Went, 1935)

translocated to the shaded and unshaded side of the coleoptile, leading to the increased elongation of the shaded side, causing the tip to bend toward the light. In 1931, Kögl and Haagen Smit named the "influence" auxin, from the Greek "auxein" meaning "to grow". In 1928, experiments by Went had also showed that translocation in the coleoptile was predominantly in an apical to basal direction, establishing the idea of polar auxin transport (PAT). Kenneth Thimann was the first to demonstrate the acidic nature of the auxin and in 1934 (Kögl and Kostermans) and in 1937 (Went and Thimann), the structure was determined to be indole-3-acetic acid (IAA) (Pennazio, 2002; Woodward and Bartel, 2005). Although many other auxins, both natural and synthetic, have subsequently been discovered, IAA is the predominant active form in the plant.

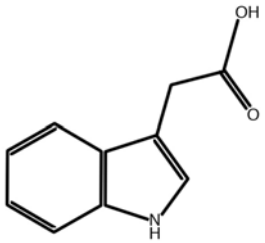

Figure 3: Indole-3-acetic acid

Functions

For a small, fairly simple compound, auxin (in general, IAA is meant when auxin is referred to) has a bewildering array of effects in the plant. The effects of auxin can be broadly divided into categories of development, cell elongation (auxin also influences cell division, but this aspect is not as well studied), patterning, and responses to the environment (Teale et al., 2006).

Figure 4: *Arabidopsis thaliana* with sites of some of the major auxin functions

Development

From the very first cell division in early embryonic development, an auxin gradient is established that will define the shoot-root axis of the plant for the rest of its life (Fleming, 2006). A high auxin concentration in the part of the embryo that will eventually become the shoot shifts to the base of the embryo at the globular stage, marking the site of future root development (Petrásek and Friml, 2009). As the embryo develops, auxin concentration differences in various parts of the embryo both maintain the overall shoot-root axis and begin the delicate task of patterning, distinct sites of high auxin already manifest at points of the triangular phase that will become the site of cotyledon formation. Fruit development is yet another important developmental stage that is influenced by auxin. This is shown especially well by the manipulation of auxin levels of developing fruit. In one case, all auxin producing achenes of a strawberry compound fruit are removed, leading to an entire lack of fruit development. Conversely, external application of auxins, or increasing the level of response to auxin in unfertilized ovules, (Serrani et al., 2010) will induce parthenocarpic fruit.

Figure 5 Auxin concentrations (blue) and flow during early embryo development (Adapted from (Berleth et al., 2007))

Patterning

Auxin gradients determine the sites of cotyledon formation and the root apical meristem (RAM). Later, local auxin maxima established by differential transporter localization define the shoot apical meristem (SAM) that will, in turn, define much of the shoot development. A local maximum determines the site of a leaf primordium. Once the leaf begins to develop, transport of auxin from the SAM as well as local auxin synthesis create auxin streams that determine sites of vein formation. In the stem, auxin streams also act as a precursor to vasculature, enhanced flux (Sachs, 1991) or concentration (Merks et al., 2007) enhancing the stream of auxin along a particular path that eventually develops into vasculature.

Overall above-ground patterning is also influenced by auxin. Thimann and Skoog showed in 1934 that application of auxin to a plant with the SAM removed would continue to repress outgrowth of secondary shoots, i.e. would retain apical dominance. Recently, this has been shown to be one of the many instances of complicated hormone cross-talk (Chandler, 2009).

Auxin also has a role in root patterning and development. After establishment of the RAM in the early embryo, the local synthesis and transport from the SAM sets up a complicated variety of gradients in the root. The location of the auxin maximum in the tip determines the site of the quiescent center (QC). Although the QC is called "quiescent" for its low rate of cell division, the gradients it maintains control the pattern development for the whole root. Local auxin maxima also develop at other sites along the root, and become the sites for lateral root formation. Once

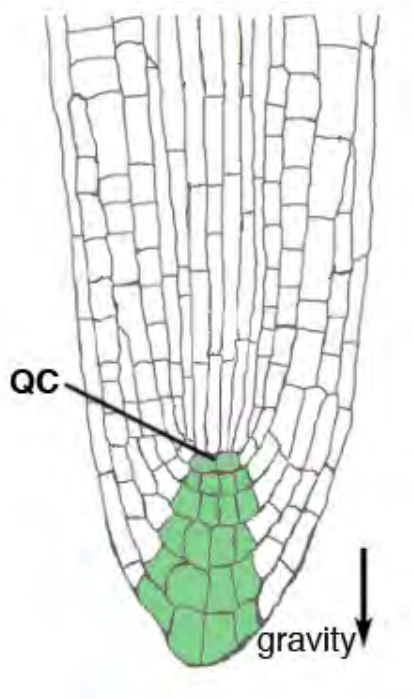

Figure 6: High auxin concentration is in the root tip and the quiescent center (Adapted from Tanaka et al., 2006)

the lateral root has started growing, it develops its own root tip auxin maximum to maintain growth and proper patterning.

Cell elongation

In addition to these stages of differentiation and patterning, auxin plays a key role in growth of the plant. Auxin influences shoot growth by triggering cell elongation. In a natural and intact state, stems and coleoptiles are not much influenced by additional auxin, so most information on auxin enhancement of cell elongation comes from studies where the endogenous supply has been depleted through decapitation. The cellular machinery requires some time, at least 10 minutes, to begin elongation, after which activated proton and K^+ transporters help in cell wall acidification and loosening (Christian et al., 2006), while cell wall polysaccharides building also seems to be increased (Baker and Ray, 1965), both of which lead to the possibility of a larger cell. The whole process is energy dependent and is inhibited by generic metabolic inhibitors. Interestingly, although roots also require a certain amount of auxin to grow, root cell elongation is inhibited at concentrations at which shoot cells still expand. (Summary in Taiz and Zeiger, 2006, Chapter 19)

Environmental responses

Of course, the most historical role for auxin is phototropism, since that is how it was first discovered. Shifting light conditions in a natural environment mean that a plant has to respond in order to get maximally beneficial light exposure. As mentioned in section 1, during unilateral illumination of a shoot, auxin is differentially transported to the

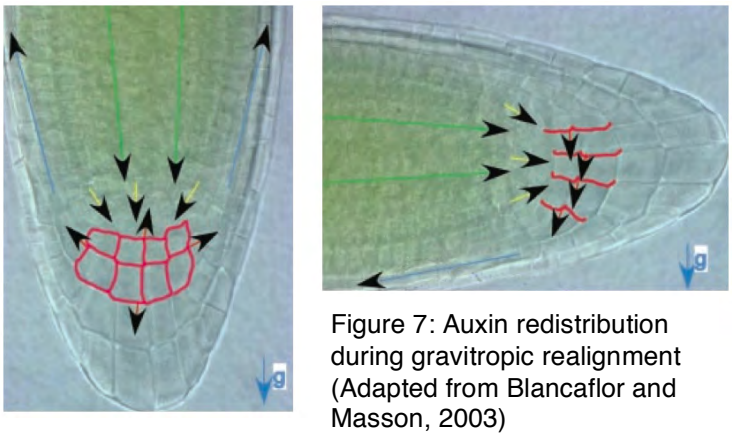

Figure 7: Auxin redistribution during gravitropic realignment (Adapted from Blancaflor and Masson, 2003)

shaded side of the shoot. This induces cell elongation on that side of the root, causing it to bend toward the light. In a similar way, auxin also plays a role in gravitropism, both positive, in the root, and negative, in the shoot. In both root and shoot, placing the organ horizontally will cause auxin to be transported to the lower part. In the shoot, as with phototropism, this will cause the side with the increased auxin concentration to elongate more rapidly, leading to the curvature of the shoot away from gravity. In the root however, the side with an elevated auxin concentration elongates more slowly, causing the tip of the root to turn toward gravity. This paradox of differential responses to auxin is puzzling, but can be explained by the fact that the root is much more sensitive to auxin, and reaches the maximum level of growth promotion at lower concentrations of added auxin. After this maximum level, growth is inhibited, leading to the idea that the increased auxin felt by the lower side of the root during gravitropism is most likely simply at this level.

Finally, in addition to these natural functions in growth and differentiation, auxins have interesting agricultural functions as well. Besides being used to produce parthenocarpic, and thus seedless, fruits, auxin is also used in clonal propagation, as it will initiate roots in plant cuttings. Synthetic auxins such as 2,4-D (2,4-Dichlorophenoxyacetic acid) can also be used as herbicides against broad-leaf weeds among grassy crops. In fact, a mixture of 2,4-D and 2,4,5-Trichlorophenoxyacetic acid was used during the Vietnam War as a defoliant called Agent Orange.

Signaling

For some time, the biggest question in auxin was how it got its message across. That is, what was the auxin receptor. An Auxin Binding Protein (ABP1) had been identified as necessary for auxin-related cell elongation (Chen et al., 2001), but in 2005, two groups simultaneously identified the F-box protein TIR1 as the auxin receptor responsible for auxin-

stimulated gene expression (Dharmasiri et al., 2005; Kepinski and Leyser, 2005). Auxin binds to TIR1, a component of an SCF (SKP1 protein, Cullin, F-box protein, and RBX1) complex, which then binds to an ubiquitnylates Aux/IAA proteins bound to genetic Auxin Response Factors (ARFs). The ubiquitinylation leads to degradation of the Aux/IAAs, releasing the block on transcription on the genes regulated by ARFs, thus leading to the genes being expressed (Quint and Gray, 2006).

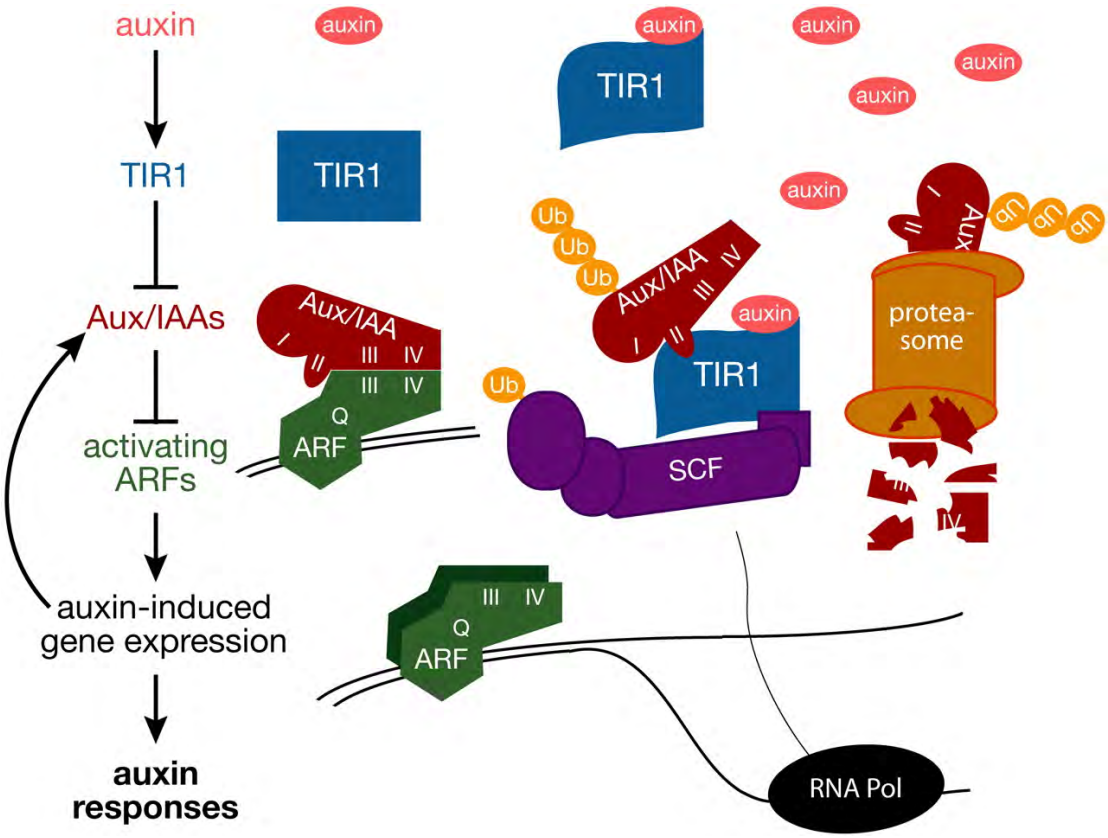

Figure 8: Overview of auxin perception and signaling in the nucleus. (Woodward and Bartel, 2005)

Theories of function

The discovery of auxin and its mode of action led to the concept of phytohormones, generally defined as "substances [in plants] which are synthesized in particular cells and which are transferred to other cells where extremely small quantities influence developmental processes" (Phillips, 1971). Although it is a generally accepted term now applied to a wider range of signaling compounds in plants (Santner et al., 2009), currently there is

discussion on whether the mode of auxin action is best described as a hormone, or using the more specific term, morphogen. "Morphogens are secreted signaling molecules that organize a field of surrounding cells into patterns" (Gurdon and Bourillot, 2001). Auxin seems to fulfill the criteria of a morphogen, namely, that it uses a concentration gradient in a specific subset of cells to act directly on cells by regulating gene expression that defines those cells (Benková et al., 2009). The concept of a morphogen also implicates movement of the compound away from its source, setting up certain patterns as it does so (Turing, 1952). The essential difference in the hormone definition and the morphogen is that the gradient set up by a morphogen is generally considered to be an important factor in establishing the desired pattern, and different concentrations can have different effects, whereas only a small, set concentration of a hormone is required to affect development, with no implications for varying concentration. As this kind of gradient-mediated patterning has still not been determined for auxin, it is still to early to say if it can rightly be called a morphogen or not.

Another recent theory of auxin function focuses on the mechanism of auxin transmission, suggesting a vesicle-mediated secretion across the membrane (Baluška et al., 2003). The involvement of actin in this kind of cell-to-cell communication indicates a similarity to neurotransmitter transport across synapses (Baluška et al., 2005), leading to the suggestion of a view of auxin signaling called "plant neurobiology" (Brenner et al., 2006), with the root apex acting as an integrator of signaling. Although this view has incurred some criticism (Alpi et al., 2007), it can still be useful as a way of interpreting the many components of the auxin signaling pathway (Brenner et al., 2007; Trewavas, 2007).

2: Auxin & Transport

The Chemiosmotic Model

One of the defining characteristics of auxin is its polar movement from the tip of the shoot to the tip of the root, and throughout the plant. Therefore, an important question in auxin research has always been how does it move the way it does? At a velocity of around 1 cm h^{-1}, auxin is transported faster than diffusion, inverted sections still transport in their original direction, and early agar-block experiments showed transport against a concentration gradient. This indicates that auxin is being directed by some mechanism. Since efflux had been shown to be more susceptible to inhibition than influx, early theories rested on the concept only of active energy-dependent secretion from only the lower end of the cell (Goldsmith, 1977). However, in the 70s, Rubery and Sheldrake, as well as Raven, proposed an important model for influx that is known as the chemiosmotic model (Rubery and Sheldrake, 1974; Raven, 1975).

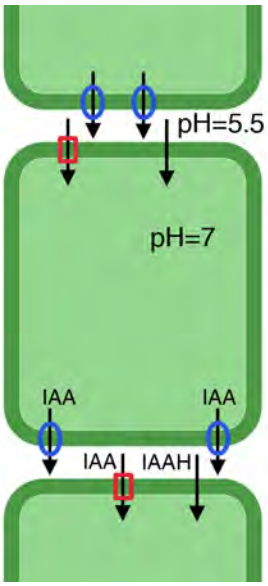

Figure 9: Representation of the chemiosmotic model

IAA is a weak acid with a pK_a of 4.75. Thus, at the pH present in the intercellular space of about 5-5.5, a significant percentage of the IAA will be present in the undissociated form, with the carboxyl group protonated. In this form, the molecule is lipophilic and can readily diffuse through the plasma membrane. The cytosolic pH of around 7 means that upon entering the cell, IAA is found mostly in the anionic form, which cannot pass the plasma membrane, and is therefore trapped in the cell. In this way, higher concentrations than exist outside of a cell can accumulate in a cell, and control of efflux, whether by carriers of active transporters, is the only

regulation necessary for directed auxin transport throughout the plant. Later, auxin importers were also found, to be discussed in the next section.

Auxin Transporters

The AUX/LAX transporters

The proposal and widespread acceptance of the chemiosmotic model for auxin uptake into cells rendered questionable the necessity of an auxin influx carrier. However, early studies had in fact shown that influx was saturable in higher plants, especially at a higher external pH, indicating the presence of and influx carrier (Goldsmith, 1977). When a an agravitropic mutant with altered IAA and 2,4D responses (Maher and Martindale, 1980), *aux1,* was found to correspond to a gene coding for multiple transmembrane domains with similarity to plant amino acid transferases (Bennett et al., 1996), it was speculated that this could be an auxin carrier. It was then demonstrated (Marchant et al., 1999) that AUX1 did indeed specifically support the uptake of auxin, and further members of the family, termed LAX1, 2, and 3 (for *L*ike *AUX*1) were found based on sequence similarity (reviewed in Parry et al., 2001). The AUX/LAX proteins are $2H^+$--IAA^- symporters that allow for a greater accumulation of auxin in a cell than would be by the chemiosmotic model alone, due to the high concentration of protons outside the cell pushing the IAA through with them. AUX1 is localized in the root to the lateral root cap, where uptake can be a particularly important driving force for proper auxin distribution (Kramer and Bennett, 2006). Besides the root cap, it is also found in a subset of columella and stele cells (Swarup et al., 2001), and in general appears to function in basipetal auxin transport in the root, as well as mediating the gravitropic response. Interestingly, another member of the family, LAX3, has a very different and specific function, being localized to cells surrounding an emerging root hair and apparently working as architects in allowing the proper emergence of the hair (Swarup et al., 2008).

The PINs

A central role in the chemiosmotic hypothesis of Polar Auxin Transport (PAT) is ascribed to a polarly localized auxin efflux carrier, which would direct the flow in a specific way. The pin-formed mutation (*pin1)* that had shown a similarity to wild-type plants treated with Auxin Transport Inhibitors (ATIs) as well as a reduction in PAT (Okada et al., 1991) became the main candidate for this role when it was shown to be a transmembrane protein localized to the basal end of conducting cells (Gälweiler et al., 1998). At the same time, another member (PIN2) of the family was demonstrated to play a role in the control of gravitropism (Müller et al., 1998). There are eight members of the PIN family of proteins, divided into two groups. PINs 1, 2, 3, 4, and 7 are so-called full-length PINs, with varying plasma membrane polar localizations (see Figure 10) (Petrásek and Friml, 2009) and at least 1, 2, 4 and 7 show evidence of direct auxin transport (Petrásek et al., 2006; Yang and Murphy, 2009)(Review in Zazimalova et al., 2009). Interestingly, the short loop PINs, 5, 6, and 8, which are missing a hydrophilic loop in the middle of the protein, between transmembrane domains 5 and 6, seem to demonstrate an ER localization (Mravec et al., 2009; Ganguly et al., 2010), indicating a role in maintaining auxin homeostasis and and not direct involvement in PAT. The

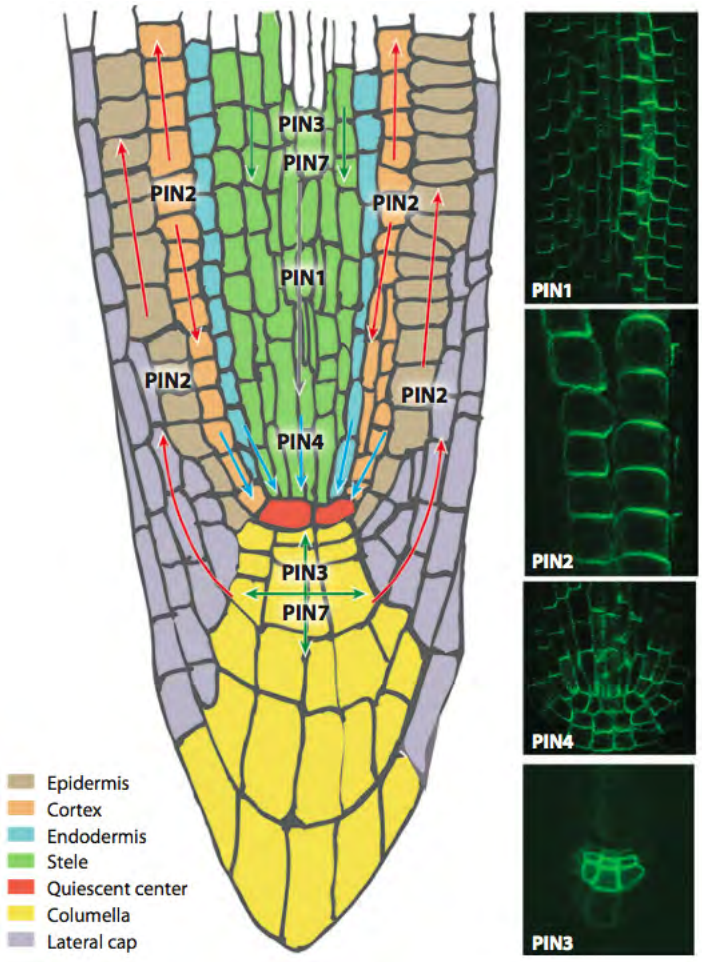

Figure 10: PIN localizations, showing also polar location in cells (Kleine-Vehn and Friml, 2008)

polar localization of the long-loop PINs is dynamic and appears to result from continual cycling to and from the plasma membrane (Geldner et al., 2001); review (Muday et al., 2003). This flexible polar localization makes the PIN family of efflux carriers the main directors of the flow of auxin, as well as giving them key roles in many developmental phases of the plant, like embryogenesis (1, 4, 7) and lateral organ development (2, 3) as well as plant responses to the environment by gravi- and phototropism (2, 3) (Petrásek and Friml, 2009). They work together with the influx carriers and other classes of auxin transporters to keep correct concentrations of auxin in the right place at the right time.

ABCBs

As discussed above, PINs are undoubtedly a key determinant of auxin streams in multi-cellular land plants, but although auxin is known even in one-celled algae, the PINs do not appear on plant evolution until land plants (Galván-Ampudia and Offringa, 2007). Therefore, there must be another system capable of auxin efflux. One of the early indications of this was the discovery that dwarf mutants of maize and sorghum, a mutation that often indicates malfunction in some part of the auxin pathway, were found to result from the loss of function of a P-glycoprotein transporter that appeared to modulate auxin transport in the stalk (Multani et al., 2003) Unrelated research later found a homologous protein,

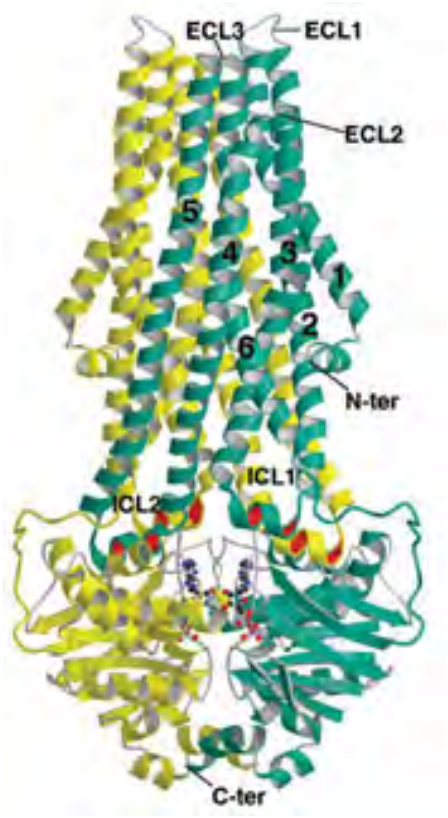

Figure 11: Overall structure of a bacterial ABC transporter. The two subunits are green and yellow, with the trans-membrane alpha helices numbered for the green subunit. Nucleotide binding domains at the bottom show bound ADP in ball-and-stick representation. (Dawson and Locher, 2006)

ABCB1/PGP1, in A. thaliana that also demonstrated auxin transport (Geisler et al., 2005), a function shared by its own closest homolog, ABCB19/PGP19/MDR1 (Bouchard et al., 2006), and a slightly more distant relative, ABCB4 (Terasaka et al., 2005). ABCB 1 and 19 have overlapping expression and apparently function, as the double loss-of-function mutant *abcb1/19* shows a much more severe dwarf phenotype than either *abcb1* or *abcb19* shows by itself (Noh et al., 2001; Geisler et al., 2003). Both ABCB1 and 19 show mostly apolar plasma membrane loclization throughout tissues of the root, although specific regions may show some polarity (Geisler et al., 2005; Titapiwatanakun et al., 2008). ABCB4 has been less studied, but has been shown concentration-dependent variation in direction of auxin transport (Terasaka et al., 2005; Yang and Murphy, 2009) and a role in root hair elongation (Santelia et al., 2005; Cho et al., 2007).

All three are members of a large and ancient class of ATP-powered primarily active transporters, the ATP-binding cassette (ABC) transporters (Reviewed by Rea, 2007), more specifically, the MDR group of ABC transporters, with twelve transmembrane domains interspersed with two nucleotide-binding sites (NBDs). ABC transporters are found in all kingdoms and have, as a family, a wide range of substrates. Some individual proteins are able themselves to transport a range of compounds, such as the medically relevant human PGP1 that is involved in multi-drug resistance cancers, working to pump out many different chemotherapeutic agents (Sarkadi et al., 1992). The mechanism of export, as currently understood, is that a substrate is bound to a binding site within the transmembrane region, after which binding of ATP to the NBDs causes a change in conformation that releases the substrate to the other side of the plasma membrane. Hydrolysis of the ATP to ADP releases the structure back to its receptive conformation (Dawson and Locher, 2007). This creates a very stable system that is able to transport against any sort of gradient whenever necessary, essential for maintaining the correct balance of auxin in a dynamic environment.

What is the use of having two very different systems of regulating auxin efflux? Here, it is important to note that the PINs and ABCBs do not function separately or alone. Both are apparently part of the complex system that the plant must maintain to balance the level of auxin necessary to grow properly. Indeed, the two classes of proteins have been shown to work together to increase substrate specificity and transport volume, and ABCB19 at least has been shown to stabilize PIN1 position in the membrane (Bandyopadhyay et al., 2007; Blakeslee et al., 2007; Titapiwatanakun et al., 2008). The two systems are regulated separately and coordinately, allowing very fine-tuning of the critical auxin flow.

Regulation of Auxin Transport

Transcriptional

If the level of auxin at the right place at the right time is so critical for the proper growth and function of the plant, it is to be assumed that several layers of regulation must exist to control the transport mechanisms that control the levels. Therefore, it is not surprising that the regulation of auxin transport begins at the regulation of transcription of the transporter genes. The binding of auxin the nuclear auxin receptor, TIR1 (Dharmasiri et al., 2005; Kepinski and Leyser, 2005), leads to the ubiquitinylation and subsequent degradation of Aux/IAA repressors. Then the auxin responsive factors (ARFs) are free to activate auxin-inducible genes. These include all known carrier proteins, the AUX/LAX family, the PINs, and the ABCBs. Thus auxin is able to itself regulate the level of its transport through transcriptional activation (review Petrásek and Friml, 2009).

Trafficking

The polar localization of the auxin efflux carriers is, as mentioned previously, a key feature of the chemiosmotic model of PAT. Therefore, correct localization is a further method of regulation. The AUX1 influx carrier undergoes subcellular trafficking and has a general polar localization, but not

much is yet known about its path, except that it is separate from that of the PINs (Kleine-Vehn et al., 2006). While the ABCBs are generally located ubiquitously on the plasma membrane, the PIN family proteins have specific polar locations that direct the flow of auxin (Wisniewska et al., 2006). Not only do known auxin transport inhibitors block the cycling of PINs as well as vesicle trafficking (Geldner et al., 2001), but auxin itself inhibits endocytosis (Paciorek et al., 2005), which would preserve the normally cycled proteins at the plasma membrane. PINs are cycled out of the plasma membrane via clathrin-coated pits. ADP-rybosylation factor (ARF)- guanine nucleotide exchange factors (GEF), which are commonly involved in endocytosis, help track the vesicles to endosomes. From there, they are either targeted for degradation to lytic vacuoles, or recycled back to the plasma membrane via the ARF-GEF GNOM (Geldner et al., 2003). There is still not much known about how the cell knows which PINs should have which polar localization, but there are some clues. For example, apically and basally located PINs have differential sensitivity to Brefeldin A (BFA) treatment, a compound known to affect endocytosis, indicating that a target of BFA is involved in directing polarity (Kleine-Vehn et al., 2008). Phosphorylation also plays a role, and will be discussed further in the next section

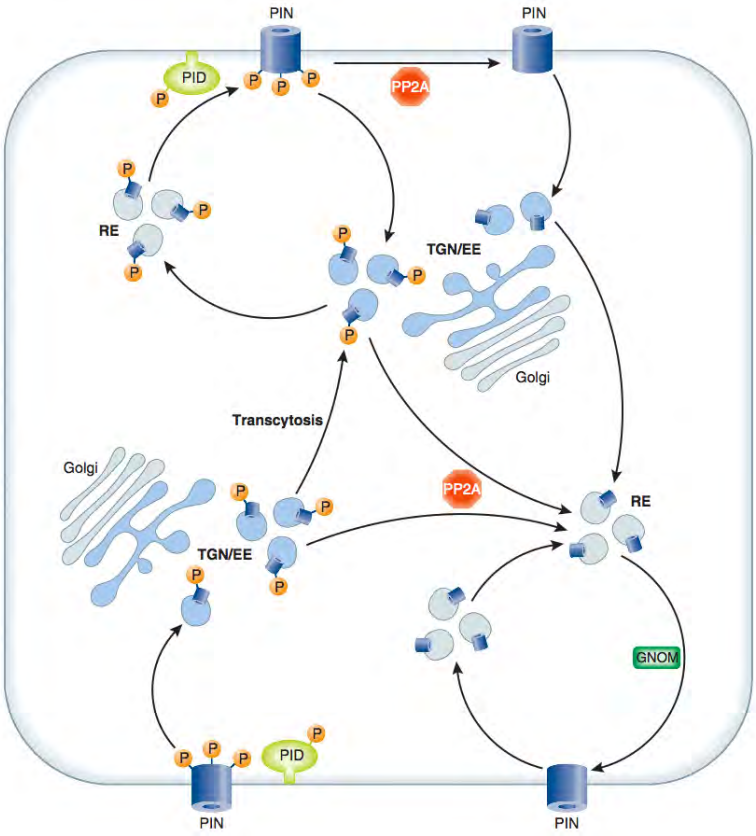

Figure 12: Schematic of PIN trafficking, and its regulation by phosphorylation. (Grunewald and Friml, 2010)

(Reviewed in Grunewald and Friml, 2010). It is well known that the actin cytoskeleton plays a role in organelle movement in the cell (Holweg and Nick, 2004; Kim et al., 2005; Ueda et al., 2010), and therefore might also be involved in the movement of PIN-carrying vesicles to and from the plasma membrane. Evidence includes ATIs affecting actin dynamics (Dhonukshe et al., 2008) and the fact that actin is involved in polar distribution of auxin transport proteins in some way (Muday, 2000), by anchoring the complex to one surface, or by acting as a track for the vesicles carrying the proteins (Muday and DeLong, 2001). The role of actin in auxin transport will be further discussed later. Interestingly, IAA itself seems to block the endocytosis of PINs, meaning that through membrane cycling, auxin is able to regulate its own flow out of the cell by maintaining the right number of efflux capacitators at the correct surface of the cell. The value of this constant recycling is not only that it maintains the proteins at the correct surface without necessitating strict membrane divisions, but also that it facilitates a rapid re-localization under changing circumstances. A pool of PINs is always ready at the center of the cell to be carried to the new basal or apical end in a shifting root.

Phosphorylation

Phosphorylation and dephosphorylation is a widespread method to quickly and reversibly post-transcriptionally modulate the activity of a protein by a kinase covalently attaching phosphate, or a phosphatase removing it, from the target. Evidence of a role for phosphorylation in regulating auxin transport has been building up over some years. The *rcn1* loos-of-function mutation was found through differential respionse to the ATI NPA, and subsequently found to code for a protein phosphatase 2A (PP2A) that has a regulatory function in auxin transport. Although mutants showed increased auxin efflux, this was not dependent on PIN2 or AUX1 (Rashotte et al., 2001) PINOID (PID) was found through phenotypic resemblance of the loss-of-function mutation to *pin1*, and discovered to enhance polar auxin transport (Benjamins et al., 2001). This kinase was found to induce a switch in polar localization of PIN1 (Friml et al., 2004) and generally recruit PIN proteins to a

specific localization path. Subsequently, PP2A and PID have been found to antagonistically regulate phosphorylation and dephosphorylation of PIN proteins, leading to apical or basal localization, dependent on phosphorylation status (Michniewicz et al., 2007). Specifically, PID mediated phosphorylation leads to apical placement, while PP2A mediated dephosphorylation switches the program to move the PINs to the basal surface (Kleine-Vehn et al., 2009). This translates to a practical function in regulating the gravitropic response (Sukumar et al., 2009). Recent work from our lab has also demonstrated a role of phosphorylation in regulation of ABCB-mediated auxin transport (Henrichs et al. In preparation).

Protein-protein interaction

As already briefly mentioned, one way PINs and ABCBs regulate each other is through direct interaction (Blakeslee et al., 2007). PIN1 co-expression with either ABCB1 or ABCB19 in a heterologous system enhanced IAA transport overall, as well as enhancing substrate specificity and sensitivity to NPA. Conversely, PIN2 co-expression with the ABCBs did not increase export, although substrate specificity and inhibitor sensitivity were still enhanced. Combined with yeast two hybrid assays showing evidence for direct interaction of ABCB19 with both PINs 1 and 2, it has been shown that where ABCB19 and PINs co-localize, they mutually enhance auxin transport and its specificity. Although evidence of direct ABCB1 interaction with the PINs was not shown, there is likely to be indirect interaction in larger complexes, or through the assistance of other proteins. In addition, direct ABCB19 interaction has been demonstrated to stabilize at least PIN1 in certain domains of the plasma membrane, meaning that a greater concentration will be focused in the desired direction (Bandyopadhyay et al., 2007; Titapiwatanakun et al., 2008). Both the specific interaction and stabilizing of plasma membrane domains as regulators of auxin transport must be very tissue-specific, as the expression patterns of PINs and ABCB19 only partially overlap. Besides these, an important protein-protein interaction regulates the activity of ABCB1 and 19. A small (42kD) peripheral plasma membrane

protein TWisted Dwarf 1, (TWD1) has been found to physically interact with both ABCBs 1 and 19 (Geisler et al., 2003). A distinct FK506-like Binding Domain (FKBD) at the N-terminal of TWD1 interacts with the C-terminal NBDs, forming a complex on the plasma membrane. This direct interaction was found to influence auxin efflux by the ABCBs (Bailly et al., 2006; Bouchard et al., 2006). The influence is specific, and interaction enhances the rate of auxin efflux in plants and human cells, although the effect is reverse in yeast cells for unknown reasons, possibly because of regulatory or membrane composition differences. The exact mechanism of the influence is still unknown. Further details on TWD1 will be given in a later section.

Chemical regulators

An important tool in auxin transport research has been the use of chemical auxin transport inhibitors (ATIs). Early on, two of the most effective were found to be 2,3,5-triiodobenzoicacid (TIBA) and N-1-naphthylphthalamic acid (NPA) (Keitt and Baker, 1966). Since then, researchers have been trying to elucidate the mechanism of the inhibition. The solubilization of the NPA receptor (Sussman and Gardner, 1980) led to investigation of its binding sites, with findings of high and low affinity sites (Michalke et al., 1992) and that the sites are perpheral to the membrane as well as associated with the cytoskeleton (Cox and Muday, 1994), and face the cytoplasm (Dixon et al., 1996). More recently, NPA has been found to bind the ABCBs (Murphy et al., 2002). Also, flavonoids, a class of non-essential plant polyphenolics of so-far unknown function widely found in plants, have been suggested as the native counterpart of NPA, possibly acting to subtly regulated auxin flow during such events as the root gravitropic response (Murphy et al., 2000; Santelia et al., 2008). Investigations into the mechanism of TIBA inhibition have not been as wide, but some studies have shown it to have and effect on AUX1

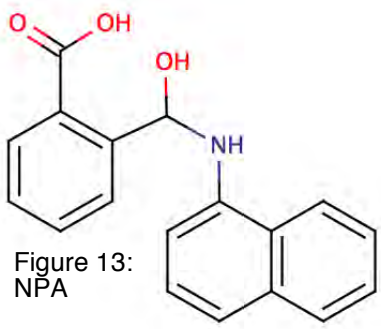

Figure 13: NPA

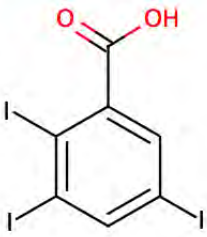

Figure 14: TIBA

localization (Kleine-Vehn et al., 2006) and vesicle trafficking (Dhonukshe et al., 2008), and that there is a difference in TIBA and NPA, namely that TIBA reduces the length of the growth zone at the root tip, while NPA reduces the cell production rate and slows down cytoplasmic streaming (Rahman et al., 2007). ATIs are thus useful for investigating auxin transport, and differentiating between various components of the transport complex. Further elucidation of inhibitors could help refine which components act where and when.

Actin

Actin is a one of the components of the cytoskeleton that gives structure to a cell and organizes the cytosol. The actin filament (F-actin), 7nm in diameter, is made up of individual, 42 kD globular proteins (G-actin) (Holmes et al., 1990; Kabsch et al., 1990). Each individual unit binds an ATP, and is then capable of binding to other units to form the double-helical filament (Review in Pollard and Cooper, 1986). After a delay, the ATP is hydrolyzed to ADP. The filament is extremely flexible and dynamic, growing and shrinking from each end.

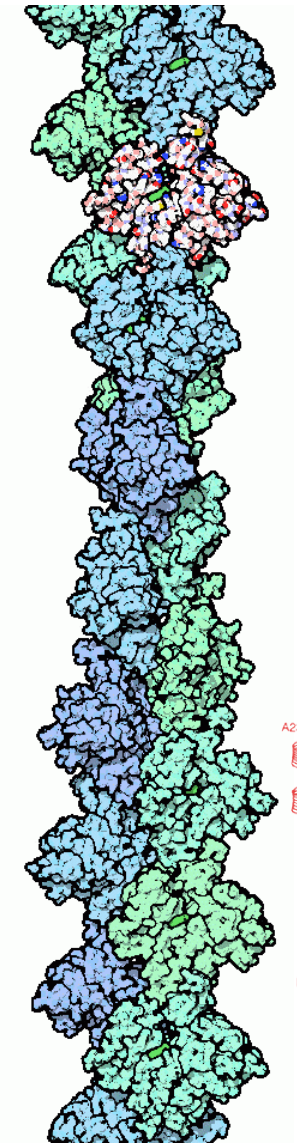

As actin was originally found in mammalian muscles, it was not at first known if plants contained actin at all. The first plant actin was found in large filamentous algal cells (summary in Lloyd, 1988), and it has since been found not only in all plants, but all eukaryotes. In *Arabidopsis thaliana*, there are eight actin genes and two pseudogenes. These are widely dispersed through the genome, and fall into two classes (McKinney and Meagher, 1998). ACT1, 3, 4, 11, and 12 are in the reproductive class, mostly found in the reproductive cells of the plant,

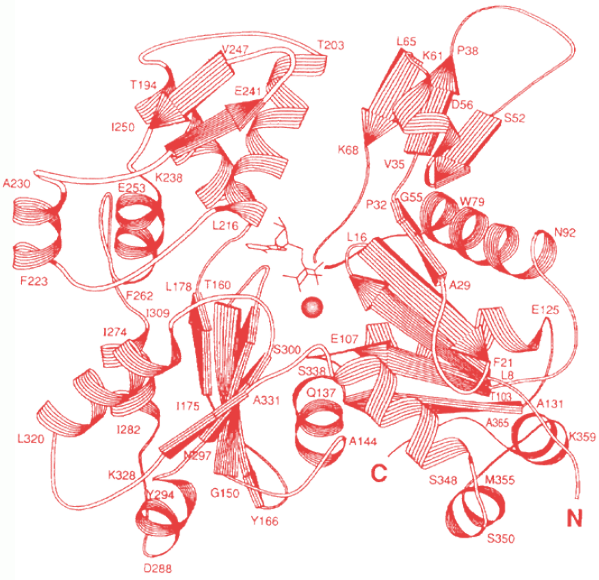

Figure 15: Single actin monomer and filament (Holmes and Kabsch, 1991)

although there is some evidence of expression in other parts of the plant of ACT4 and 12 (review Blancaflor et al., 2006). ACT 2, 7, and 8 are the vegetative actins, found throughout most of the plant. Although their function and expression overlap, individual loss-of-function mutations show varying phenotypes, and double mutant combinations show more severe phenotypes, indicating some specialization of role. ACT7 has been especially well studied, from being found in rapidly developing tissues (McDowell et al., 1996), through being induced by auxin (Kandasamy et al., 2001) to playing an essential role in germination and root growth (Gilliland et al., 2003). The *act7-4* loss of function mutation shows one of the most severe *act* mutations, with severely reduced and disorganized root growth.

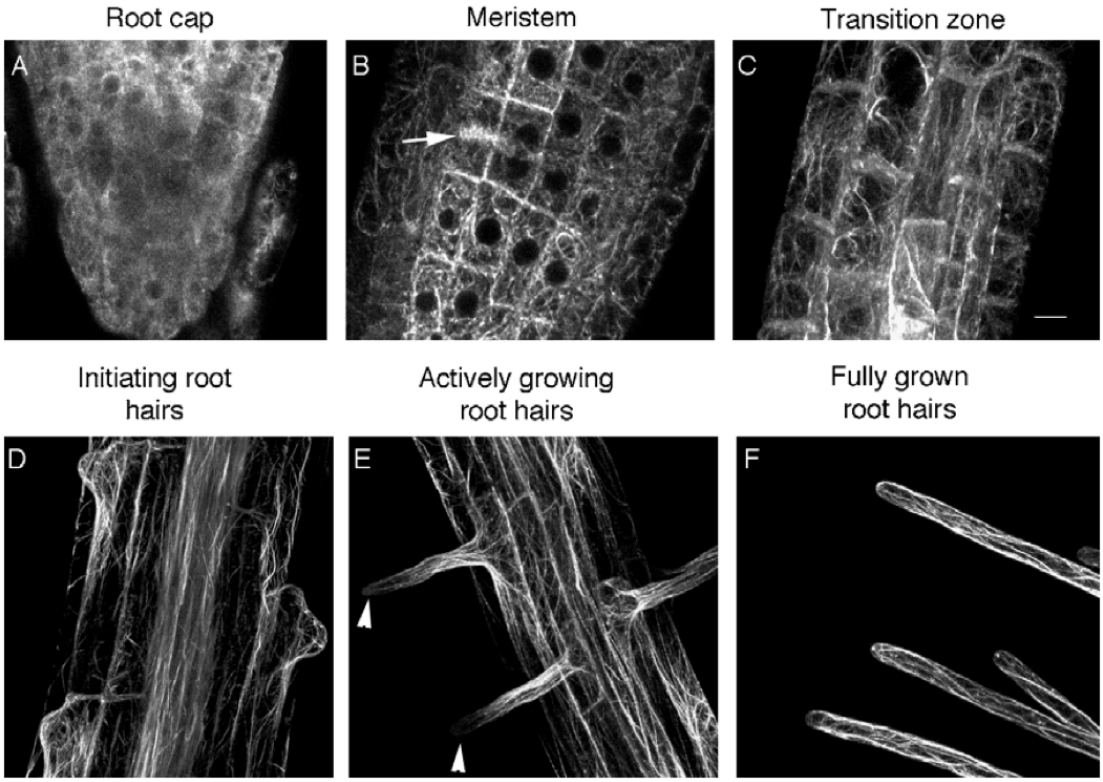

Figure 16: Actin organization in the root (Blancaflor et al., 2006)

Of course actin cannot do the structural and regulatory work it does without a lot of interaction with other proteins. There are many large classes of actin-interacting proteins. Some classes shape the actin filaments, like the Actin Related Protein 2/3 complex (ARP2/3), which is an actin nucleator that helps make new branches on existing filaments (review (Blancaflor et al., 2006) and

also correlates actin/plasma membrane interaction (Kotchoni et al., 2009). Profilins bind to G-actin, preventing their addition to filaments, whereas actin-depolymerization factors (ADFs) cause the filaments to dissociate into monomers. Several classes are known as actin bundling proteins because they group strands of actin into different formations. These include Villins, Fimbrins, and LIMs that generally group two filaments to each other, either parallel or anti-parallel, depending on the particular member of the group. Formins can create more complex organizations, first helping to nucleate the filament and promote its rapid elongation, and then arranging groups of filaments in broader arrays (review in Thomas et al., 2009). Other proteins, the myosins, which interact with actin, do not reshape the actin itself, but rather use the actin as a scaffold for moving cellular compartments or other materials through the cell (Holweg and Nick, 2004). In addition to protein-protein interaction-based regulation of actin shape and form, chemical compounds can also play a role. Latrunculin B depolymerizes actin, leading to dwarf plants (Baluska et al., 2001) and jasplakinolide induces nucleation, which can lead to stabilized F-actin (Bubb et al., 2000).

All this organizing and bundling, dynamic instability and nucleating, has a purpose. Actin serves many functions in the plant cell, and is very important for shaping both the internal architecture of the cell and the overall shape of the plant. A good example is found in single cells that grow out of their surroundings, like trichomes (Mathur et al., 1999) and root hairs (Gilliland et al., 2002; Voigt et al., 2005; Ketelaar et al., 2007). Both need a stable and functioning actin cytoskeleton to properly elongate and take their own shapes. Treatment with actin-destabilizing chemicals generates non-branching trichomes and loss of function of even one actin gene can lead to stunted and misshapen root hairs. Also, root hairs and pollen tubes grow via tip-growth, that is, only one end of the cell expands. Both have been shown to require actin cables and networks to carry vesicles supplying materials to the growing end (Gibbon et al., 1999; Ketelaar and Emons, 2001). In many life-forms, actin plays an active role in endocytosis (Kaksonen et al., 2006) and

seems to be involved in endocytosis-related processes in plants as well (Samaj et al., 2004; Dhonukshe et al., 2008), although the level and mechanism of involvement is still unclear.

Interestingly, actin also seems to be involved in many auxin-related processes. Particularly, the disruption of actin by latrunculin-B enhances the gravitropic response in inflorescence stems, hypocotyls (Yamamoto and Kiss, 2002) and in roots (Hou et al., 2003), which is caused by the persistence of an auxin gradient in the absence of actin (Hou et al., 2004).

There are also many lines of evidence directly linking actin to auxin's role in plant development. A mutation in a myosin is defective in auxin transport (Holweg and Nick, 2004). Auxin transport inhibitors can mimic the effect of actin inhibitors (Rahman et al., 2007) and thus alter vesicle motility (Dhonukshe et al., 2008). Auxin even seems to be directly involved in bundling of actin filaments (Nick et al., 2009). Due to these lines of evidence and the fact that PIN proteins are known to maintain their polar localization by cycling to and from the plasma membrane via vesicles, a theory directly linking this trafficking to actin has been proposed, but not yet conclusively proven. However, and older idea links the NPA-binding protein (NBP) component of the auxin efflux complex to the actin cytoskeleton, (Muday and DeLong, 2001), either by trafficking the proteins to the membrane or stabilizing them there. Further evidence shows that auxin transport inhibitor TIBA (as well as the less-studied PBA) directly influence actin dynamics, as well as affecting trafficking, clearly linking the two (Dhonukshe et al., 2008). This study did not show NPA to have a direct effect on actin, but another (Rahman et al., 2007) showed that NPA can directly reduce actin filaments, without affecting PIN2 localization. Thus the answer to how actin, PIN localization, and auxin transport overall remains not entirely resolved.

4: TWISTED DWARF 1

FKBPs

TWD1, mentioned above as an ABCB1 and 19 interactor, is a member of a large family of proteins identified as the FK506 Binding Proteins. Also in 1989, a protein with similar characteristics as cyclophilin was discovered (Harding et al., 1989). These enzymes exhibit Peptidyl-Prolyl cis-trans Isomerase (PPIase) activity, and bind an immunosuppressive compound, FK506 (Harding et al., 1989). FKBPs are quite a large and varied family of proteins found in all branches of life, with many different functions. Overall, they can be split into two broad groups, the low-molecular weight FKBPs and the high molecular weight ones. The low molecular weight proteins generally consist of only one FK506 binding domain (FKBD), whereas the high molecular weight ones may contain one or more FKBDs, as well as other domains, including, but not necessarily limited to, tetratricopeptide repeat (TPR) domains, a degenerate repeat domain involved in protein-protein interactions, a calmodulin (CaM) binding domain (CaMBD), and even membrane anchors, although the vast majority of FKBPs are soluble proteins. Interestingly, these domains tend to function independently, with the deletion of one domain not affecting the

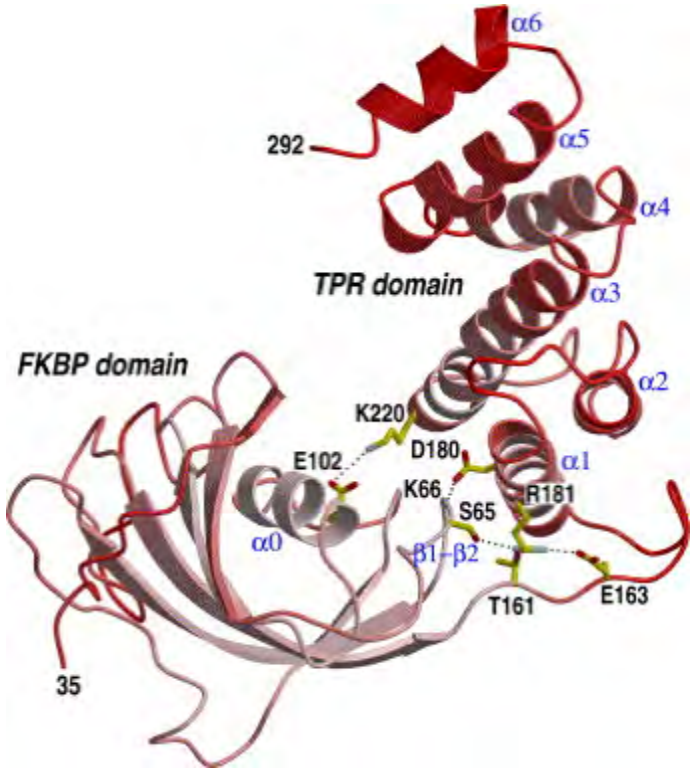

Figure 17: Full-length structure of TWD1, minus the membrane anchor. Alpha helices are numbered comprehensively over the entire structure. An interesting feature is the orientation of the subunits to each other. (Granzin et al., 2006)

ability of the other domains to perform their tasks (Barik, 2006). The structure of the smallest member of the FKBPs, FKBP12, demonstrates the common FKBD structure. Large molecule weight FKBPs in humans interact with many partners, such as FKBP38, which regulates the anti-apoptotic protein Bcl-2 (Kang et al., 2005) as well as interacting with a viral protein NS5A (Wang et al., 2006).

In plants, the *Arabidopsis* genome has revealed a large number of FKBPs, 23 in all, with 16 low molecular weight and seven high molecular weight FKBPs. Eleven of the low molecular weight proteins are found localized to the chloroplast lumen, a real hotbed of FKBP activity (He et al., 2004; Geisler and Bailly, 2007). Arabidopsis FKBP12 shows only 63 percent similarity with its human homolog (Harrar et al., 2001), but has a somewhat similar function in regulating the cell cycle. Only one interacting partner was found for AtFKBP12 (Faure et al., 1998), AtFIP37 (FKBP12 interacting protein), which is essential in controlling endoreduplication, especially in trichomes, although it is also expressed in embryonic cells. Knockouts in fact cause an embryo-lethal phenotype (Vespa et al., 2004). One high molecular

Figure 18: The phenotypes of *abcb* and *twd1* loss-of-function mutants. From left: Wild type, *abcb1*, *abcb19*, *abcb1x19*, *twd1*. Inset: detail of , *abcb1x19* and *twd1*. (Geisler and Bailly, 2007)

weight FKBP is PASTICCINO1 (PAS1), interacts with FAN (FKBP associated NAC), a transcription factor, and through this interaction controls cell proliferation and differentiation (Smyczynski et al., 2006). As a family, FKBPs are involved in many phases of plant development, mainly by supporting and modulating protein-protein interactions of various classes of proteins, from transporters to transcription factors (Geisler and Bailly, 2007).

TWD1 (TWISTED DWARF1) was originally studied after the *twd1* phenotype was identified in a screen for plant architecture mutants (Kamphausen et al., 2002). Its formulaic name is AtFKBP42, indicating that it is a high-molecular weight (42 kDa) FKBP from *Arabidopsis thaliana*. Another *Arabidopsis* mutation, *ucu2* (*ultracurvata2*) (Pérez-Pérez et al., 2004) is allelic to *twd1*. TWD1 has a single FKBD, one three-part TPR domain, a CaM binding domain, and, uncommonly, a membrane anchor, which localizes it to the plasma membrane as well as the tonoplast. Its closest homolog is in fact the human FKBP38, which also has a membrane anchor (Kang et al., 2005). Unusually, TWD1 shows neither FK506 binding nor PPIase activity (Kamphausen et al., 2002). The crystal structure of the FKBD shows the canonical FKBP12 structure, with the exception of an extended loop, altering the FK506 binding pocket (Weiergraber et al., 2006). Subsequent crystal structure elucidation of the entire TWD1, minus the membrane anchor, revealed an unexpected orientation of

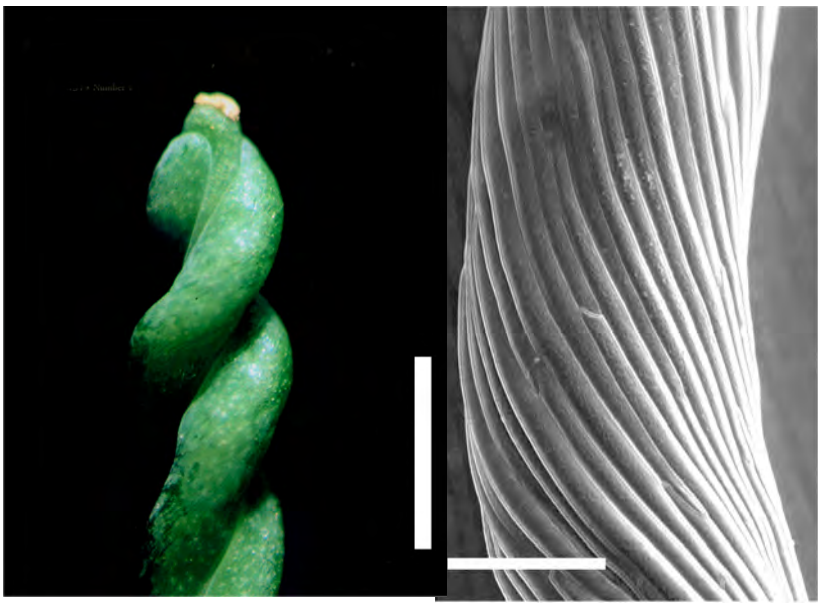

Figure 20: Details of the twist at the silique and hypocotyls (Bailly et al., 2006)

FKBD and TPR domain subunits, forming an overall C-shape (Granzin et al., 2006). Also, characterization of the membrane anchor separately showed it to lie parallel to the lipid membrane (Scheidt et al., 2007).

The Phenotype and ABCB interaction

The *twd1* loss-of-function mutation shows a striking phenotype. The plants have a dwarf architecture, they are fertile and develop fully though slowly. They have epinastically growing cotyledons and leaves. The most interesting feature is the twist, which manifests itself both at the epidermal, organ, and whole plant level. Yeast two-hybrid screen revealed the interacting partners of TWD1 to be ABCB1 and ABCB19 (Geisler et al., 2003). The ABCBs co-localize with TWD1 on the plasma membrane, and interact via their C-

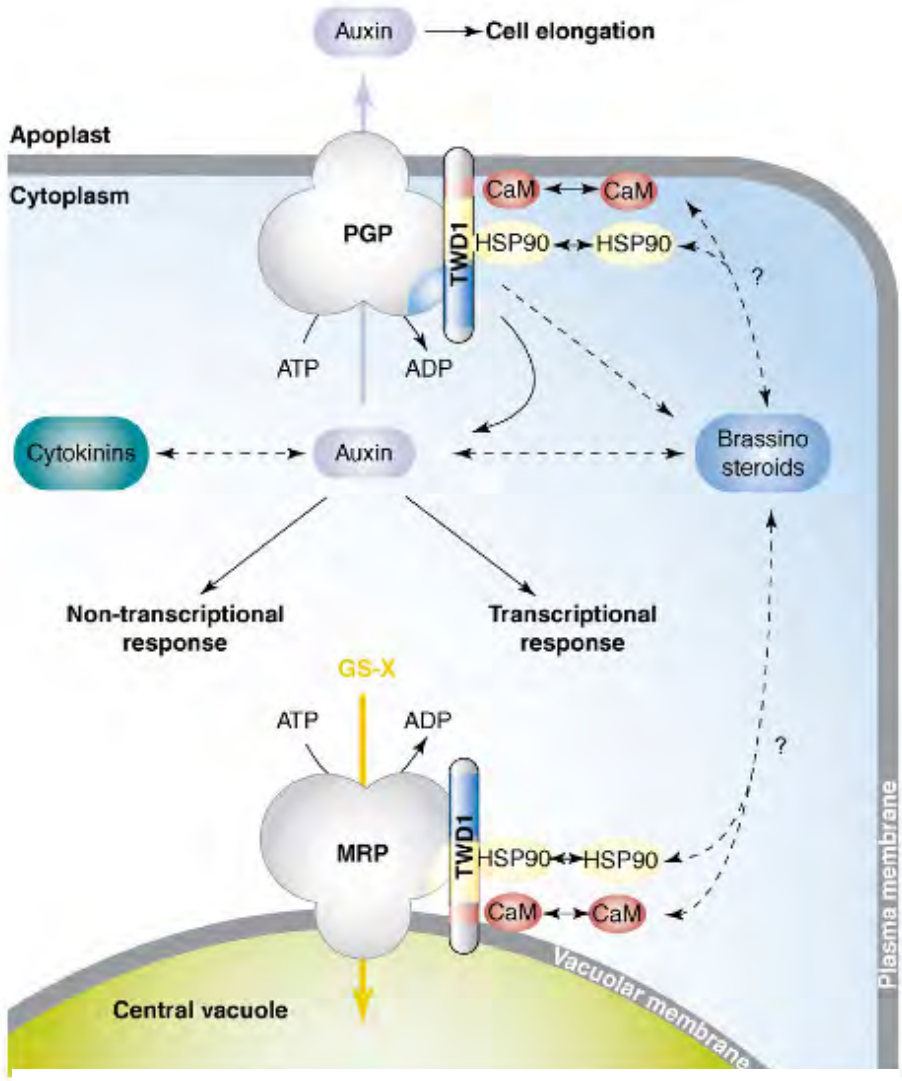

Figure 21: Overview of TWD1-interacting proteins and the related functions. (Geisler and Bailly 2007)

termini with the FKBD of TWD1. The *abcb1/abcb19* double knockout shows a very similar phenotype to *twd1,* minus the twist, indicating that TWD1 also has a function independent of these transporters. Further investigation revealed interaction of the TWD1 TPR domain with MRP1 and MRP2 on the tonoplast (Geisler et al., 2004). Then, when ABCB1 was shown to catalyze the cellular efflux of auxin (Geisler et al., 2005), the question was what role TWD1 could play in this activity. The *twd1* plants do show a reduced efflux, but overexpression of the TWD1 protein does not enhance efflux. However, it was shown that direct interaction of TWD1 with ABCB1 and 19 enhances the efflux capabilities of those proteins (Bouchard et al., 2006). Other functions of TWD1 may involve the heat shock protein 90 (HSP90), a ubiquitous member of an important chaperone complex. AS TWD1 is know to bind HSP90, it could well be that brassinosteroid signal transduction involving TWD1 is connected to this chaperone, which is known be implicated in steroid-hormone signaling in other organisms (Sangster and Queitsch, 2005). Despite this level of enquiry into TWD1 functions, the most striking component of the loss-of-function mutation is still not adequately explained, and may depend on further interactions by this promiscuous immunophilin.

The Identity of the NPA-binding protein

The role of TWD1 in the modulation of ABCB1 and 19 mediated auxin efflux by ATIs, especially NPA, as well as the as-yet underexplained twisting phenotype of *twd1* brings up an interesting connection. As previously mentioned, the importance of NPA in auxin transport research cannot be overstated, and thus the identity of the NPA-binding protein (NBP) is crucial to understanding auxin transport. Early on it was found that the protein was like to be membrane associated and to non-covalently and reversibly bind NPA (Thomson et al., 1973), but only later was it conclusively shown that the plasma membrane protein was really the NBP involved in auxin transport (Bernasconi et al., 1996). Some studies have demonstrated the possibility of two binding sites, one abundant low-affinity one, and another of lower

abundance but higher affinity (Michalke et al., 1992). Interestingly, both the assertion of two sites (Muday et al., 1993) and the NBP's integral membrane status have been refuted (Cox and Muday, 1994). While the latter claim still associates the binding site with the plasma membrane, it gives it only a peripheral location, as well as associating it with the cytoskeleton, specifically actin. Later studies specifically aimed at purifying NPA-binding proteins identified several candidates (Murphy et al., 2002). Although the study focused on plasma membran associated aminopeptidases, and interesting result also showed NPA-binding activity for ABCBs, specifically ABCB1 and ABCB19, and especially the latter (Noh et al., 2001). The existence of this integral membrane protein with auxin efflux capacity seems to fulfill the criteria for one of the described NBPs. However, there remains the idea of a membrane-peripheral protein with a link to the cytoskeleton, neither of which fits the ABCBs. The idea that this component of the auxin efflux would integrate the efflux units with the actin cytoskeleton (Muday and DeLong, 2001) and the striking structural abnormalities of *twd1* plants led to the question whether TWD1, linked to auxin transport and peripheral to the plasma membrane might be this NBP, connected to actin. Although many twisting phenotypes are related to microtubules and not actin, the non-handed twisting demonstrated by *twd1* could indicate simply its auxin transport deficiency (Ishida et al., 2007). Also,

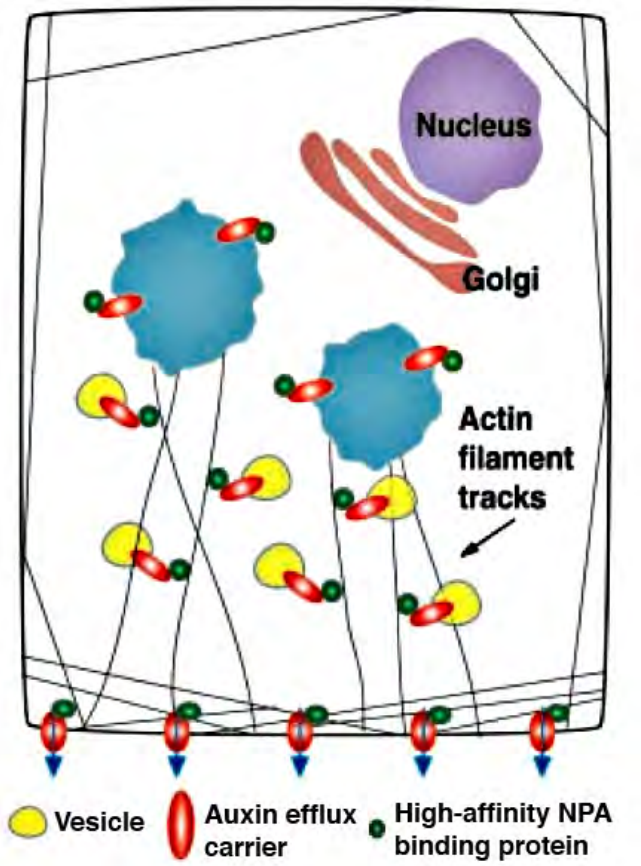

Figure 22: A theory of actin filament and NBP involvement in auxin transport. (Muday and DeLong, 2001)

microtubules do not seem to play a significant role in auxin-mediated responses (Hasenstein et al., 1999) as actin seems to. These ideas led to the aims for this thesis.

Aims

- Does TWD1 function in NPA inhibition of auxin transport?
- Is TWD1 associated with actin?
- Do TWD1 and actin directly interact?
- Is this interaction associated with NPA inhibition?
- Are there other inhibitors that work on this mechanism?

Chapter 2:

Modulation of P-glycoproteins by Auxin Transport Inhibitors Is Mediated by Interaction with Immunophilins

Chapter 2

Personal Contributions

Figure 1C: Mutagenesis and BRET experiments

Figure 3B: Mutagenesis and export experiments

Figure 4: Mutagenesis and binding assays

Supplemental Material can be found at:
http://www.jbc.org/cgi/content/full/M709655200/DC1

THE JOURNAL OF BIOLOGICAL CHEMISTRY VOL. 283, NO. 31, pp. 21817–21826, August 1, 2008
© 2008 by The American Society for Biochemistry and Molecular Biology, Inc. Printed in the U.S.A.

Modulation of P-glycoproteins by Auxin Transport Inhibitors Is Mediated by Interaction with Immunophilins*[S]

Received for publication, November 27, 2007, and in revised form, May 19, 2008 Published, JBC Papers in Press, May 22, 2008, DOI 10.1074/jbc.M709655200

Aurélien Bailly[‡], Valpuri Sovero[‡], Vincent Vincenzetti[‡], Diana Santelia[‡1], Dirk Bartnik[§], Bernd W. Koenig[§¶], Stefano Mancuso[‖], Enrico Martinoia[‡], and Markus Geisler[‡2]

From the [‡]Institute of Plant Biology and Zurich-Basel Plant Science Center, University of Zurich, CH-8008 Zurich, Switzerland, the [§]Institute of Neuroscience and Biophysics, Research Centre Jülich, D-52425 Jülich, Germany, the [¶]Institute of Physical Biology, Heinrich-Heine University Düsseldorf, D-40225 Düsseldorf, Germany, and the [‖]Department of Horticulture, University of Firenze, I-50019 Sesto Fiorentino, Italy

The immunophilin-like FKBP42 TWISTED DWARF1 (TWD1) has been shown to control plant development via the positive modulation of ABCB/P-glycoprotein (PGP)-mediated transport of the plant hormone auxin. TWD1 functionally interacts with two closely related proteins, ABCB1/PGP1 and ABCB19/PGP19/MDR1, both of which exhibit the ability to bind to and be inhibited by the synthetic auxin transport inhibitor *N*-1-naphylphtalamic acid (NPA). They are also inhibited by flavonoid compounds, which are suspected modulators of auxin transport. The mechanisms by which flavonoids and NPA interfere with auxin efflux components are unclear. We report here the specific disruption of PGP1-TWD1 interaction by NPA and flavonoids using bioluminescence resonance energy transfer with flavonoids functioning as a classical established inhibitor of mammalian and plant PGPs. Accordingly, TWD1 was shown to mediate modulation of PGP1 efflux activity by these auxin transport inhibitors. NPA bound to both PGP1 and TWD1 but was excluded from the PGP1-TWD1 complex expressed in yeast, suggesting a transient mode of action *in planta*. As a consequence, auxin fluxes and gravitropism in *twd1* roots are less affected by NPA treatment, whereas *TWD1* gain-of-function promotes root bending. Our data support a novel model for the mode of drug-mediated P-glycoprotein regulation mediated via protein-protein interaction with immunophilin-like TWD1.

Bioactive flavonoids derived from plant secondary metabolism serve as important nutraceuticals (1). They have health-promoting effects, including antioxidant, anticarcinogenic, antiviral, and anti-inflammatory activities; however, the cellular targets of the *in vivo* protein remain largely unknown (1, 2). In plants, among other functions, flavonoids such as quercetin, kaempferol, and other aglycone molecules have been shown to inhibit cell-to-cell/polar auxin transport (PAT)[3] and consequently to enhance localized auxin accumulation (1, 3–6). During PAT, the plant hormone auxin, which determines many aspects of plant physiology and development, is moved directionally in a cell-to-cell mode (7–9).

The regulatory impact of flavonoids on PAT initially was based on their ability to compete with N-1-naphtylphtalamic acid (NPA), a synthetic auxin transport inhibitor (ATI) (4, 10–12) and herbicide (naptalam, alanap), for transporter binding sites. This concept is further supported by auxin-related phenotypes of *Arabidopsis* mutants with altered flavonoid levels (1, 3, 13), although fundamental physiological processes occur in the absence of flavonoids. Currently the flavonoids are seen as transport regulators or modulators (14); nevertheless, the mechanisms by which flavonoids interfere with auxin efflux components are not yet clear (1).

The auxin efflux complex is thought to regulate PAT on the molecular level and consists of at least two proteins: a membrane integral transporter and an NPA-binding protein (NBP) regulatory subunit (11, 15–17). Recently, ABCB/P-glycoprotein (PGP)/multidrug resistance (MDR) proteins, members of the expanded *Arabidopsis* ABC (ATP-binding cassette) transporter family (18, 19), have been identified as both auxin transporters (20–24) and high-affinity NBPs (25, 26).

High NPA concentrations cause inhibition of auxin efflux catalyzed by ABCB1/PGP1 and ABCB19/PGP19/MDR1 (20, 21) (hereafter referred to as PGPs), most probably by binding to the transporter itself (26). This is in analogy to flavonoids functioning as inhibitors of plant (20, 21, 24) and mammalian PGPs (2) probably by mimicking ATP and competing for PGP nucleotide-binding domains (27). Overexpression of certain PGPs is associated with increased MDR, whereas loss of function often results in diverse diseases (28) in mammalians.

The immunophilin-like FKBP42, TWISTED DWARF1 (TWD1) (29–31), belongs to the FKBP (FK506-binding protein)-type family of PPIases (peptidyl-prolyl *cis-trans* isomerases, EC

* This work was supported by funds from the Swiss National Fonds (to M. G. and E. M.) and the Novartis Foundation (M. G.). The costs of publication of this article were defrayed in part by the payment of page charges. This article must therefore be hereby marked "*advertisement*" in accordance with 18 U.S.C. Section 1734 solely to indicate this fact.

[S] The on-line version of this article (available at http://www.jbc.org) contains supplemental Experimental Procedures," references, and Figs. S1–S6.

[1] Present address: Zurich-Basel Plant Science Ctr., ETH Zürich Inst. of Plant Science, CH-8092 Zurich, Switzerland.

[2] To whom correspondence should be addressed: University of Zurich, Inst. of Plant Biology and Zurich-Basel Plant Science Ctr., CH-8008 Zurich, Switzerland. Tel.: 41-44-634-8277; Fax: 41-44-634-8204; E-mail: markus.geisler@botinst.uzh.ch.

[3] The abbreviations used are: PAT, polar auxin transport; NPA, *N*-1-naphylphtalamic acid; ATI, auxin transport inhibitor; NBP, NPA-binding protein; PGP, P-glycoprotein; MDR, multidrug resistance; ABC, ATP-binding cassette; FKBP, FK506-binding protein; PPIase, peptidyl-prolyl *cis-trans* isomerase; TWD, Twisted Dwarf; BRET, bioluminescence resonance energy transfer; YFP, yellow fluorescent protein; GFP, green fluorescent protein; CFP, cyan fluorescent protein; IAA, indole-3-acetic acid; BA, benzoic acid; rLuc, *Renilla* luciferase; NBD, nucleotide-binding domain; HA, hemagglutinin.

Downloaded from www.jbc.org at SMAC Consortium - University of Zürich on August 6, 2008

5.1.2.8) (29, 31, 32). Many but not all PPIases catalyze the *cis-trans* isomerization of *cis*-prolyl bonds and have been identified as targets of immunosuppressant drugs such as FK506 (tacrolimus) (29, 31, 32). The TWD1 C terminus forms a so-called amphipathic in-plane membrane anchor, which probably confers a perpendicular orientation (33) on both the vacuolar (34) and the plasma membrane (30, 35).

TWD1 docks with its N-terminal FK506-binding domain (FKBD), shown to lack PPIase activity and FK506 binding (30, 35), to C-terminal nucleotide-binding domains (18) of PGP1 and PGP19 (see Fig. 1*A*). In this way, TWD1 acts *in planta* as a positive regulator of PGP1- and PGP19-mediated auxin efflux by means of protein-protein interaction (20, 30), modulating the movement of auxin out of apical regions and long range auxin transport on the cellular level (20, 36).

Here, we employed a yeast-based bioluminescence resonance energy transfer (BRET) system to investigate PGP1-TWD1 interaction on a molecular level. Auxin transport inhibitors and flavonoids, inhibitors of mammalian and plant PGPs, disrupt PGP1-TWD1 interaction. Auxin transport inhibitors modulate the regulatory effect of TWD1 on PGP1 activity, supporting a novel mode of PGP regulation via immunophilin-like TWD1 (20). This represents a new concept of drug-mediated ABC transporter modulation via membrane-anchored immunophilins and may have important agronomic and clinical implications.

EXPERIMENTAL PROCEDURES

Yeast Constructs, Growth, and Expression Analysis—cDNA covering the N-terminal FKBD of *Arabidopsis* TWD1 (TWD1-(1–187); At3g21640) were cloned into BamHI and SalI sites of the copper-inducible yeast shuttle vector pRS314CUP (20) resulting in pRS314CUP-FKBD. Point mutations in TWD1 and a stop codon in PGP1 (bp 3.240) were introduced using the QuikChange XL site-directed mutagenesis kit (Stratagene, La Jolla, CA) resulting in pRS314CUP-TWD1^{C70D,L72E} and pNEV-PGP1$^{\Delta NBD2}$-YFP (20). Empty vector controls pNEV and pRS314CUP as well as pNEV-PGP1, pNEV-PGP1-YFP, pNEV-PGP1$^{\Delta NBD2}$-YFP, pRS314CUP-FKBD, pRS314CUP-FKBD-rLuc, pRS314CUP-TWD1, and pRS314CUP-TWD1-rLuc were transformed into *Saccharomyces cerevisiae* strain JK93dα (37), and single colonies were grown in SD-UT (synthetic minimal medium without uracil and tryptophan, supplemented with 2% glucose and 100 μM $CuCl_2$).

Cells co-expressing PGP1-YFP and TWD1-CFP (20) grown in the presence of 10 μM drugs or solvent control to an A_{600} around 0.8 were washed and incubated in mounting media containing 4,6-diamidino-2-phenylindole, and fluorescence pictures were collected by confocal laser scanning microscopy (Leica, DMIRE2) equipped with argon (488 nm) and UV lasers (410 nm). Fluorescence and DIC (differential interference contrast) images were processed using Adobe Photoshop 7.0. Vector controls showed no detectable fluorescence. Plasma membrane fractions were separated via continuous sucrose gradient centrifugation (34) and subjected to 4–20% PAGE (Long Life Gels, Life Therapeutics), and Western blots were immunoprobed using anti-GFP (Roche Applied Science) and anti-*Renilla* luciferase (rLuc; Chemicon Int.).

For auxin analogue detoxification assays (20, 38), transformants grown in SD-UT to an A_{600} of ~0.8 were washed and adjusted to an A_{600} of 1.0 in water. Cells were diluted 10× five times, and each 5 μl was spotted on minimal media plates supplemented with 750 μM 5-fluoroindole (Sigma). Growth at 30 °C was assessed after 3–5 days. Assays were performed with three independent transformants.

BRET Constructs and Assays—*Renilla* luciferase (rLuc, GenBank™ accession number AY189980) was amplified by PCR from plasmid pRL-null (Promega) and inserted in-frame into AscI sites generated in the coding regions of pRS314CUP-FKBD and pRS314CUP-TWD1 (64 bp) using the QuikChange XL site-directed mutagenesis kit (Stratagene). In this way, rLuc was inserted into the very N terminus of TWD1. Single colonies co-expressing PGP1-YFP (20) and TWD1-rLuc were grown in selective synthetic minimal medium (SD-UT) in the presence of inhibitors or adequate amounts of solvents. 200 ml of overnight cultures were harvested at $A_{600} = 1$ by centrifugation for 10 min at 1500 × *g* and washed two times with ice-cold milliQ water. The resulting pellet was suspended in 4 ml of ice-cold lysis buffer (50 mM Tris, 750 mM NaCl, 10 mM EDTA) supplemented with proteases inhibitors (Complete tablets, Roche Diagnostics) and an equivalent volume of acid-washed glass beads (inner diameter, 0.5 mm, Biospec Products Inc.) was added. Cells were broken by vortexing 10 times for 1 min, with 1-min intervals on ice for cooling. The supernatant was decanted, and the beads were washed four times with 10 ml of ice-cold lysis buffer. Supernatants were centrifuged at 4,500 × *g* (S1) and 12,000 × *g* (S2) for 10 min at 4 °C to remove unbroken cells and other debris. Membranes were collected by centrifugation at 100,000 × *g* (P3) for 1 h at 4 °C. The membrane pellet was homogenized using a pestle in 300 μl of ice-cold STED10 buffer (10% sucrose, 50 mM Tris, 1 mM EDTA, 1 mM dithiothreitol) supplemented with proteases inhibitors to give a suspension of about 3 mg of proteins/ml as measured using the Bradford assay (Bio-Rad). All preparations were stored at −80 °C for subsequent use. *In vitro* measurement of the BRET signal was performed using 200 μl of yeast membrane suspension (~600 μg of proteins) in a white 96-well microplate (OptiPlate-96, PerkinElmer Life Sciences). 5 μM coelenterazine (Biotium Inc.) was added, and sequential light emission acquisition in the 410 ± 80 nm and 515 ± 30 nm windows was started after 1 min using the Fusion microplate analyzer (PMT = 1100 V, gain = 1, reading time = 1 s; PerkinElmer Life Sciences). BRET ratios were calculated as described (39) as follows: [(emission at 515 ± 30 nm) − (emission at 410 ± 80 nm) × C_f]/(emission at 410 ± 80 nm), where C_f corresponds to (emission at 515 ± 30 nm)/(emission at 410 ± 80 nm) for the rLuc fusion protein expressed alone in the same experimental conditions. The results are the average of 10 readings collected every minute; presented are average values from 6–10 independent experiments with four replicates each.

Yeast Auxin Transport Assays—IAA transport experiments were performed as in (20). In short, *S. cerevisiae* strains JK93dα (37) were grown as described above, loaded with [^{3}H]-IAA (20 Ci/mmol; American Radiolabeled Chemicals Inc.) for 20 min on ice, washed twice with cold water, and resuspended in 15 ml of SD, pH 5.5. 0.5 ml-aliquots were filtered prior to $t = 0$ min

Downloaded from www.jbc.org at SMAC Consortium - University of Zürich on August 6, 2008

and after 10 min were incubated at 30 °C. PGP1-mediated IAA export is expressed as relative retention of initial (maximal) loading ($t = 0$ min), which is set to 100%. Presented are average values from 6–8 independent experiments with four replicates each.

Drug Binding Assays—Whole yeast NPA binding assays were performed essentially as described previously (26). 10 ml of yeast cultures were grown as described above to an A_{600} of 1, and cells were resuspended in 10 ml of SD, pH 4.5. To 1-ml aliquots (for each experiment four replicates were used) 10 nM [^{3}H]NPA (60 Ci/mmol) and 10 nM [^{14}C]benzoic acid (BA, 58 mCi/mmol; all from American Radiolabeled Chemicals Inc.) were added in the presence and absence of 10 μM NPA (±10 μM BA for competition experiments; 1000-fold excess). Cells were incubated for 1 h at 4 °C under shaking and washed with ice-cold MilliQ water, and the tips of centrifuge tubes including pellets were subjected to scintillation counting. Reported values are the means of specific binding ([^{3}H]NPA bound in the absence of cold NPA (total) minus [^{3}H]NPA bound in the presence of cold NPA (unspecific)) from 4–8 independent experiments with four replicates each.

For PPIase Affi-Gel pulldown assays, 2 mg of the PPIase domain/FKBD of TWD11–180 expressed in *Escherichia coli* and purified as described previously (40) was coupled to 2 ml of Affi-Gel-15 beads (Bio-Rad). 50 μl of Affi-Gel-PPIase or empty Affi-Gel beads (50% slurry) was resuspended in 450 μl of phosphate-buffered saline, pH 7.4, and 5 μl of radiolabeled [7-^{14}C]BA (58 mCi/mmol, 0.1 mCi/ml) and [^{3}H]NPA (60 Ci/mmol, 1 mCi/ml; all from American Radiolabeled Chemicals Inc.), diluted 20× in phosphate-buffered saline was added to four replications of each. After shaking for 1 h at 4 °C, the beads were filtered on nitrocellulose, and the filters washed three times with cold MilliQ water and finally subjected to scintillation counting. Reported values are the means of specific binding ([^{3}H]NPA bound to Affi-Gel-PPIase minus [^{3}H]NPA bound to empty Affi-Gel beads) per 1 μg of coupled protein as measured using the Bradford assay (Bio-Rad). Presented are average values from 4–8 independent experiments with four replicates each.

For microsomes of *Arabidopsis* NPA binding assays, *Arabidopsis* seedlings were grown in liquid cultures, and microsomes were prepared as described elsewhere (34). Four replicates of each 20 μg ($Pro_{CaMV35S}$-TWD1-HA) or 100 μg of protein (wild-type and *twd1*) in STED10 were incubated with 10 nM [^{3}H]NPA (60 Ci/mmol) and 10 nM [^{14}C]BA (58 mCi/mmol) in the presence and absence of 10 μM NPA (±10 μM BA for competition experiments; 1000-fold excess). After 1 h at 4 °C under shaking, membranes were filtered over nitrocellulose filters (MF 0.45 μm, Millipore) and washed three times with cold MilliQ water, and filters were subjected to scintillation counting. Reported values are the means of specific binding ([^{3}H]NPA bound in the absence of cold NPA (total) minus [^{3}H]NPA bound in the presence of cold NPA (unspecific)) from three independent experiments with four replicates each.

Plant Growth Conditions and Quantitative Analysis of Root Gravitropism—*Arabidopsis thaliana* plants were grown as described previously (30). For quantification of gravitropism in the presence of light (Fig. 5*A*, supplemental Fig. S6*A*), wild type, *pgp1* (At2g36910) and *pgp19* (At3g28860), and *pgp1/pgp19* and *twd1* (At3g21640) mutants (all ecotype Wassilewskija (Ws Wt)), seeds were surface sterilized and grown on 0.5× Murashige and Skoog medium, 0.7% phytoagar (Invitrogen) under continuous light conditions in the presence or absence of 5 μM NPA as described previously (20). The angle of root tips from the vertical plane was determined using Photoshop 7.0. (Adobe Systems, Mountain View, CA), and each gravistimulated root was assigned to one of twelve 30° sectors in the circular histograms; the length of each bar represents the percentage of seedlings showing the same direction of root growth. (Figs. 5 and 6, supplemental Fig. S6). Helical wheels were plotted using PolarBar software.

For quantification of root bending rates (Figs. 5*B* and 6, supplemental Fig. S6*B*), 5 dag seedlings, grown vertically on 0.5× strength Murashige and Skoog medium, 0.7% agar, 1% sucrose were transferred for an additional 12 h onto new plates containing 5 μM NPA or the solvent DMSO. Plates were rotated 90° from the vertical for 7–12 h of gravity stimulation in the dark. The angle of root tips from the vertical plane (root curvature) was determined using Photoshop 7.0. (Adobe Systems), and the rate of curvature was calculated as first derivative of root curvature. The number of seedlings for each genotype was between 72 and 96.

Analysis of IAA Responses—Homozygous T4 generations (20) of *A. thaliana* wild-type (ecotypes Ws and Columbia (Col)), *pgp1*, *pgp19*, *pgp1/pgp19*, and *twd1* mutants (all in Ws Wt) expressing the maximal auxin-inducible reporter Pro_{DR5}-GFP (41) were grown vertically for 5 days as described above and analyzed by confocal laser scanning microscopy (Leica, DMIRE2) equipped with an argon laser (488 nm). In some cases, seedlings were transferred for an additional 12 h onto new plates containing 5 μM NPA or the solvent DMSO and gravistimulated for 2 h by turning the plates 90°. For histological signal localization, differential interference contrast and GFP images were merged electronically using Photoshop 7.0 (Adobe Systems).

Recording of Root Apex Auxin Fluxes Using an IAA-specific Microelectrode—A platinum microelectrode was used to monitor IAA fluxes in *Arabidopsis* roots as described previously (20, 42). For measurements, plants were grown in hydroponic cultures and used at 5 days after germination. Differential current from an IAA-selective microelectrode placed 2 μm from the root surface was recorded in the absence and presence of 5 μM NPA. Relative NPA inhibition was calculated by dividing peak influx values (at 200 nm from the root tip) in the absence of NPA by those in the presence.

Data Analysis—Data were analyzed using Prism 4.0b (GraphPad Software, San Diego, CA), and statistical analysis was performed using SPSS 11.0 (SPSS Inc., Chicago). FKBD structure alignment was performed using PyMol 0.99.

RESULTS

Establishment of a Yeast-based PGP1-TWD1 BRET System—Despite the fact that FKBPs are well known subunits and modulators of multiprotein complexes (20, 37, 43), ABC transporter regulation by FKBPs has been reported only for murine MDR3 and *Arabidopsis* PGP1 (20, 30, 34, 37). On the other hand, the

Downloaded from www.jbc.org at SMAC Consortium - University of Zürich on August 6, 2008

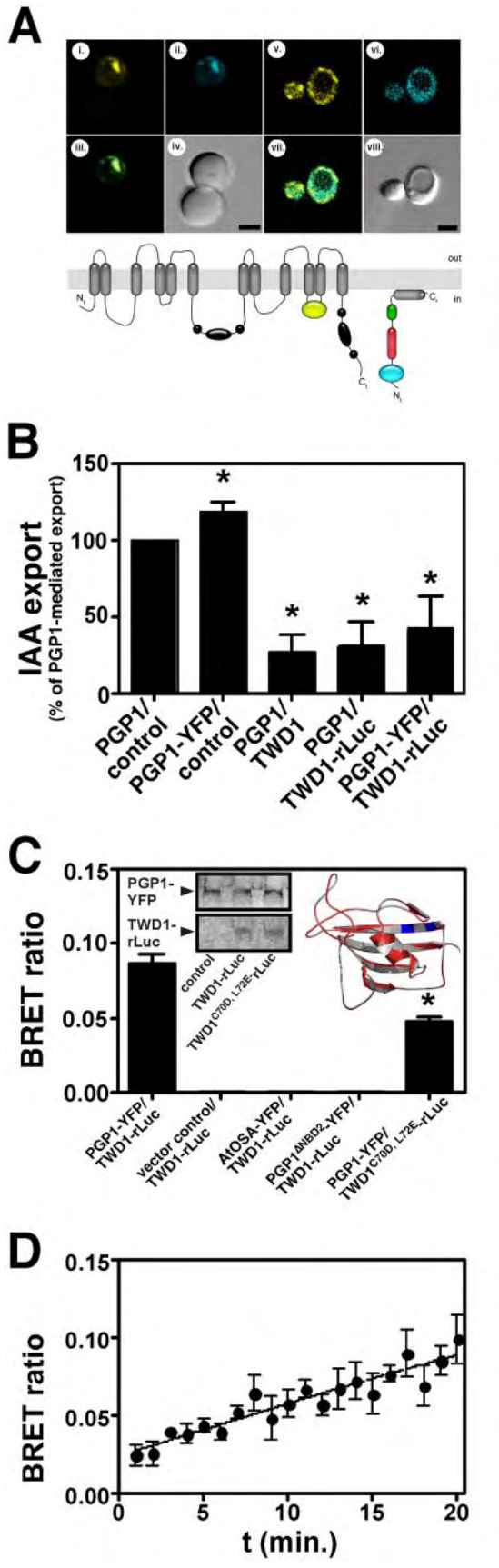

FIGURE 1. **A yeast-based BRET system of TWD1-PGP1 interaction.** *A*, co-localization of PGP1-YFP (*yellow*) and TWD1-CFP (*blue*) in yeast (*upper panels*). The model illustrates PGP1-YFP and TWD1-rLuc interactions resulting in BRET (*lower panels*). *Black*, NBDs; *yellow*, YFP; *red*, FKBD; *green*, tetratricopetide repeat; *blue*, rLuc. The perpendicular orientation of the TWD1 C terminus, forming a so-called amphipatic in-plane membrane anchor, is based on the findings of Scheidt *et al.* (33). *B*, PGP1-YFP and TWD1-rLuc are active. PGP1-YFP exports IAA comparably to native PGP1 (set to 100%), and co-expression of TWD1-rLuc reduces PGP1-mediated IAA efflux to a similar extent as wild type TWD1. Reductions in auxin retention (efflux) were calculated as relative export of initial loading. Data are the means ± S.E. ($n = 4$); means significantly different from native PGP1 control (unpaired *t* test with Welch's correction, $p < 0.05$) are marked by an *asterisk*. *C*, PGP1-YFP-TWD1-rLuc interaction quantified by BRET is specific. PGP1-YFP and TWD1-rLuc were co-expressed in yeast, sequential light emission acquisition on microsomes in 410 ± 80 nm and 515 ± 30 nm windows was quantified, and BRET ratios were calculated as in Angers *et al.* (39). *Inset*, Western detection of PGP1/TWD1 on yeast microsomes (*left*) and structure comparison of native (*red*) and computed TWD1-rLuc$^{C70D,\ L72E}$ (*gray*) (exchanges shown in *blue*) FKBDs (*right*). Data are means ± S.E. ($n = 5$–10); means significantly different from PGP1-YFP/TWD1-rLuc control (unpaired *t* test with Welch's correction, $p < 0.05$) are marked by an *asterisk*. *D*, PGP1-YFP/TWD1-rLuc interaction determined by BRET is stable over time. Presented are means ± S.E. from 6–10 independent experiments with four replicates each.

mechanisms by which NPA or flavonoids interfere with auxin efflux complex components, and hence with PAT (7–9), are not clear (1, 3, 5, 36).

Therefore, and in order to analyze PGP1-TWD1 interaction and its impact on cellular auxin efflux at the molecular level, we established a yeast-based BRET assay by co-expressing TWD1 and PGP1 fused to bioluminescence donor rLuc and acceptor fluorophore YFP, respectively (Fig. 1*A*). In short, BRET is a naturally occurring phenomenon based on the Förster resonance energy transfer between a light-emitting luciferase and an acceptor fluorophore and occurs when the donor and acceptor are below 100 Å apart (44). It has been shown to be independent from substrate concentration and has been validated by its usage in yeast (45) and other cells (39). In summary, BRET offers the advantages of FRET but avoids the drawbacks of fluorescence excitation like photobleaching and direct excitation of the acceptor fluorophore (44).

PGP1-YFP and TWD1-rLuc fusion proteins are functional as shown by analysis of IAA export upon co-expression and PGP1-YFP mediated detoxification of auxin analogs in yeast (Fig. 1*B*, supplemental Fig. S1). Moreover, TWD1-rLuc inhibited PGP1- or PGP1-YFP-mediated auxin efflux to the native TWD1 level. As shown previously, TWD1 has in yeast, unlike in mammalian and plant cells, an inhibitory effect on PGP1 export activity (20, 46). As discussed in detail below (see "Discussion"), the difference might be due to the lack of higher eukaryote components in yeast, the lower abundance of TWD1 *in planta*, or competition of TWD1 with yeast FKBP12 for activation of PGP1.

PGP1-YFP and TWD1-rLuc co-localize on the plasma membrane and small plasma membrane-attached vesicles (Fig. 1, *A* and *C* (20)) and co-expression results in a stable, highly reproducible BRET signal (Fig. 1*C*), which was quantified as a ratio of the light emitted by PGP1-YFP over that emitted by TWD1-rLuc (BRET ratio (39)). This BRET signal was specific because, first, no BRET was observed in the absence of PGP1-YFP (Fig. 1*C*) or with PGP1 minus YFP (not shown) or AtOSA-YFP, an unrelated protein kinase that co-localized with TWD1-CFP (Fig. 1*A*). Second, deletion of the interacting C terminus of PGP1-YFP containing the second nucleotide-binding domain (NBD) (PGP1$^{\Delta NBD2}$-YFP) abolished BRET entirely. And third,

Downloaded from www.jbc.org at SMAC Consortium - University of Zürich on August 6, 2008

introduction of two point mutations in the β_2 sheet of the TWD1 FKBD (47) (TWD1$^{C70D,\ L72E}$-rLuc), which apparently does not significantly affect the overall FKBD structure and PGP1-YFP expression (Fig. 1*C*, *inset*), reduced BRET significantly (46% reduction; Fig. 1*C*).

Moreover, the specificity of interaction was further validated by the fact that a soluble FKBD-rLuc was specifically retained by PGP1- but not by the related auxin importer, PGP4- (23), or vector control membranes, and a soluble FKBD-rLuc restored BRET when added to PGP1-YFP membranes (supplemental Fig. S2).[4] Together, these results unambiguously demonstrate that PGP1 and TWD1 are compatible partners in yeast and that BRET was specific.

Identification of Drugs That Alter PGP1-TWD1 Interaction Using BRET—BRET signal stability and linearity over time (Fig. 1*D*) allowed us to screen a mini-library of putative ATIs for drugs that were able to alter PGP1-TWD1 interaction. The synthetic ATI, NPA, (4, 10–12) has been shown to bind to *Arabidopsis* PGPs employing whole yeast assays and NPA affinity chromatography (25, 26, 30).

NPA reduced BRET by about 50%, thus disrupting PGP1-TWD1 interaction (Fig. 2*A*). This verifies previous *in planta* data where an excess of NPA was shown to exclude TWD1 from PGP-positive NPA chromatography fractions (30). Not unexpectedly, the ATIs 2,3,5-triiodobenzoic acid (TIBA) and 2-carboxylphenyl-3-phenylpropan-1,3-dione (CPD), known to employ a different locus and mode of action than NPA (17, 48), respectively, did not alter BRET significantly.

Next, we tested representative flavonoids that are known inhibitors of PAT on one hand and of plant (20, 21, 24) and mammalian PGPs (2) on the other. Interestingly, the flavonol quercetin abolished BRET efficiently with an apparent IC_{50} of ~200 nM (Fig. 2*B*). With the exception of the flavonoid precursor chalcone, all flavonoids tested disrupted PGP1-TWD1 interaction but were less efficient than quercetin. Interestingly, quercetin-3-*O*-glucoside and kaempferol-3-*O*-glucoside, the most common *Arabidopsis* flavonol glycoside derivates (5, 13), were as effective as their aglycones in disrupting PGP1-TWD1 interaction. In summary, our data indicate that NPA and flavonoids disrupt TWD1-PGP1 interaction with quercetin being the most efficient.

TWD1 Confers Drug Modulation of PGP1 Efflux Activity—With the intention of investigating the physiological impact of these drugs, we quantified PGP1-mediated IAA transport in the presence of TWD1 in yeast. As shown previously (20, 46) and discussed above and under "Discussion," TWD1 has in yeast, unlike in mammalian and plant cells, an inhibitory effect on PGP1 export activity. NPA and the flavonols quercetin and kaempferol, shown to efficiently disrupt PGP1-TWD1 interaction as monitored by BRET (Fig. 3*A*), therefore, as expected reverted TWD1-mediated inhibition of IAA export catalyzed by PGP1. This resulted in an enhanced IAA export, which is in agreement with a dissociation and hence an activation of the PGP-TWD1 transport complex in yeast. 2,3,5-Triiodobenzoic acid, which is not a representative ATI (48) and which had no

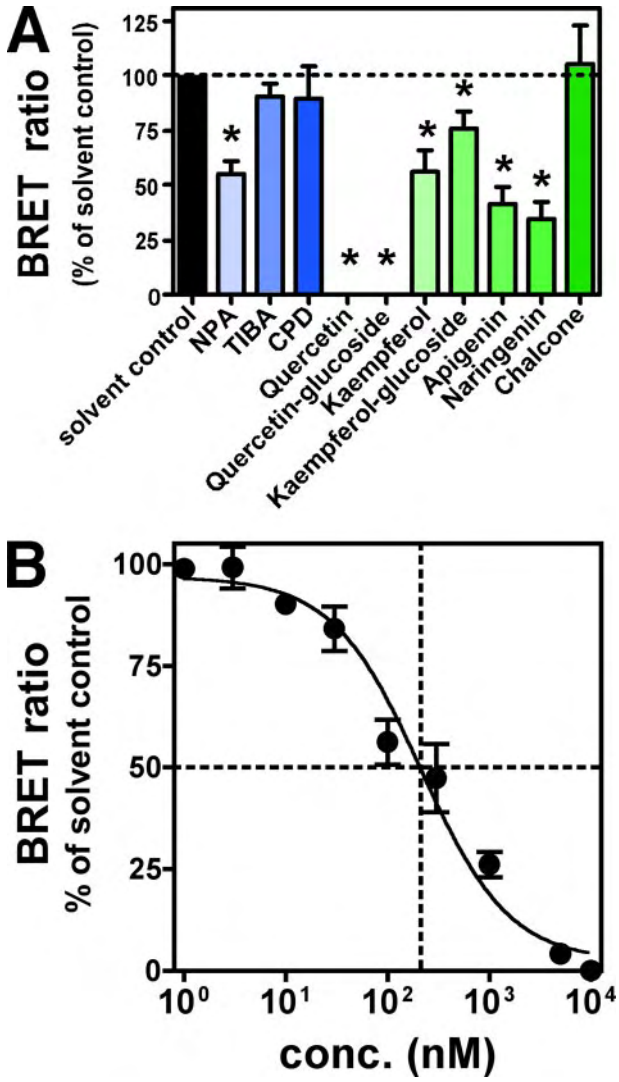

FIGURE 2. **TWD1-PGP1 interaction is disrupted by auxin transport inhibitors.** *A*, PGP1-YFP-TWD1-rLuc interaction quantified by BRET is disrupted by ATI NPA and flavonoids (10 μM). Data are means ± S.E. (n = 6–10); means significantly different from solvent control (unpaired t test with Welch's correction, $p < 0.05$) are marked by an *asterisk*. *B*, dose dependence of complex disruption by the flavonol quercetin. PGP1-YFP and TWD1-rLuc were co-expressed in yeast, sequential light emission acquisition on microsomes in 410 ± 80 nm and 515 ± 30 nm windows was quantified, and BRET ratios were calculated as in Angers *et al.* (39). Presented are the means of BRET ratios ± S.E. (n = 6–10).

significant effect on the TWD1-PGP1 complex (Fig. 2*A*), did not alter IAA transport (Fig. 2*A*).

This modulatory effect was dependent on TWD1 because drug treatments in the absence of TWD1 had no stimulating and only mildly inhibitory effects (Fig. 3*A*) as reported recently (20, 21). Indirect effects, like mistargeting or altered PGP1 expression caused by drug treatments, were excluded by co-immunolocalization (supplemental Fig. S3) and Western blotting analysis (results not shown) of yeast co-expressing TWD1-CFP and PGP1-YFP.

Point mutations in the FKBD, bisecting the PGP1-TWD1 interaction (Fig. 1*C*), completely abolished transduction of the regulatory effects of quercetin on PGP1 activity (Fig. 3*B*). Moreover, the soluble FKBD of TWD1 alone was sufficient to functionally substitute full-length TWD1 in both PGP1 repression

[4] Direct measurement of PGP1-YFP/FKBD-rLuc BRET was not possible because of the high FKBD-rLuc expression and its strong light emission.

Downloaded from www.jbc.org at SMAC Consortium - University of Zürich on August 6, 2008

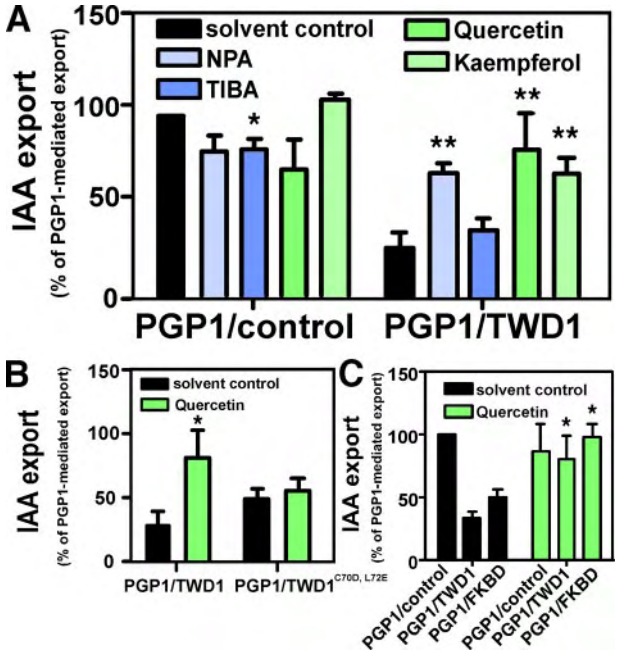

FIGURE 3. **TWD1 confers ATI modulation of PGP1-mediated auxin efflux activity.** *A*, effect of TWD1 on PGP1-mediated IAA export (20) assayed in the presence of auxin transport inhibitors. Data are means ± S.E. ($n = 4–6$). Reductions in auxin retention (efflux) were determined as relative retention of initial loading; PGP1-mediated IAA export was set to 100%. Data are means ± S.E. ($n = 4–6$). *Single asterisks*, significantly different from PGP-mediated IAA transport; *double asterisks*, significantly different from PGP/TWD1-mediated IAA transport. (unpaired *t* test with Welch's correction, $p < 0.05$). *TIBA*, 2,3,5-triiodobenzoic acid . *B*, two point mutations in TWD1-rLuc$^{C70D, L72E}$ abolish the modulatory effect of quercetin on PGP1 activity. Data are means ± S.E. ($n = 4–6$). Reductions in auxin retention (efflux) were determined as relative retention of initial loading; PGP1-mediated IAA export was set to 100%. Data are means ± S.E. ($n = 4–6$); means significantly different from solvent control (unpaired *t* test with Welch's correction, $p < 0.05$) are marked by *asterisks*. *C*, the FKBD of TWD1 is responsible for PGP1 regulation. Co-expression of the soluble FKBD of TWD1 reduces PGP1-mediated IAA efflux to a similar extent as membrane-bound, full-length TWD1. Quercetin (10 μM) disrupts the inhibitory effect of TWD1 and FKBD on PGP1 activity. Data are means ± S.E. ($n = 4–6$); means significantly different from solvent control (unpaired *t* test with Welch's correction, $p < 0.05$) are marked by an *asterisk*.

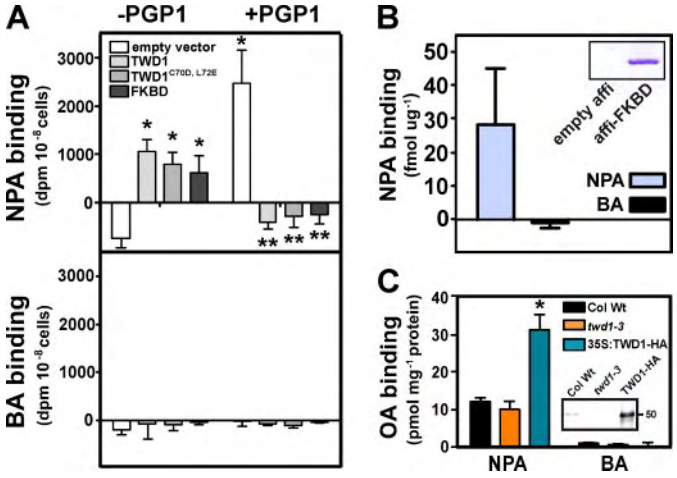

FIGURE 4. **PGP1 and TWD1, but not the PGP1-TWD1 complex, bind NPA.** *A*, binding assays of whole yeast expressing TWD1 and PGP1 assay NPA and BA in parallel. Reported values are means ± S.E. of specific binding from 4–8 independent experiments with four replicates each. *, significantly different from empty vector control; **, significantly different from PGP1 control (unpaired *t* test with Welch's correction, $p < 0.05$). *B*, NPA binding assay using purified Affi-Gel-coupled TWD1 FKBD (PPIase Affi-Gel pulldown assays). Reported values are means of specific binding ± S.E. ($n = 4–6$). *Inset*, Coomassie stain of coupled FKBD. *C*, binding of organic acids (*OA*), NPA and BA (to microsomal fractions of *twd1* and Pro$_{CaMV35S}$-TWD1-HA *35S*.TWD1-HA). Data are means of specific binding ± S.E. ($n = 4$). *Inset*, Western detection of TWD1 from microsomes (each 10 μg of protein). Data are means ± S.E. ($n = 4$); means significantly different from wild type (Col Wt) control (unpaired *t* test with Welch's correction, $p < 0.05$) are marked by an *asterisk*.

and quercetin-mediated reversal of PGP1 activity (Fig. 3*C*). These results taken together indicate that TWD1 functions as an associated modulator of PGP1-mediated auxin transport by mediating the regulatory impact of ATIs via its FKBD.

NPA Binding to PGP1 and TWD1 Is Abolished in the PGP1-TWD1 Complex—NPA was shown to inhibit and bind to PGPs (20, 21); however, an excess of NPA was shown to exclude TWD1 from PGP-positive NPA chromatography fractions (30). To test the hypothesis that TWD1 competes for NPA binding on PGP1, we quantified the binding of radiolabeled NPA using established whole yeast assays (26). NPA binding was specific, as it was outcompeted by an excess of NPA (see "Experimental Procedures") but was not displaced by benzoic acid (not shown). Moreover, whole yeast NPA binding assays (WYNBA) are independent from transport events (supplemental Fig. S4).

PGP1-expressing yeast specifically bound NPA (Fig. 4*A*) as was shown previously for the close homolog PGP19 (26). Surprisingly, a lesser but significant NPA binding was also observed for yeast expressing TWD1 or its FKBD (Fig. 4*A*). NPA binding was specific, as neither PGP1 nor TWD1 bound the organic acid BA, commonly used as a negative control in auxin research. Indirect effects, like TWD1-induced NPA binding to yeast endogenous proteins, were excluded by demonstrating NPA binding to highly purified Affi-Gel-immobilized FKBD (Fig. 4*B*), which was used for crystallization studies (47). In agreement, NPA binding was strongly enhanced in microsomal fractions prepared from *TWD1* gain-of-function plants (Pro$_{CaMV35S}$-TWD1-HA; Fig. 4*C*) compared with wild type. *twd1* microsomes showed reduced but not significant differences in NPA binding compared with wild type, most probably because of the low expression level of *TWD1* (Fig. 4*C*, *inset*) (20, 30).

However, co-expression of PGP1 with TWD1 abolished NPA binding to PGP1 and TWD1 (Fig. 4) but did not significantly alter the expression level of the two proteins (Fig. 1*B*), suggesting that the PGP1-TWD1 (FKBD) complex has a lower affinity for NPA or that binding pockets were simply masked. Again, in analogy to auxin transport assays, co-expression of the FKBD eliminated NPA binding to PGP1, indicating that the N-terminal FKBD was sufficient to perform TWD1 function.

TWD1 Mediates Drug Modulation of P-glycoproteins in Vivo—To test our conclusions derived from the yeast model and to substantiate the physiological relevance of the proposed TWD1 function *in planta*, we investigated NPA sensitivity of *twd1* roots in comparison with those of *pgp* plants using three different assays.

First, we quantified the gravitropic responses, a hallmark of auxin-controlled physiological responses, of *twd1* and *pgp* roots in the presence of NPA, known to disrupt gravitropism in the wild type (49). Performing root gravitropism assays in the presence and absence of light (see "Experimental Procedures")

Downloaded from www.jbc.org at SMAC Consortium - University of Zürich on August 6, 2008

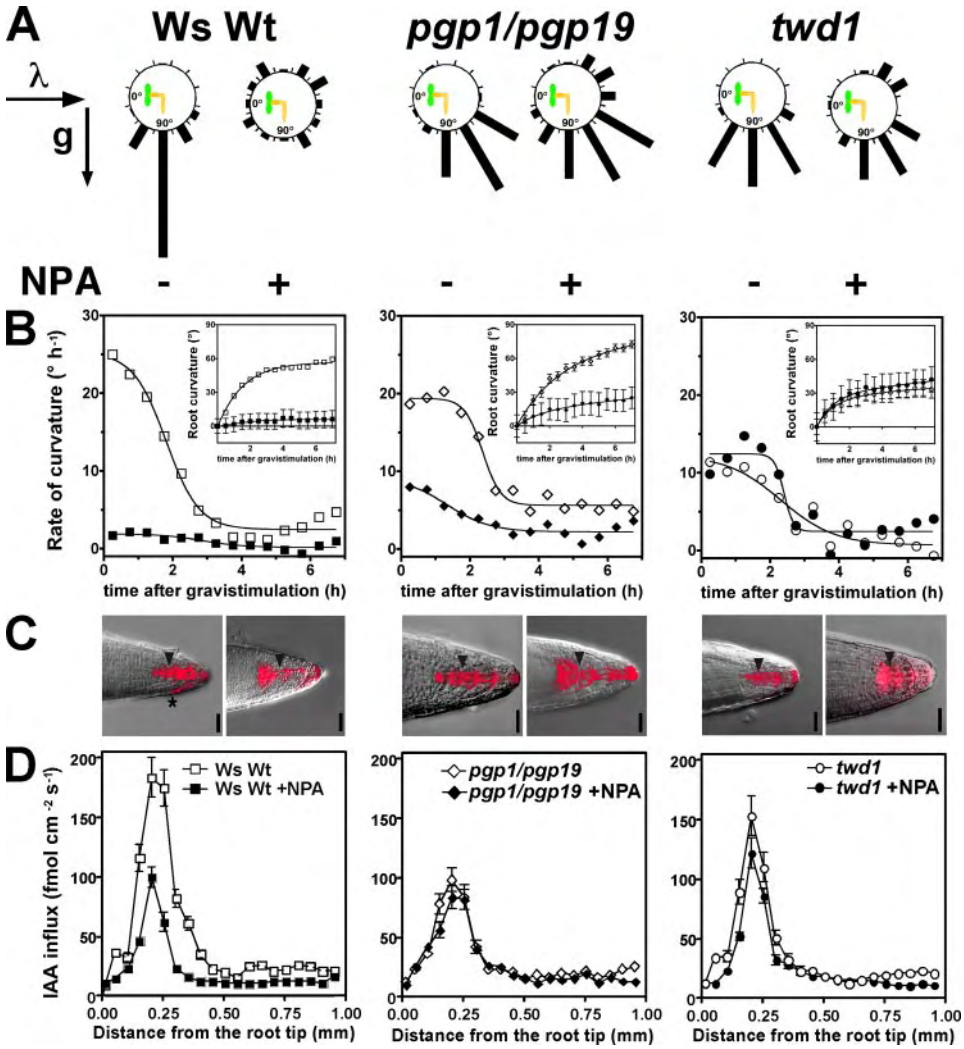

FIGURE 5. **twd1 roots are less sensitive to the auxin transport inhibitor NPA.** *A* and *B*, NPA disrupts gravitropic responses in wild type and, to a lesser extent, in *twd1* roots. Root curvature of *twd1* and *pgp1/pgp19* alleles in comparison with wild type (*Ws Wt*). Seedlings were either grown under continuous light (*A*) as described by Bouchard *et al.* (20) or in the dark (*B*) (see "Experimental Procedures"). Root curvatures were assigned to one of twelve 30° sectors in the *circular histograms*; the length of each *bar* represents the percentage of seedlings showing the same direction of root growth. Data are means ± S.E. ($n = 3$ with each 72–96 seedlings). Shown in *B* is the rate of curvature calculated as first derivative of root curvature (*insets*), with the same description as in *D*. *Arrows* in *A* indicate the direction of light (λ) and gravitropism (*g*). *C*, expression of the auxin-responsive reporter Pro_{DR5}-GFP (20), shown in *red*, upon gravistimulation (from the top). Note that asymmetric auxin accumulation is more pronounced in the commonly used Columbia than in the Wassilewskija ecotype (Fig. S5). *Scale bars*, 200 μm. *D*, IAA influx profile along wild type, *pgp1/pgp19*, and *twd1* roots measured using an IAA-specific microelectrode (20, 23, 42); positive fluxes represent a net IAA influx. Data are means ± S.E. ($n = 6–8$).

revealed that NPA affected *pgp1* and *pgp19* root gravitropism to a similar extent as in the wild type (supplemental Fig. S6). Of special interest was a comparison of *twd1* and *pgp1/pgp19* plants because, based on interaction and transport studies, TWD1 has been proposed to function as a positive modulator of PGP1 and PGP19 auxin transport activities (20, 29, 30, 46). This biochemical evidence is supported by widely overlapping mutant phenotypes (20, 29, 30, 46). Compared with the single *pgp* mutants (supplemental Fig. S6), *pgp1/pgp19* roots were less inhibited by NPA, which was most obvious during the initial, first 3 h of bending (Fig. 5*B*). As shown previously (20, 30), *twd1* showed a more variable and reduced curvature rates compared with the wild type and *pgp* mutants. Interestingly, *twd1* roots were only slightly affected by NPA treatment compared with the solvent control, which is most obvious in the early rates (<3 h) of root curvature (Fig. 5*B*), which were calculated as the first derivative of root curvatures (Fig. 5*B*, *insets*).

Second, asymmetric auxin accumulation along the lower side of the root tip, the primary cause of root bending, was monitored by expression of the auxin-responsive reporter construct Pro_{DR5}-GFP (20, 41) upon gravistimulation. Compared with wild type, basipetal reflux was reduced in *pgp1* but was abolished in *pgp19* (supplemental Fig. S6), *pgp1/pgp19 and twd1* roots (Fig. 3*B*), which is in line with the reported roles for PGP19 and to lesser extent for PGP1 in a coordinated basipetal re-export of auxin out of the root tip (21, 30, 36). However, NPA disrupted basipetal reflux and enhanced the DR5-GFP signal in the quiescent center, the columella initials, the S1 cells in wild type (41), *pgp1*, *pgp19* (supplemental Fig. S6), and *pgp1*/*pgp19* but not in *twd1* roots, which showed instead a faint, diffuse columella DR5-GFP signal (Fig. 5*B*).

Third, we employed an IAA-specific microelectrode that is able to noninvasively record IAA influxes into the root transition zone (20, 23, 42). IAA influx in this zone is characterized by a distinct peak at ~200 μm from the root tip and is consistent with the current auxin "reflux model" (53). *Pgp1*, *pgp19* (supplemental Fig. S6), *pgp1*/*pgp19*, and *twd1* showed reductions of IAA influx compared with wild type (Fig. 3*C* (20, 21)). In agreement with DR5-GFP imaging, relative NPA inhibition of IAA influx was significant in *pgp1* in comparison with wild type but low in *pgp19* and *pgp1/pgp19*. However, NPA had only a negligible inhibitory effect on IAA influx into *twd1* roots (relative inhibition: wild type ≫ *pgp1* > *pgp19* ≅ *pgp1/pgp19* > *twd1*).

To test the impact of TWD1 on PGP-mediated auxin transport in gain-of-function alleles, we measured gravitropic responses of $Pro_{CaMV35S}$-TWD1-HA roots (20). Plants overexpressing TWD1-HA (Fig. 4*C*) perform a more efficient and sharper root curvature compared with wild type and agravitope *twd1–3* (Fig. 6*A*). The kinetics of root bending and rates of curvature clearly indicate that $Pro_{CaMV35S}$-TWD1-HA roots initially bend faster (149%) than those of wild type, whereas *twd1* roots respond more slowly (15%) (Fig. 6*B*). Together,

Downloaded from www.jbc.org at SMAC Consortium - University of Zürich on August 6, 2008

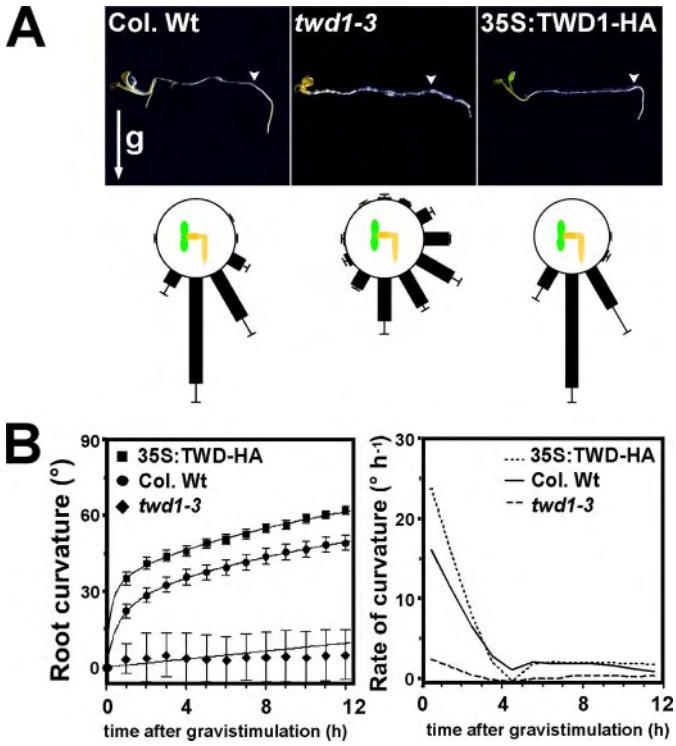

FIGURE 6. **Overexpression of *TWD1* promotes root gravitropism.** *A*, gravitropic root responses of *TWD1* loss- (*twd1–3*) and gain-of-function, $Pro_{CaMV35S}$-TWD1-HA (35S-TWD1-HA) alleles in comparison with wild type (*Col. Wt*). *Triangle* indicates direction of gravitropism (*g*); *triangles* mark time point of 90° plate rotation (*upper panel*). Root curvatures was assigned to one of twelve 30° sectors in the circular histograms; the length of each *bar* represents the percentage of seedlings showing the same direction of root growth. Data are means ± S.E. ($n = 3$ with each 72–96 seedlings). *B*, time series of root curvature (*left panel*) and rate of curvature calculated as first derivative of root curvature (*right panel*).

these data indicate that *TWD1* loss-of-function results in reduced sensitivities to NPA, whereas *TWD1* gain-of-function promotes root gravitropism and NPA binding.

DISCUSSION

Drug Modulation of P-glycoprotein Activity Is Conferred by FKBPs—Previous work has established a role for FKBP42 TWD1 as a positive regulator of PGP-mediated auxin efflux by means of protein-protein interaction (20, 29, 30, 46). Loss of positive regulation of PGP1- and PGP19-mediated auxin efflux activity on the cellular level blocks long range auxin transport *in planta* (20, 36). As a consequence, *PGP1* and *PGP19* single, and more strikingly, double loss-of-function alleles show elevated root auxin levels and defects in root gravitopism (20).

Here, by employing yeast-based, specific TWD1-rLuc/PGP1-YFP BRET and auxin transport systems, we have demonstrated functional disruption of TWD1-PGP1 interaction by NPA and flavonoids, synthetic and *bona fide* native auxin transport inhibitors, respectively. TWD1-PGP1 disruption by NPA is in line with previous findings demonstrating NPA binding to plant PGPs and inhibition of PGP-mediated auxin transport by NPA (20, 23, 24). In contrast to NPA, the ATIs 2,3,5-triiodobenzoic acid and 2-carboxylphenyl-3-phenylpropan-1,3-dione had no significant effect on the TWD1-PGP1 complex stability and auxin transport. This is not unexpected, as 2,3,5-triiodobenzoic acid is structurally unrelated and has been shown to displace NPA binding only partially and even to own weak auxin activity, suggesting a different locus and mode of action compared with NPA (48).

The flavonol quercetin (and its glucose conjugate), of the drugs tested, was the most capable of disrupting TWD1-PGP1. This is of interest because quercetin was the most efficient flavonoid in competing with NPA for auxin transporter binding sites (4). Further, nanomolar IC_{50} values are in agreement with the effective working concentrations of flavonols in blocking PAT (5).[5] Disruption of the TWD1-PGP1 complex by NPA and flavonols leads to activation of auxin transport by the TWD1-PGP1 complex (Figs. 2 and 3), which is reflected by reversal of TWD1-mediated inhibition of PGP1 auxin transport activity. This reversing, inhibitory effect on PGP1 activity in yeast is, as shown previously (20, 23, 24), the opposite of what has been found for mammalian and plant cells. This (reversing, inhibitory) effect or finding either reflects a lack of regulatory components in the lower eukaryotic system (22, 46) or is due to the higher abundance of TWD1 in yeast compared with plant (compare Fig. 1*C versus* Fig. 4*C*) and mammalian cells (20). Therefore, it has been speculated that the TWD1-PGP interaction is of a transient nature *in planta* (20). Alternatively, TWD1 might compete with endogenous yeast FKBP12 for PGP1 binding. scFKBP12 has been shown to activate *Arabidopsis* PGP1 (20) and murine MDR3 (37); assuming enhanced activation of PGP1 by ScFKBP12 but lower affinities to PGP1 compared with TWD1, PGP1-TWD1 co-expression would *de facto* result in an inhibition.

Despite this discrepancy, the disrupting effect of ATIs is in agreement with its proposed inhibitory role in PAT (14). Interestingly, and in opposition to what is seen *in planta,* the inhibitory effect of μM concentration of ATIs on PGP1 expressed alone in yeast is low (around 20–30%), whereas the reversing effect on the TWD1-PGP1 complex is far higher (Fig. 3).

Interaction, transport, and NPA binding studies suggest that the TWD1 FKBD provides the surface for PGP1-TWD1 interaction (21) and is responsible for PGP1 regulation (20, 46) but also confers drug-mediated regulation of PGP1. The soluble FKBD alone can fully complement the full-length, membrane-bound TWD1 in respect to both PGP1 regulation and drug binding and sensing. However, two amino acid exchanges that minimally affect the overall structure and only bisect the interaction (Fig. 1*C*) fully destroy the impact of quercetin on TWD1-PGP1 activity (Fig. 3*B*).

Based on specificity patterns, PGP as a common protein (or protein complex) that mediates hormone efflux as well as hormone action has been proposed (55). Indeed our data support a sensor-like function of TWD1 in PGP regulation by integrating the modulatory impact of flavonoids, the intracellular key signaling molecules of auxin transport and action (1, 7, 9). This concept is sustained by *in planta* data demonstrating reduced NPA sensitivities for TWD1 modulation of root gravitropism and PAT (Fig. 5). Moreover, TWD1 gain-of-function alleles show highly improved initial root-bending performance. These findings together suggest that TWD1 controls PGP-mediated gravisensing by ATIs.

[5] D. Santelia, S. Henrichs, V. Vincenzetti, M. Sauer, L. Bigler, M. Klein, A. Bailly, Y. Lee, J. Friml, M. Geisler, and E. Martinoia, manuscript in preparation.

Downloaded from www.jbc.org at SMAC Consortium - University of Zürich on August 6, 2008

TWD1 and PGP1 Are Key Components of the NPA-binding Auxin Efflux Complex—NPA binding to PGP1 and TWD1, shown by employing binding studies using either whole yeast, immobilized, highly purified FKBD protein or plant microsomes, respectively is in line with past and recent findings on the regulatory roles of NPA (and flavonoids) on auxin export (7, 10, 14). Until today the identity, number, and affinity of putative NBPs is still controversial (11, 16, 17, 56). But there is apparently a consensus that PIN-formed proteins (57), recently shown to interact functionally with PGPs in auxin transport (58), do not act as NBPs (10). However, our data are in agreement with the broadly accepted current concept that the efflux complex consists of at least two proteins, a transporter and an NPA-binding regulatory subunit (11, 12, 48). Binding to PGP1 (this work and Refs. 25 and 30) and PGP19 (25, 26, 30, 60) support the idea that P-glycoproteins represent the integral, membrane-embedded, NPA-binding proteins identified previously (15, 61). On the other hand, TWD1 might be the peripheral NPB described previously (16), which is in line with the recently proposed perpendicular orientation of the TWD1 C terminus forming a so-called amphipathic in-plane membrane anchor (33). However, this perception is also supported by the fact that the NBP has been suggested to be required for auxin efflux transporter positioning (62). Interestingly, a low-affinity NPA binding site has been associated with the transporter because its block results in transport inhibition, whereas the high-affinity site does not interfere directly with auxin transport (17). However, binding affinities for TWD1 from *Arabidopsis* total microsomes seem to be lower than found for the peripheral NBP from zucchini hypocotyls (16), which might reflect species- and/or tissue-dependent differences in binding affinities.

NPA binding to PGP1 and TWD1 is abolished in the yeast PGP1-TWD1 (FKBD) complex, suggesting that the FKBD apparently competes for NPA binding sites on PGP1. The fact that NPA binding to *pgp* (26, 60) and *twd1* microsomes (60) is reduced compared with the wild type suggests that NPA interrupts transient TWD1-PGP1 interaction *in planta* before they take place and argues against a tight complex as apparently found in yeast. However, individual functional domains on the FKBD are apparently independent, as TWD1$^{C70D,\ L72E}$-rLuc showed reduced affinities to PGP1 (Fig. 1*B*) but was fully capable of blocking NPA binding to PGP1 (Fig. 4*A*). Two more lines of evidence support the identity of more than one NBP: displacement of NPA from microsomes by flavonoids is biphasic (6), but in *Arabidopsis* the membrane-integral NPA-flavonoid interaction site was shown to be associated with PGP1, PGP2, and PGP19, whereas a weaker interaction site correlated with periperal membrane proteins TWD1 and aminopeptidase APM1 (25). Finally, our data provide a mechanistic explanation for the fact that an excess of NPA during washing steps leads to loss of TWD1 in NPA chromatographies (30). Although the exact role of two individual NBPs remains open (see below), our data provide good evidence that TWD1 and PGP1 represent the high- and low-affinity NPA binding sites, key components of the long sought after NBP auxin transport complex (15, 17, 25).

Flavonoid Modulation of P-glycoprotein-mediated Auxin Transport Conferred by TWD1—Our data highlight the functional importance of the PGP1-TWD1 complex but also support a novel mode of action for ATIs, namely the drug-mediated modulation of transport activity conferred by means of protein-protein interaction. In this scenario, plant endogenous or synthetic ATIs would compete with TWD1 for NPA binding sites on the PGP1 nucleotide binding folds, keeping the TWD1-PGP efflux complex in a dissociated, inactive state, thus allowing flexible fine modulation of activity. However, our data do not unambiguously clarify whether NPA and flavonols employ the same or adjacent, but functionally related, binding sites of a multifaceted ligand binding region (54).

Disruption and inhibition of the TWD1-PGP complex by flavonoids, as supported by our data, is an intriguing option supported by several findings. 1) Lesions in the genes encoding for PGP1 homologs result in reductions in long-distance transport of auxin and consequent dwarfism in mutant plants. These data together with tissue-specific accumulation of flavonols in *Arabidopsis* seedlings that coincide with regions of high auxin levels (5, 6) suggest that flavonols affect polar auxin transport in apical tissues by modulating auxin loading into the long-distance auxin stream (5). Moreover, genetic evidence that flavonoids generally act on PGPs transporting auxin is provided by the epistatic relationship of *pgp4* (*mdr4*, *abcb4*) to the *tt4* phenylpropanoid pathway mutation (36). 2) Aglycone flavonols were localized in a developmentally and tissue-specific manner in the plasma membrane (13, 50) of tissues that strongly overlap with *PGP1* and *PGP19* expression (30, 58). Accordingly, flavonol glucoside contents are drastically altered in *twd1* and *pgp1/pgp19* mutants (results not shown).

Agronomic and Clinical Implications of Drug-mediated ABC Transporter Modulation via Immunophilins—Loss-of *PGP1* gene function has been shown to increase stem diameter in the agriculturally important *brachytic2* and *dwarf3* mutants in maize and sorghum (51). Our yeast-based BRET system will allow rapid and sensitive chemical genetic screens to be performed to identify novel growth promoters or inhibitors that influence plant development and thus plant productivity (agrochemicals) in efforts to confer structural stability to crops.

Moreover, two findings imply that this novel mode of ABC transporter regulation via sensor-like immunophilins might be of interest beyond the plant field. Flavonoids have, as in plants, a modulatory impact on mammalian PGP activity and thus on MDR (27, 52), but the data support both inhibitory and stimulating effects (52). Our findings that inhibitory flavonoid modulation is conferred by interacting FKBPs might explain the conflicting results of flavonoid action, which might be due to tissue-specific immunophilin-PGP complex formation. Moreover, the mammalian TWD1 homolog, FKBP38, is localized to the outer membrane of mitochondria where it helps to anchor the anti-apoptosis proteins Bcl-2 and Bcl-xL (59). Taken together, membrane-anchored FKBPs and their interactive partners might be a promising target for genetic or chemical manipulation for new drug development and disease treatments.

Downloaded from www.jbc.org at SMAC Consortium - University of Zürich on August 6, 2008

Acknowledgments—We thank Aileen Funke for help with protein purification, Christian Fankhauser for assistance during gravity assays, Sina Henrichs and Shaun Peters for critical comments on the manuscript, Bo Burla for PolarBar software, and Michal Jasinski for the donation of yeast expression plasmid pNEV-AtOSA-YFP (At5g64940). Special thanks go to Rainer Hertel for sharing timely historical information and encouraging discussions.

REFERENCES

1. Taylor, L. P., and Grotewold, E. (2005) *Curr. Opin. Plant Biol.* **8,** 317–323
2. Morris, M. E., and Zhang, S. (2006) *Life Sci.* **78,** 2116–2130
3. Brown, D. E., Rashotte, A. M., Murphy, A. S., Normanly, J., Tague, B. W., Peer, W. A., Taiz, L., and Muday, G. K. (2001) *Plant Physiol.* **126,** 524–535
4. Jacobs, M., and Rubery, P. H. (1988) *Science* **241,** 346–349
5. Peer, W. A., Bandyopadhyay, A., Blakeslee, J. J., Makam, S. N., Chen, R. J., Masson, P. H., and Murphy, A. S. (2004) *Plant Cell* **16,** 1898–1911
6. Murphy, A., Peer, W. A., and Taiz, L. (2000) *Planta* **211,** 315–324
7. Blakeslee, J. J., Peer, W. A., and Murphy, A. S. (2005) *Curr. Opin. Plant Biol.* **8,** 494–500
8. Kerr, I. D., and Bennett, M. J. (2007) *Biochem. J.* **401,** 613–622
9. Vieten, A., Sauer, M., Brewer, P. B., and Friml, J. (2007) *Trends Plant Sci.* **12,** 160–168
10. Lomax, T. L., Muday, G. K., and Rubery, P. H. (1995) in *Plant Hormones: Physiology, Biochemistry and Molecular Biology* (Davies, P. J., ed) pp. 509–530, Kluwer, Dordrecht, Netherlands
11. Luschnig, C. (2001) *Curr. Biol.* **11,** R831–833
12. Morris, D. A. (2000) *Plant Growth Regul.* **32,** 161–172
13. Peer, W. A., Brown, D. E., Tague, B. W., Muday, G. K., Taiz, L., and Murphy, A. S. (2001) *Plant Physiol.* **126,** 536–548
14. Peer, W. A., and Murphy, A. S. (2007) *Trends Plant Sci.* **12,** 556–563
15. Bernasconi, P. (1996) *Physiol. Plant.* **96,** 205–210
16. Cox, D. N., and Muday, G. K. (1994) *Plant Cell* **6,** 1941–1953
17. Michalke, W., Katekar, G. F., and Geissler, A. E. (1992) *Planta* **187,** 254–260
18. Martinoia, E., Klein, M., Geisler, M., Bovet, L., Forestier, C., Kolukisaoglu, U., Muller- Rober, B., and Schulz, B. (2002) *Planta* **214,** 345–355
19. Verrier, P. J., Bird, D., Burla, B., Dassa, E., Forestier, C., Geisler, M., Klein, M., Kolukisaoglu, U., Lee, Y., Martinoia, E., Murphy, A., Rea, P. A., Samuels, L., Schulz, B., Spalding, E. J., Yazaki, K., and Theodoulou, F. L. (2008) *Trends Plant Sci.*
20. Bouchard, R., Bailly, A., Blakeslee, J. J., Oehring, S. C., Vincenzetti, V., Lee, O. R., Paponov, I., Palme, K., Mancuso, S., Murphy, A. S., Schulz, B., and Geisler, M. (2006) *J. Biol. Chem.* **281,** 30603–30612
21. Geisler, M., Blakeslee, J. J., Bouchard, R., Lee, O. R., Vincenzetti, V., Bandyopadhyay, A., Titapiwatanakun, B., Peer, W. A., Bailly, A., Richards, E. L., Ejendal, K. F., Smith, A. P., Baroux, C., Grossniklaus, U., Muller, A., Hrycyna, C. A., Dudler, R., Murphy, A. S., and Martinoia, E. (2005) *Plant J.* **44,** 179–194
22. Geisler, M., and Murphy, A. S. (2006) *FEBS Lett.* **580,** 1094–1102
23. Santelia, D., Vincenzetti, V., Azzarello, E., Bovet, L., Fukao, Y., Duchtig, P., Mancuso, S., Martinoia, E., and Geisler, M. (2005) *FEBS Lett.* **579,** 5399–5406
24. Terasaka, K., Blakeslee, J. J., Titapiwatanakun, B., Peer, W. A., Bandyopadhyay, A., Makam, S. N., Lee, O. R., Richards, E. L., Murphy, A. S., Sato, F., and Yazaki, K. (2005) *Plant Cell* **17,** 2922–2939
25. Murphy, A. S., Hoogner, K. R., Peer, W. A., and Taiz, L. (2002) *Plant Physiol.* **128,** 935–950
26. Noh, B., Murphy, A. S., and Spalding, E. P. (2001) *Plant Cell* **13,** 2441–2454
27. Conseil, G., Baubichon-Cortay, H., Dayan, G., Jault, J. M., Barron, D., and Di Pietro, A. (1998) *Proc. Natl. Acad. Sci. U. S. A.* **95,** 9831–9836
28. Dean, M. (2005) *Methods Enzymol.* **400,** 409–429
29. Geisler, M., and Bailly, A. (2007) *Trends Plant Sci.* **12,** 465–473
30. Geisler, M., Kolukisaoglu, H. U., Bouchard, R., Billion, K., Berger, J., Saal, B., Frangne, N., Koncz-Kalman, Z., Koncz, C., Dudler, R., Blakeslee, J. J., Murphy, A. S., Martinoia, E., and Schulz, B. (2003) *Mol. Biol. Cell* **14,** 4238–4249
31. Romano, P., Gray, J., Horton, P., and Luan, S. (2005) *New Phytol.* **166,** 753–769
32. Fanghanel, J., and Fischer, G. (2004) *Front. Biosci.* **9,** 3453–3478
33. Scheidt, H. A., Vogel, A., Eckhoff, A., Koenig, B. W., and Huster, D. (2007) *Eur. Biophys. J.* **36,** 393–404
34. Geisler, M., Girin, M., Brandt, S., Vincenzetti, V., Plaza, S., Paris, N., Kobae, Y., Maeshima, M., Billion, K., Kolukisaoglu, U. H., Schulz, B., and Martinoia, E. (2004) *Mol. Biol. Cell* **15,** 3393–3405
35. Kamphausen, T., Fanghanel, J., Neumann, D., Schulz, B., and Rahfeld, J. U. (2002) *Plant J.* **32,** 263–276
36. Lewis, D. R., Miller, N. D., Splitt, B. L., Wu, G., and Spalding, E. P. (2007) *Plant Cell* **19**
37. Hemenway, C. S., and Heitman, J. (1996) *J. Biol. Chem.* **271,** 18527–18534
38. Luschnig, C., Gaxiola, R. A., Grisafi, P., and Fink, G. R. (1998) *Genes Dev.* **12,** 2175–2187
39. Angers, S., Salahpour, A., Joly, E., Hilairet, S., Chelsky, D., Dennis, M., and Bouvier, M. (2000) *Proc. Natl. Acad. Sci. U. S. A.* **97,** 3684–3689
40. Weiergraber, O. H., Eckhoff, A., and Granzin, J. (2006) *FEBS Lett.* **580,** 251–255
41. Ottenschlager, I., Wolff, P., Wolverton, C., Bhalerao, R. P., Sandberg, G., Ishikawa, H., Evans, M., and Palme, K. (2003) *Proc. Natl. Acad. Sci. U. S. A.* **100,** 2987–2991
42. Mancuso, S., Marras, A. M., Magnus, V., and Baluska, F. (2005) *Anal. Biochem.* **341,** 344–351
43. Chelu, M. G., Danila, C. I., Gilman, C. P., and Hamilton, S. L. (2004) *Trends Cardiovasc. Med.* **14,** 227–234
44. Xu, Y., Piston, D. W., and Johnson, C. H. (1999) *Proc. Natl. Acad. Sci. U. S. A.* **96,** 151–156
45. Gehret, A. U., Bajaj, A., Naider, F., and Dumont, M. E. (2006) *J. Biol. Chem.* **281,** 20698–20714
46. Bailly, A., Sovero, V., and Geisler, M. (2006) *Plant Signal. Behav.* **1,** 277–280
47. Granzin, J., Eckhoff, A., and Weiergraber, O. H. (2006) *J. Mol. Biol.* **364,** 799–809
48. Petrasek, J., Cerna, A., Schwarzerova, K., Elckner, M., Morris, D. A., and Zazimalova, E. (2003) *Plant Physiol.* **131,** 254–263
49. Rashotte, A. M., Brady, S. R., Reed, R. C., Ante, S. J., and Muday, G. K. (2000) *Plant Physiol.* **122,** 481–490
50. Buer, C. S., Muday, G. K., and Djordjevic, M. A. (2007) *Plant Physiol.*
51. Multani, D. S., Briggs, S. P., Chamberlin, M. A., Blakeslee, J. J., Murphy, A. S., and Johal, G. S. (2003) *Science* **302,** 81–84
52. Zhang, S., Yang, X., Coburn, R. A., and Morris, M. E. (2005) *Biochem. Pharmacol.* **70,** 627–639
53. Blilou, I., Xu, J., Wildwater, M., Willemsen, V., Paponov, I., Friml, J., Heidstra, R., Aida, M., Palme, K., and Scheres, B. (2005) *Nature* **433,** 39–44
54. Brunn, S. A., Muday, G. K., and Haworth, P. (1992) *Plant Physiol.* **98,** 101–107
55. Hossel, D., Schmeiser, C., and Hertel, R. (2005) *Plant Biol.* (*Stuttg*) **7,** 41–48
56. Sussman, M. R., and Gardner, G. (1980) *Plant Physiol.* **66,** 1074–1078
57. Petrasek, J., Mravec, J., Bouchard, R., Blakeslee, J. J., Abas, M., Seifertova, D., Wisniewska, J., Tadele, Z., Kubes, M., Covanova, M., Dhonukshe, P., Skupa, P., Benkova, E., Perry, L., Krecek, P., Lee, O. R., Fink, G. R., Geisler, M., Murphy, A. S., Luschnig, C., Zazimalova, E., and Friml, J. (2006) *Science* **312,** 914–918
58. Blakeslee, J. J., Bandyopadhyay, A., Lee, O. R., Mravec, J., Titapiwatanakun, B., Sauer, M., Makam, S. N., Cheng, Y., Bouchard, R., Adamec, J., Geisler, M., Nagashima, A., Sakai, T., Martinoia, E., Friml, J., Peer, W. A., and Murphy, A. S. (2007) *Plant Cell* **19,** 131–147
59. Shirane, M., and Nakayama, K. I. (2003) *Nat. Cell Biol.* **5,** 28–37
60. Rojas-Pierce, M., Titapiwatanakun, B., Sohn, E. J., Fang, F., Larive, C. K., Blakeslee, J., Cheng, Y., Cutler, S. R., Peer, W. A., Murphy, A. S., and Raikhel, N. V. (2007) *Chem. Biol.* **14,** 1366–1376
61. Ruegger, M., Dewey, E., Hobbie, L., Brown, D., Bernasconi, P., Turner, J., Muday, G., and Estelle, M. (1997) *Plant Cell* **9,** 745–757
62. Gil, P., Dewey, E., Friml, J., Zhao, Y., Snowden, K. C., Putterill, J., Palme, K., Estelle, M., and Chory, J. (2001) *Genes Dev.* **15,** 1985–1997

Downloaded from www.jbc.org at SMAC Consortium - University of Zürich on August 6, 2008

Chapter 3:

Identification of an ABCB/P-glycoprotein-specific inhibitor of auxin transport by chemical genomics

Chapter 3

Personal Contributions

Figure 6AC: NPA binding assays

Figure 6D: BRET assays

Supplemental Material can be found at:
http://www.jbc.org/content/suppl/2010/05/14/M110.105981.DC1.html

THE JOURNAL OF BIOLOGICAL CHEMISTRY VOL. 285, NO. 30, pp. 23309–23317, July 23, 2010
© 2010 by The American Society for Biochemistry and Molecular Biology, Inc. Printed in the U.S.A.

Identification of an ABCB/P-glycoprotein-specific Inhibitor of Auxin Transport by Chemical Genomics*[S]

Received for publication, January 20, 2010, and in revised form, April 29, 2010 Published, JBC Papers in Press, May 14, 2010, DOI 10.1074/jbc.M110.105981

Jun-Young Kim[‡1], Sina Henrichs[§1], Aurélien Bailly[§], Vincent Vincenzetti[§], Valpuri Sovero[§], Stefano Mancuso[¶], Stephan Pollmann[‖], Daehwang Kim[**], Markus Geisler[§2], and Hong-Gil Nam[‡3]

*From the [‡]Laboratory of Plant Systems Bio-Dynamics, Pohang University of Science and Technology, 790-784 Pohang, Korea, the [§]Institute of Plant Biology, University of Zurich and Zurich-Basel Plant Science Center, Zolliker Strasse 107, CH-8008 Zurich, Switzerland, the [¶]Department of Horticulture, University of Firenze, I-50019 Sesto Fiorentino, Italy, the [‖]Lehrstuhl für Pflanzenphysiologie, Ruhr-Universität Bochum, D-44801 Bochum, Germany, and the **Biomaterials Research Center, Korea Research Institute of Chemical Technology, 305-600 Dae-jon, Korea*

Plant development and physiology are widely determined by the polar transport of the signaling molecule auxin. This process is controlled on the cellular efflux level catalyzed by members of the PIN (pin-formed) and ABCB (ATP-binding cassette protein subfamily B)/P-glycoprotein family that can function independently and coordinately. In this study, we have identified by means of chemical genomics a novel auxin transport inhibitor (ATI), BUM (2-[4-(diethylamino)-2-hydroxybenzoyl]benzoic acid), that efficiently blocks auxin-regulated plant physiology and development. In many respects, BUM resembles the functionality of the diagnostic ATI, 1-*N*-naphtylphtalamic acid (NPA), but it has an IC_{50} value that is roughly a factor 30 lower. Physiological analysis and binding assays identified ABCBs, primarily ABCB1, as key targets of BUM and NPA, whereas PIN proteins are apparently not directly affected. BUM is complementary to NPA by having distinct ABCB target spectra and impacts on basipetal polar auxin transport in the shoot and root. In comparison with the recently identified ATI, gravacin, it lacks interference with ABCB membrane trafficking. Individual modes or targets of action compared with NPA are reflected by apically shifted root influx maxima that might be the result of altered BUM binding preferences or affinities to the ABCB nucleotide binding folds. This qualifies BUM as a valuable tool for auxin research, allowing differentiation between ABCB- and PIN-mediated efflux systems. Besides its obvious application as a powerful weed herbicide, BUM is a *bona fide* human ABCB inhibitor with the potential to restrict multidrug resistance during chemotherapy.

In plants, the auxin indolyl-3-acetic acid (IAA)[4] serves as a hormone-like signaling molecule that is a key factor in plant development and physiology (1–4). Many of its functionalities are controlled by a unique, plant-specific process, the cell-to-cell or polar auxin transport (PAT) (3). However, cellular efflux is the rate-limiting step of PAT, and in agreement with the chemiosmotic hypothesis, putative exporters of the PIN (pin-formed) and B subfamily of ABC transporter, ABCB/PGP/MDR (P-glycoprotein, multidrug resistance), families have been identified (5–7).

Most PIN efflux carriers show predominantly polar locations in PAT tissues and developmental, organogenetic loss-of-function phenotypes and are thought to be the determinants of a "reflux loop" in the root apex (3, 8). ABCB isoforms have been identified as primary active (ATP-dependent) auxin pumps showing auxin-related, developmental (but not organogenetic) loss-of-function phenotypes (5, 9, 10). Despite their mostly apolar locations, they have been demonstrated to contribute to PAT and long range auxin transport (5, 11, 12). Moreover, ABCB1/PGP1 and ABCB19/PGP19/MDR1 coordinately function in basipetal reflux of auxin maxima out of the root and shoot tip (9). The immunophilin-like FKBP42, TWD1 (twisted DWARF1) protein, was characterized as a central regulator of ABCB-mediated auxin transport by means of protein-protein interaction (11, 12). Positive regulation of ABCB1- and ABCB19-mediated auxin transport accounts for overlapping phenotypes between *twd1* and *abcb1 abcb19* (11, 12).

ABCB- and PIN-mediated auxin efflux can function independently and play identical cellular but separate developmental roles (10). However, ABCBs and PINs are also able to interactively and coordinately transport auxin (9). The current picture that emerges is that in interacting cells, multilaterally expressed ABCBs minimize apoplastic reflux, whereas polar ABCB-PIN interactions provide specific vectorial auxin stream (10). However, the individual roles of ABCB- and PIN-mediated auxin flows are far from being understood.

The investigation of PAT streams was facilitated by using synthetic compounds that act as auxin transport inhibitors (ATIs), with the non-competitive IAA efflux inhibitor 1-*N*-naphtylphtalamic acid (NPA) being the most prominent. Until today, the identity, number, and affinity of putative NPA-bind-

* This work was supported by grants from the Forschungskredit of the University of Zurich (KN57150702, to A. B.), from the Novartis Foundation (to M. G.), from the Swiss National Funds (NF31-125001, to M. G.), from the National Research Foundation of Korea (NRF) funded by the Korea government (MEST) (no. 2009-0091504), and from the Crop Functional Genomics Frontier Research Program (CG3132) (to H.-G. N.).

[S] The on-line version of this article (available at http://www.jbc.org) contains supplemental Figs. S1–S7.

[1] Both authors contributed equally to this work.
[2] To whom correspondence may be addressed. Tel.: 41-44-634-8277; Fax: 41-44-634-8204; E-mail: markus.geisler@botinst.uzh.ch.
[3] To whom correspondence may be addressed. E-mail: nam@postech.ac.kr.

[4] The abbreviations used are: IAA, indole-3-acetic acid; PAT, polar auxin transport; PGP, phosphoglycoprotein; TMD, transmembrane domain; NBD, nucleotide-binding domain; dag, day(s) after germination; ATI, auxin transport inhibitor; NPA, 1-*N*-naphtylphtalamic acid; NBP, NPA-binding protein; gravacin, 3-(5-[3,4-dichlorophenyl]-2-furyl)acrylic acid; GFP, green fluorescent protein; BA, benzoic acid; BRET, bioluminescence resonance energy transfer.

Downloaded from www.jbc.org at SMAC Consortium - University of ZÃƒÂ¼rich, on October 25, 2010

ing proteins (NBPs) is still controversial (13–17). However, the current consensus is that the auxin efflux complex consists of at least two proteins: a membrane-integral transporter and an NBP-regulatory subunit (13–15, 18). Several lines of evidence suggest that PIN proteins do not themselves act as NBPs (19), although NPA application results in a pin-formed inflorescence, mimicking *PIN1* loss of function (20). Therefore, it was suggested that NPA blocks PAT by interfering with the cycling of auxin transporters, like PIN1 (21). However, NPA itself does not directly affect PIN cycling, and concentrations necessary to perturb PIN cycling were much higher than was needed for efficiently blocking PAT (16, 21). Independently, ABCB1 and ABCB19 have been identified as targets of NPA (5, 22, 23) and high affinity NBPs (23–25). Surprisingly, NPA was additionally shown to bind to TWD1, and NPA binding disrupted TWD1-ABCB1 interaction (11). *In planta*, this leads to disruption of ABCB1 activity, suggesting that TWD1 and ABCB1 represent high and low affinity components of the NPA-sensitive efflux complex (11).

In the last few years, chemical genomic screens have allowed for the identification of several synthetic compounds and, in some cases, respective molecular targets that interfere with auxin signaling (26, 27), membrane trafficking (28–30), and auxin transport (23, 31). 3-(5-[3,4-dichlorophenyl]-2-furyl)-acrylic acid (gravacin) was recently identified as a strong inhibitor of root and shoot gravitropism, auxin responsiveness, and protein trafficking to the tonoplast in *Arabidopsis* (30). In a follow-up screen, inhibition of gravitropism and protein trafficking was shown to employ independent mechanics (23). Mutations in *ABCB19* confer resistance to the effect of gravacin on hypocotyl gravitropism and result in reduced binding of gravacin to microsomal fractions, implicating ABCB19 as the major target of gravacin (23). Consequently, gravacin was found to be a strong inhibitor of ABCB19-mediated auxin transport in *Arabidopsis* and HeLa cells.

In this study, we screened chemical libraries of small organic compounds for plant physiological and developmental regulators and identified a novel, highly potent ATI by means of chemical genomics. A direct comparison of compound 10824 (BUM) and NPA effects on auxin-controlled plant physiology, auxin transport, and drug binding reveals that BUM shares many features with NPA, like induction of pin-formed inflorescences and ABCB binding and blocking of transport. Unlike NPA and gravacin, BUM lacks growth activation at lower concentrations and does not interfere with membrane trafficking, respectively. BUM might therefore act as a powerful tool in dissecting ABCB- and PIN-mediated auxin streams in plant physiology.

EXPERIMENTAL PROCEDURES

Chemical Library Screens—Arabidopsis thaliana ecotype Columbia (Col) seeds were surface-sterilized, stratified at 4 °C for 3 days, and grown horizontally in 24-well plates (3 seeds/well; 0.5× B5 medium, 2% sucrose, 0.8% agar) at 22 °C under continuous light. Seven days after germination (dag), 2 μM organic compounds of a chemical library (containing 6,500 small organic chemicals at 50 μM in DMSO) from the Korea Chemical Bank was added manually. Plant phenotypes in respect to plant morphology, growth rate, leaf color, flowering time, and senescence were monitored every 2 days by visual examination in comparison with the solvent (DMSO) control on each plate up to 14 dag.

In a secondary screen, plants were treated with various concentrations (up to 10 μM) of compounds from the Korea Chemical Bank that were structurally related to compound 10824 and thus contained the 2-(formyl)-benzoic acid core (Fig. 1*B* and supplemental Fig. S1). Phenotypes were screened for induction of pin-formed inflorescences (see Fig. 1*C*).

Plant Material and Quantification of Growth—For long term experiments, *abcb1/pgp1–1* (At2g36910), *abcb19/pgp19–1/mdr1-1* (At3g28860) (all ecotype Wassilewskija), and *pin2/eir1-4* (At5g57090, ecotype Columbia) were grown on 0.5× B5 medium, 2% sucrose, 0.8% phytagar under continuous light for 18 dag in sterilized plastic boxes (SPL, Korea). For all other experiments, seedlings were grown if not indicated otherwise for 5 dag on vertical plates containing 0.5× Murashigge and Skoog medium, 1% sucrose, 1% phytagar in the dark or at 16 h of light/day. For growth quantification, seedlings were transferred on drug-containing plates (0–50 μM). After 5, 7, 9, and 11 dag, seedlings were aligned on 1% phytoagar medium, images were scanned, and root and hypocotyl lengths and lateral root numbers (7, 9, and 11 dag) were measured using Scion Image software (Scion Corp., Frederick, MD). For determination of IC_{50} values, root lengths of 7-dag seedlings grown on 0–80 μM NPA and 0–20 μM BUM were quantified, and IC_{50} values were calculated using sigmoidal dose-response fits. All experiments were performed at a minimum as triplicates with 20–30 seedlings per experiment.

In Planta Analysis of Auxin Responses and Transport—Homozygous F4 generations of *A. thaliana* wild-type, *pin2/eir1-4* (32), *abcb1/pgp1–1*, and *abcb19/pgp19-1/mdr1-1* (25) mutants expressing the maximal auxin-inducible reporter Pro_{DR5}:GFP (41) were grown vertically for 5 dag and analyzed by confocal laser-scanning microscopy (Leica; DMIRE2). In some cases, seedlings were transferred for an additional 12 h onto new plates containing 0.5 μM BUM, 5 μM NPA, or the solvent DMSO. For histological signal localization, differential interference contrast and GFP images were merged electronically using Photoshop 10.0.1 (Adobe Systems).

For measurements of basipetal root and hypocotyl (shoot) transport, seedlings were grown for 9 or 7 dag on vertical plates containing 0.5× Murashigge and Skoog medium, 1% sucrose, 1% phytagar at 16 h of light/day at 100 microeinsteins (root) or 10 microeinsteins (hypocotyl), respectively. Measurements were performed as described in Ref. 33, using radiolabeled IAA that was applied by placing solified agar droplets next to the seedlings root tips or at the apical (cut) end of the hypocotyls. In some cases, solified IAA droplets contained 1 μM BUM or 10 μM NPA. Data are means of three independent experiments with each four replica of 10 seedlings each.

A platinum microelectrode was used to monitor IAA fluxes in *Arabidopsis* roots as described previously (11, 12, 34, 35). For measurements, plants were grown in hydroponic cultures and used at 5 days after germination. Differential current from an IAA-selective microelectrode was recorded in the absence and presence of 5 μM NPA, BUM, or gravacin (23).

Endogenous free IAA was quantified from shoot and root segments of MeOH-extracted seedlings by using gas chroma-

Downloaded from www.jbc.org at SMAC Consortium - University of ZÃƒÂ¼rich, on October 25, 2010

tography-mass spectrometry, as described by Bouchard *et al.* (12). Seedlings were analyzed after 24-h treatments with 5 μM NPA or 0.5 μM BUM. Data are means of four independent lots of 40–50 seedlings each.

Yeast Auxin Loading Assays—PIN1,2- and ABCB1,19-mediated IAA transport was measured by assaying IAA loading into *Schizosaccharomyces pombe* mutant strains *ael1* and *mam1 pdr1*, respectively, as described (36), with the following modifications. Retained radioactivity was quantified by vacuum filtration after 0 and 10 min of incubation at 30 °C, and inhibitors at 10 μM were added for 30 min prior to loading and during loading. Relative ABCB1,19- and PIN1,2-mediated IAA and benzoic acid (BA) loading is calculated from retained radioactivity as follows: (radioactivity in the yeast at t = 10 min) − (radioactivity in the yeast at t = 0)) × (100%)/(radioactivity in the yeast at t = 0 min). Presented are mean values from four independent experiments (independent transformants) with four replicates each.

NPA Binding Studies—NPA binding assays using *Arabidopsis* or yeast microsomes were performed as described elsewhere (11). In short, four replicates of 10 μg each of protein were incubated with 10 nM [^{3}H]NPA (80 Ci/mmol) and 10 nM [^{14}C]BA (55 mCi/mmol) in the presence and absence of 10 μM NPA. For competition experiments, 10 μM BUM was added. Reported values are the means of specific binding ([^{3}H]NPA bound in the absence of cold NPA (total) minus [^{3}H]NPA bound in the presence of cold NPA (nonspecific)) from four independent experiments (independent transformants) with four replicates each.

Point mutations E502K and F792K in ABCB1 (pNEV-PGP1 (5)) were introduced using the QuikChange XL site-directed mutagenesis kit (Stratagene, La Jolla, CA), resulting in pNEV-ABCB1^{E502K} and pNEV-ABCB1^{F792K} (see Fig. 6*B*).

BRET Analysis—Microsomes from yeast JK93da expressing PGP1-YFP and TWD1-rLuc (11) were prepared in the presence or absence of 5 μM NPA, BUM, or gravacin or adequate amounts of solvents. BRET signals were recorded in the presence of 5 μM coelenterazine (Biotium Inc.), and BRET ratios were calculated as described (11). The results are the average values from four independent experiments with four replica each of 10 readings collected every minute.

Data Analysis—Data were analyzed using Prism 4.0b (GraphPad Software, San Diego, CA). *A. thaliana* ABCB1 structure modeling was performed using PyMOL version 0.99 (DeLano Scientific LLC, San Carlos, CA) and maximum entropy-based ligand binding was computed using MEDock (available on the World Wide Web). Drug docking was confirmed by using ZDOCK (available on the World Wide Web). Drug three-dimensional structures were energy-minimized using PRODRG2 (available on the World Wide Web), and solely polar hydrogens are displayed (usual atom *color code*).

RESULTS

A Chemical Library Screen for Growth and Developmental Regulators—To identify growth and developmental regulators, we screened *A. thaliana* (ecotype Columbia; Col Wt) seedlings with a chemical library (Korean Chemical Bank, KRICT, Korea) composed of 6,500 small organic compounds. Seeds were germinated in 24-well plates, and at 7 dag, a 2 μM concentration of a different library compound was added to each well. Plant phenotypes with respect to plant morphology, growth rate, leaf color, flowering time, and senescence were monitored every 2 days by visual examination in comparison with solvent (DMSO) controls. Among the various chemical compounds that led to altered plant morphology, compound number 10824 (2-[4-(diethylamino)-2-hydroxybenzoyl]benzoic acid) produced a drastic phenotype, including dark green, epinastic leaves (Fig. 1*A*), suppression of primary and secondary roots (Fig. 1*D*), and abnormal, pin-formed inflorescences (Fig. 1*C*). We narrowed our focus to this compound 10824, subsequently named BUM,[5] verifying consistently growth inhibition under a variety of assay conditions in follow-up screenings.

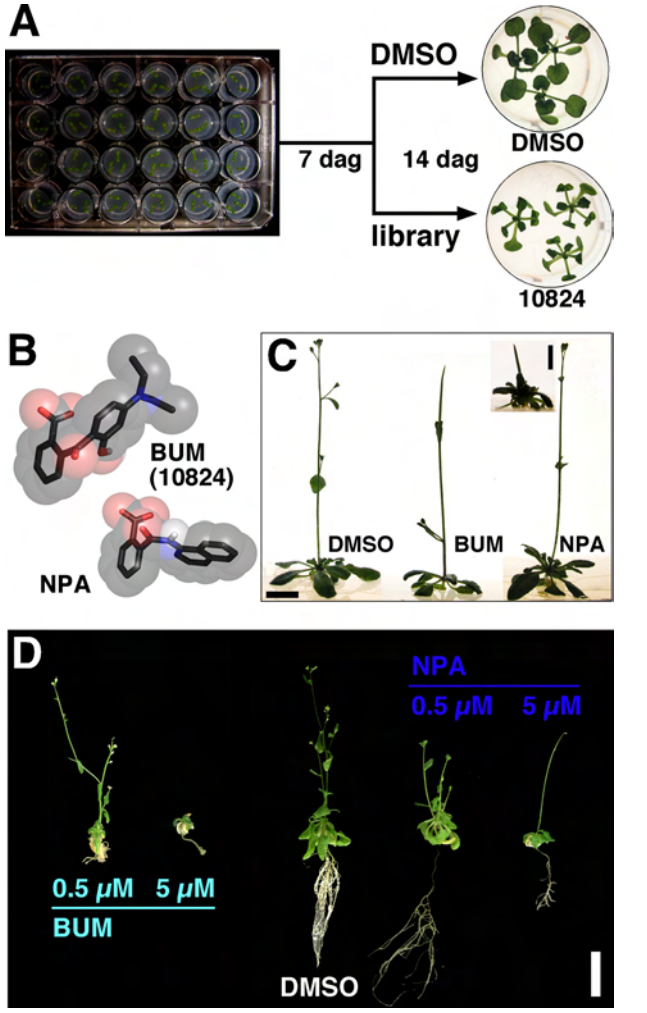

FIGURE 1. **A chemical genomic screen identified a novel auxin transport inhibitor-like compound inducing pin-formed inflorescences.** *A*, a microtiter-based screening strategy using a chemical library from the Korean Chemical Bank identified compound 10824 (BUM) as a strong modifier of plant development. *B*, three-dimensional structures of BUM in comparison with established auxin efflux inhibitor, NPA. *C*, BUM-induced pin-formed inflorescences. Note that BUM concentrations necessary for pin-formed inflorescence induction are roughly 20-fold lower compared with NPA (10 μM NPA; *inset*). *D*, BUM strongly reduces primary root growth, which is not found with NPA. *Scale bars*, 2 cm.

[5] Named after the famous Korean football player, Cha Kun-Bum. BUM is available for academic institutions upon request from M. G.

Downloaded from www.jbc.org at SMAC Consortium - University of ZÃƒÂ¼rich, on October 25, 2010

The fact that BUM/10824 produced pin-formed inflorescences in analogy to the well established ATI, NPA (15, 16, 37), and that both contain a 2-(formyl)-benzoic acid core (Fig. 1*B*), prompted us to compare growth defects between BUM and NPA over a wide concentration range. BUM induces pin-shaped inflorescences and reduces primary root growth at 0.5 μM, which is roughly 20 times lower than what is needed for NPA (Fig. 1, *C* and *D*).

In a secondary screen, we tested compounds that contained a 2-(formyl)-benzoic acid core taken from the Korea Chemical Bank and Chembridge chemical libraries. None of the six tested compounds A–F was able to induce pin-shaped inflorescences over a wide concentration range up to 10 μM (supplemental Fig. S1), suggesting that not the 2-(formyl)-benzoic acid core alone but side chains determine functionality.

BUM Affects Auxin-controlled Plant Growth—These findings suggested that BUM influences plant growth and development in analogy to the ATI, NPA, but has a stronger effect. Therefore, we quantified root and hypocotyl lengths, known to be inversely controlled by auxin, in the presence of BUM and NPA in more detail. BUM drastically reduced primary root growth of light-grown wild type seedlings (Fig. 2, *A* and *B*) with an apparent IC_{50} of 0.4 μM (supplemental Fig. S5), which is roughly a factor of 30 less than what is needed with NPA (IC_{50} = 12.8 μM). A similar effect was found also for hypocotyl elongation of light-grown seedlings. NPA shows, in agreement with previous reports on roots (38), a stimulating and inhibitory result upon hypocotyl elongation under light at nanomolar and micromolar concentrations, respectively. Such a biphasic behavior was not found for BUM in the concentration range used (0–20 μM), suggesting, despite widely overlapping effects, a different mode of action or targets (Fig. 2).

A shoot-derived auxin pulse known to be efficiently inhibited by NPA (39–41) tightly controls lateral root emergence (42). Not unexpectedly, 0.1 μM BUM drastically blocked lateral root formation in both of the tested *Arabidopsis* ecotypes, Col and Ws, by roughly 50%; enhanced sensitivities compared with 0.5 μM NPA (roughly 25% inhibition) were in line with what was found for primary root growth.

Interestingly, root and hypocotyl growth inhibition by BUM and NPA was light-dependent and less pronounced in dark-grown, etiolated seedlings (supplemental Fig. S4). Moreover, shoot hook formation and opening of etiolated seedlings was inhibited by 5 μM BUM but not by NPA (Fig. 2*A*), which requires higher concentrations, as was shown before (43–45). This is in agreement with the concept that auxin has a more important role in elongation and bending responses in light-grown than in dark-grown seedlings (44, 45).

Next we tested root gravitropism, another hallmark of auxin-controlled plant physiology (46, 47). BUM disrupted root bending in wild type seedlings drastically (supplemental Fig. S2). Interestingly, the ecotype Col revealed higher sensitivities (77% inhibition) compared with the ecotype Ws (58% inhibition) not found for NPA (11, 38). Similarly to lateral root formation, 0.1 μM BUM (supplemental Fig. S2) was more efficient than 5 μM NPA assayed in both ecotypes in parallel (not shown) (11, 38). Recently, single loss-of-function roots, *pin2*, *abcb1*, or *abcb19*, were shown to be NPA-sensitive using gravitropism assays (11, 38). In agreement, DR5-GFP imaging (Fig. 3) revealed no dramatic differences between *pin2* and *abcb1* roots in comparison with corresponding wild types. However, based on gravitropism assays (supplemental Fig. S2) and in contrast to what was

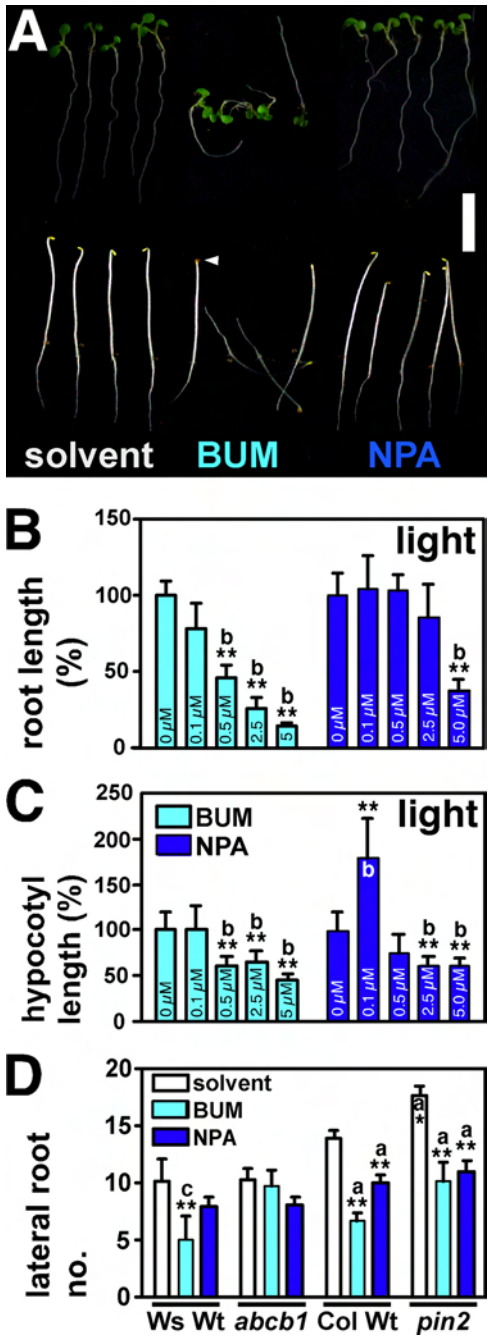

FIGURE 2. **BUM reduces root and hypocotyl growth in the light.** *A*, phenotype of BUM- and NPA-treated (each 0.5 μM) light- (*top*) and dark-grown (*bottom*) seedlings 5 dag (days after germination). Note that seedlings grown in the presence of BUM are hookless (*white arrow*). *Scale bar*, 1 cm. *B* and *C*, dose dependence of BUM and NPA treatments on primary root (*C*) and hypocotyl (*D*) lengths; absolute root and hypocotyl lengths were 29.5 ± 4.4 and 2.7 ± 0.5 mm, respectively. *D*, reduction of lateral root numbers caused by BUM (0.1 μM) and NPA (0.5 μM) treatments 11 dag. Note that *abcb1* in contrast to wild-type and *pin2* is less sensitive to BUM. Data are mean ± S.D. (*error bars*) (n = 3 with each 20–30 seedlings). Significant differences from wild type or between inhibitor and solvent treatments (0 μM) are indicated by *one* or *two asterisks*, respectively, and were calculated using Dunnett's multiple comparison test (*A* and *B*) or analysis of variance (*C*) (Tukey's test for multiple comparisons) with the following p values: $p < 0.001$ (*a*); $p < 0.01$ (*b*); $p < 0.05$ (*c*).

Downloaded from www.jbc.org at SMAC Consortium - University of ZÃƒÂ¼rich, on October 25, 2010

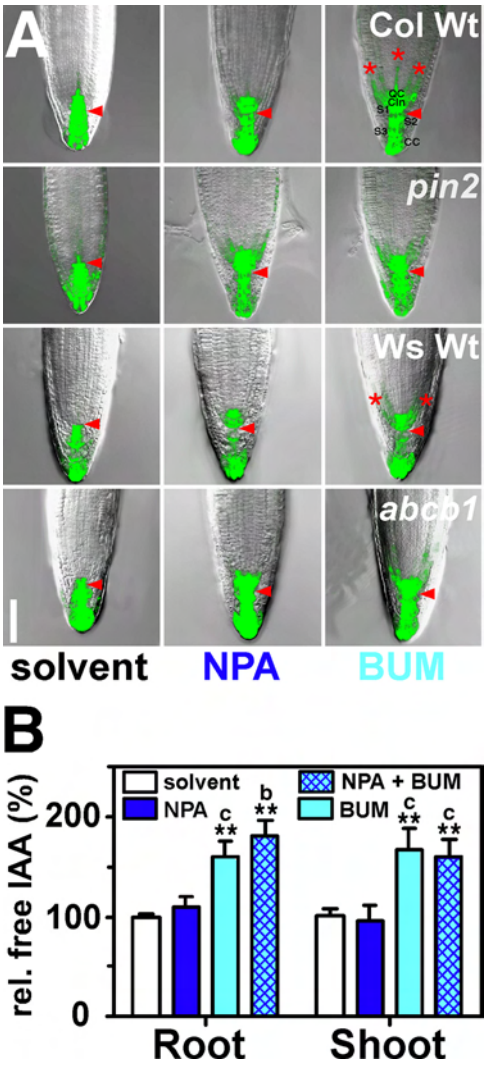

FIGURE 3. **BUM alters auxin responses and levels *in planta*.** *A*, expression of the auxin-responsive reporter DR5-GFP (*green*) upon BUM (0.5 μM) and NPA (5 μM) treatments (24 h) in root tips. BUM and NPA enhance DR5-GFP signals in the quiescent center (*QC*), columella initials (*CIn*), and S1 cells but reduce signals in columella S2, S3, and cap cells (*CC*); S2 and S3 borders are marked with *arrowheads*. Note stronger extensions of GFP signals from quiescent center, columella initials, and S1 cells into initials of epidermis, endodermis, and stele upon BUM treatment (*asterisks*) compared with NPA. *Scale bar*, 200 μm. *B*, root and shoot free IAA concentrations of BUM-treated (0.5 μM) and NPA-treated (5 μM) wild type seedling. Data are mean ± S.D. (*error bars*) (n = 4 with each 40–50 seedlings); absolute wild-type values were 42.2 ± 5.7 and 49.9 ± 6.1 pg/mg (fresh weight) for roots and shoots, respectively. Significant differences (analysis of variance using the Tukey's test for multiple comparisons: $p < 0.001$ (*a*); $p < 0.01$ (*b*); $p < 0.05$ (*c*)) between inhibitor and solvent treatments are indicated by *two asterisks*.

recently found for NPA (11, 38), *abcb1* roots were significantly less affected by BUM: 35.3% (percentage occurrence of 60, 90, and 120° bending between inhibitor and solvent control (see "Experimental Procedures")) of *abcb1* roots bent efficiently on BUM but only 26.8% of the corresponding wild type. Even higher resistance was found for *pin2* root gravitropism (supplemental Fig. S2). However, similar inhibition by BUM in the wild type suggests that this is mainly due to the strong genetic effect of the *pin2* mutation. Only partial resistance found for *abcb1* toward BUM is probably caused by functional redundancy between ABCB1 and ABCB19 that was recently confirmed by the finding that *abcb1abcb19* and *twd1* roots have reduced sensitivities toward NPA (11). These results provide evidence that BUM, like NPA, blocks many aspects of plant physiology that are controlled by the polar transport of auxin.

BUM Alters Auxin Accumulation—To test our conclusions derived from growth experiments and to substantiate the physiological relevance of the proposed BUM function *in planta*, we investigated BUM sensitivity of wild type roots in comparison with NPA using two different approaches. First, analysis of the auxin-responsive reporter construct Pro_{DR5}:GFP (48) revealed that in analogy to NPA (11), BUM disrupts basipetal, root-to-shoot auxin reflux and enhanced the DR5-GFP signal in the quiescent center (*QC*), columella initials (*CIn*), and S1 cells but reduced signals in columella S2 and S3 and cap cells (*CC*) (Fig. 3*A*). BUM inhibition, although used at 10-fold lower concentration, was more drastic compared with NPA, resulting in enhanced DR5-GFP signal extending the quiescent center, columella initials, and S1 cells into initials of epidermis, endodermis, and stele upon BUM treatment (*asterisks*) compared with NPA. As shown before, this inhibitory effect was more pronounced in the Col ecotype than in the Ws ecotype (11).

Second, we analyzed free auxin (*IAA*) levels in vertically grown root and shoot portions of 5-dag wild type seedlings treated with BUM and NPA. Although 5 μM NPA had only a minor effect on auxin root/shoot ratios, 0.5 μM BUM significantly enhanced both root and shoot auxin levels (Fig. 3*B*), suggesting a block of basipetal delivery of IAA from the shoot to the root and *vice versa*. Elevated auxin levels are in agreement with and explain reduced root lengths caused by BUM. Effects of NPA and BUM treatments were not additive (Fig. 3*B*), indicating overlapping modes of action and/or targets. In summary, these data support the concept that BUM in analogy to NPA blocks PAT.

BUM Modifies PIN but Not ABCB1 Expression—Inhibition of PAT-driven plant growth and gravitropism can be achieved via two pathways, by blocking the trafficking (21, 22) and by the direct or indirect inhibition of auxin transporters. Accordingly, gravacin was identified in a chemical genomics screen for gravitropic modulators and shown to block trafficking of the vacuolar marker GFP-∂TIP and ABCB19 but also to bind to and inhibit ABCB19 (23). Therefore, we questioned whether BUM would interfere with the abundance and location of the major players in basipetal auxin transport, ABCB1 and ABCB19 on one hand and PIN1 and PIN2 on the other. Although BUM (like NPA) had only mild effects on the expression (ABCB1 was slightly up-regulated in the stele) and no significant effect on the location of ABCB1- and ABCB19-GFP fusion, NPA and, more pronouncedly, BUM enhanced PIN1-GFP and lowered PIN2-GFP signals in the stele and epidermal/cortical cell files, respectively (Fig. 4). Unchanged expression of ABCB proteins and reduced PIN2 abundance upon BUM and NPA addition is supported by semiquantitative reverse transcription-PCR analysis (supplemental Fig. S3) and for NPA as well by gene chip analysis (see the Genevestigator site on the World Wide Web).

Interestingly, NPA and, again more strongly, BUM induced ectopic PIN1-GFP expression in PIN2 locations (epidermis and cortex; see Fig. 4, *inset*), as described previously for the auxin transport modulator quercetin (38, 49). In light of these findings, up- and down-regulation of PIN proteins in their non-

Downloaded from www.jbc.org at SMAC Consortium - University of ZÃƒÂ¼rich, on October 25, 2010

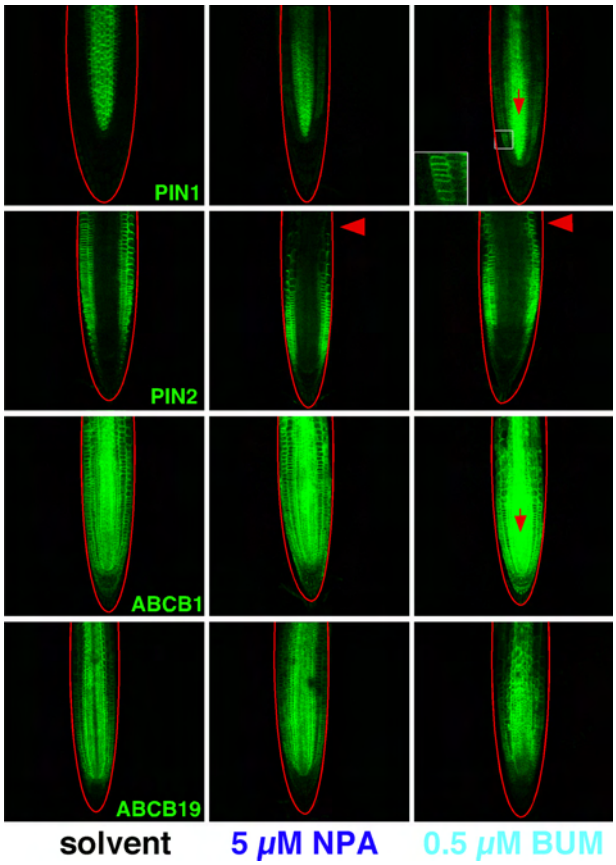

FIGURE 4. **Effect of BUM and NPA on PIN and ABCB abundance and locations.** Localization of PIN1-GFP, PIN2-GFP (8), ABCB1-GFP, and ABCB19-GFP (10) fusion proteins (*green*) in *Arabidopsis* roots 5 dag upon BUM (0.5 μM) and/or NPA (5 μM) treatments (24 h). Note enhanced polar (*arrowheads*) and non-polar PIN1 signals in PIN2 locations upon BUM (*inset*) and NPA treatments and reduced PIN2 expression upon NPA treatment in the elongation zone (*arrowheads*). Root borders are marked in *red*.

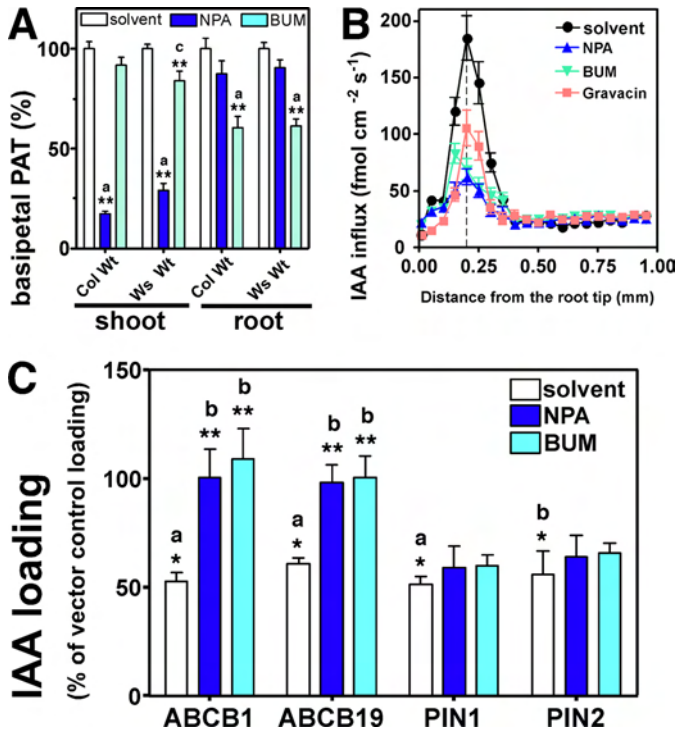

FIGURE 5. **BUM inhibits ABCBs and polar auxin transport in the root.** *A*, BUM and NPA inhibit basipetal IAA transport in roots, whereas NPA (and, to a lesser extent, BUM) blocks basipetal movement in the shoot. Note that concentrations for NPA and BUM were 10 and 1 μM, respectively. Shown are means of three independent experiments ± S.E. (*error bars*) with each four replicates of 10 seedlings. *B*, IAA influx profile along wild type roots in the presence of inhibitors (5 μM) measured using an IAA-specific microelectrode; positive fluxes represent a net IAA influx. Data are means ± S.E. ($n = 12$). Note that BUM results in a reduced influx peak at 200 nm from root tip (*red line*) that is shifted apically. *C*, BUM and NPA (each 10 μM) specifically inhibit ABCB1,19-mediated IAA export in the yeast *S. pombe*. ABCB1-, ABCB19-, PIN1-, and PIN2-mediated export was 52.7.2 ± 4.3, 60.9 ± 2.8, 51.5 ± 3.6, and 56.1 ± 10.6%, respectively, of the corresponding solvent vector control (mean ± S.E.; $n = 4$). Significant differences (analysis of variance using Tukey's test for multiple comparisons: $p < 0.001$ (*a*); $p < 0.01$ (*b*); $p < 0.05$ (*c*)) from vector controls or between inhibitor and solvent treatments are indicated by *one* or *two asterisks*, respectively.

native environments might be of an indirect nature and triggered by elevated auxin levels in these tissues caused by the blocking of PAT. An inverse impact of IAA on PIN1 and PIN2 expression was reported recently (38, 49, 50). In summary, BUM has, unlike gravacin, only a minor impact on ABCB expression and abundance, but it, like NPA, indirectly interferes with PIN expression probably via altered IAA levels.

BUM Alters Auxin Responses and Levels—Next we aimed to analyze the impact of BUM on PAT *in planta* using two independent approaches. First, we measured polar basipetal root and shoot (hypocotyl) transport of radiolabeled IAA that was applied by placing solified agar droplets next to the seedling root tips or at the apical (cut) end of the hypocotyls using recently described standard protocols (33). In agreement with DR5-GFP auxin reporter analysis, 1 μM BUM inhibited root basipetal (up) PAT in both commonly used *Arabidopsis* wild-type ecotypes, Ws and Col, by roughly 40% (Fig. 5*A*). In contrast, 10 times higher NPA concentrations had only a mild effect, as described in Refs. 42 and 46), where 100 μM NPA was needed for a roughly 30% inhibition. Shoot basipetal (down) PAT IAA transport, known to be (in contrast to root PAT) highly NPA-sensitive (46), was strongly reduced (70–80%) by 10 μM NPA but, surprisingly, less effected by 1 μM BUM (8–16% reduction). However, 10 μM BUM resulted in a similar block of shoot PAT (76% reduction) compared with NPA (not shown). This demonstrates the ability of BUM to act as a PAT inhibitor but suggests different affinities to transporters or an altered presence of targets in the root and shoot.

Second, we employed an IAA-specific microelectrode that has become a reliable tool for non-invasively recording IAA influxes into the root transition zone (11, 12, 34, 35). IAA influx in this zone is characterized by a distinct peak at 200 μm from the root tip and is consistent with the current auxin reflux model (8) and a measure for PAT. In agreement with DR5-GFP imaging and PAT measurements, IAA influx peaks were strongly and similarly reduced by 5 μM BUM or NPA (Fig. 5*B*). The magnitude of inhibition caused by BUM and NPA phenocopies genetic reductions of influx peaks found for single *ABCB1 or ABCB19* auxin transporter loss-of-function roots (11). However, gravacin, a recently identified inhibitor of gravitropism (23), had a less pronounced inhibitory effect on IAA influx as with *abcb1* or *abcb19* single mutant roots (11). This is in good agreement with the reported concept that gravacin binds to and inhibits primarily ABCB19 and not ABCB1 (23). Interestingly, BUM resulted in an additional shift of the influx

Downloaded from www.jbc.org at SMAC Consortium - University of ZÃƒÂ¼rich, on October 25, 2010

maximum ~40 nm in the apical direction (not found with NPA or gravacin) that might account for more drastic growth inhibition despite similar reduction of influx peaks. Differences in the magnitude of inhibition of root PAT caused by NPA and BUM measured by means of droplet application (Fig. 5*A*) or an IAA-selective electrode (Fig. 5*B*) might have systematic reasons caused by different inhibitor concentration and application duration and site (either applied to the (root) tip or in the electrode bath).

ABCBs Are the Primary Targets of BUM and NPA—The current picture is that ABCBs and the interacting ABCB1,19-regulator, TWD1/FKBP42, but probably not PIN proteins represent predicted low and high affinity, respectively, NPA-binding proteins (11). This is supported by recent studies demonstrating ABCB1 and ABCB19 to bind NPA resulting in inhibition of efflux activity (5, 11, 23), whereas PIN1 did not seem to bind NPA (23).

Our data so far suggested that auxin exporters, the primary control units of PAT, might be the direct targets of BUM action. Our data showing that lateral root formation in *abcb1* but not in *pin2* roots is BUM-insensitive (Fig. 2*C*) point to the subclass of ABCBs as possible BUM targets. In order to clarify which subclass of auxin exporters is a direct target of BUM, we quantified IAA export activities of the most prominent members of the ABCB and PIN subclass, ABCB1,19 and PIN1,2, by heterologous expression in yeast. IAA export analysis in bakers' yeast clearly demonstrated that ABCB1 but not PIN2 is inhibited significantly by BUM and by NPA although to a lesser extent (supplemental Fig. S6). Inhibition was specific because background (vector control) inhibition by NPA/BUM was negligible (3.3/6.3%). Moreover, background activities monitored simultaneously by the non-ABCB1 substrate benzoic acid were not significantly affected (supplemental Fig. S6). Because *Saccharomyces cerevisiae* does not allow expression of functional PIN1 and ABCB19/MDR1/PGP19, both known to provide basipetal shoot (20) and acropetal root transport (51), most probably due to hyperglycosylation and unfavorable membrane compositions (5, 9), we expressed them in the fission yeast. *S. pombe* has recently been reported as the system of choice for plant auxin transporters, most likely because it offers polarized, sterol-enriched plasma-membrane microdomains and reduced glycosylation (36, 52). As described previously (36), ABCB1,19 and PIN1,2 were able to efficiently export IAA, resulting in 50–60% of vector control loading (Fig. 5*C*). As found with bakers' yeast, BUM and NPA inhibited IAA export (increase to vector control loading of roughly 40–50%) for ABCB1,19, whereas the increase in IAA loading for PIN1,2 was in the range found for the vector control (increase of 8–10%). This indicates that ABCBs, unlike PINs, are BUM/NPA targets, whereas again BUM at the same concentrations (10 μM) used was more efficient in ABCB inhibition than NPA.

NPA binding studies using *Arabidopsis* microsomes support the yeast transport data by demonstrating that ABCB1 and ABCB19 but again not PIN2 (87.0 ± 13.5% of wild type) function as NPA-binding proteins (Fig. 6*A*).[6] Interestingly, ABCB19

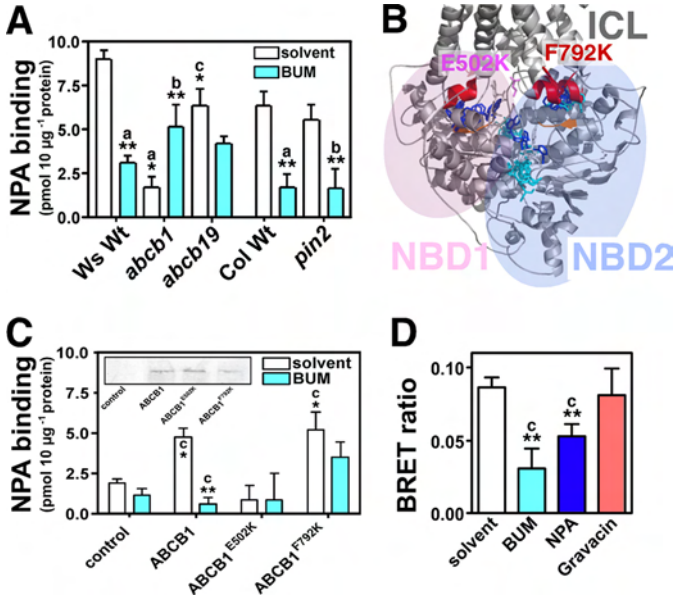

FIGURE 6. **BUM competes for NPA binding to ABCB-type auxin exporters.** *A*, BUM competes for NPA binding to wild type and *pin2* microsomes but to a lesser extent to *abcb* membranes (mean ± S.E. (*error bars*); $n = 4$). *B*, *in silico* drug binding to the N- and C-terminal ABCB1 nucleotide binding folds (NBD1 and -2) suggest overlapping and distinct inhibitor binding pockets for BUM (cyan) and NPA (*blue*). Note that NPA docks to pockets flanked by coupling helices (*red*) and Q loop (*orange*) of NBD1 and NBD2, whereas BUM docks only to the pocket corresponding to NBD2. Relevant residues Glu^{502} and Phe^{792} mutagenized under *C* are represented as *pink* and *red sticks*. *C*, site-directed mutagenesis of functional key residues predicted under *B* abolishes NPA/BUM binding (E502K) or reduces BUM competition (F792K); mean ± S.E. ($n = 4$). ABCB1 expression validated by Western analysis using anti-ABCB1/19 (5) is not significantly altered (*inset*). *D*, BUM, like NPA (each 5 μM), disrupts TWD1-ABCB1 interaction monitored by yeast BRET assays, whereas gravacin had only minor effects (mean ± S.E.; $n = 4$). Significant differences (analysis of variance using Tukey's test for multiple comparisons: $p < 0.001$ (*a*); $p < 0.01$ (*b*); $p < 0.05$ (*c*)) from wild type (*A*) or vector controls (*C*) or between inhibitor and solvent treatments are indicated by *one* or *two asterisks*, respectively.

(70.4 ± 10.8% of wild type) contributes less to NPA binding compared with ABCB1 (19.1 ± 6.5%), which is in contrast to previous data that determined ABCB19 as the primary NBP (23). However, the previous study employed different starting material and microsomal preparations for the binding studies that might influence individual ABCB abundance (23). Importantly, BUM competes drastically for NPA binding on both wild type ecotypes (65–73% reduction) and *pin2* microsomes (70%) but not on *abcb1* and only to a minor, non-significant degree on *abcb19* membranes. NPA binding and BUM competition is specific because binding of the nonspecific control, BA, assayed in parallel was a factor 10 lower, whereas BUM competition was strongly reduced on wild-type (25–58% reduction) and *pin2* (34% reduction) membranes (supplemental Fig. S7). Enhanced NPA binding caused by BUM competition on *abcb1* membranes might be indirect because the same tendency was found with BA. In line with this, our previous work has demonstrated that single loss of *abcb* or *pin* functionality reduces the transport specificity and NPA sensitivity of the ABCB-PIN export complex (9).

In order to mechanistically understand functional differences between BUM and NPA inhibitor activities, we computed BUM and NPA docking to the *Arabidopsis* ABCB1 structure that was modeled on the crystal structure of ABCB-related multidrug efflux pump Sav1866 (53). In the *in silico* analyses,

[6] Note that due to the sterility of homozygous *pin1* it is not possible to gain enough material to perform binding assays for *pin1*.

Downloaded from www.jbc.org at SMAC Consortium - University of ZÃƒÂ¼rich, on October 25, 2010

both inhibitors dock predominantly to both nucleotide binding domains (NBDs), whereas only minor apparent binding was found with the transmembrane domains (TMDs; not shown). NPA was predicted to bind interestingly primarily to grooves between coupling helices and Q loops (Fig. 6*B*), the main ABCB mechanics connecting NBDs and TMDs. In contrast, BUM was only predicted to dock to the corresponding pocket of NBD2 and additionally to an NBD1-NBD2 interface. Interestingly, BUM additionally has an apparent high affinity (around −50 kcal/mol) to a second NBD1-NBD2 interface where no NPA binding was predicted; this might account for its severe inhibition.

In order to experimentally validate our assumptions from *in silico* structure modeling and drug binding, we chose to neutralize key residues Glu^{502} and Phe^{792} situated in the ABCB1 cross-loop and coupling helix of NBD2 (53) by site-directed mutagenesis and measure subsequent NPA binding. Not unexpectedly, the E502K mutation abolished NPA binding and thus also BUM competition because mutations in the cross-loop have been suggested to alter drastically ABCB architecture (53). More interestingly, F792K mutagenesis in the C-terminal coupling helix did not affect NPA binding but significantly reduced BUM competition. This suggests that a single point mutation is able to exclude selectively BUM (but not NPA) from a putative BUM/NPA binding pocket (Fig. 6*B*). Although one should keep in mind that the drastic mutagenesis in essential mechanical key units of ABCB1, such as the cross-loop and the coupling helix, might as such affect fundamentally the functional interaction of NBDs and TMDs, our data provide a mechanistically explanation for overlapping and distinct effects of BUM/NPA on plant physiology development.

NPA was recently demonstrated to block ABCB-mediated auxin export by disrupting TWD1-ABCB1 interaction (5, 11). Not surprisingly, BUM also disrupted TWD1-ABCB1 interaction as monitored by established yeast BRET assays (11) (Fig. 6*D*). The fact that, based on docking studies, BUM probably binds, like NPA, to the ABCB1 NBD2 is in line with experimental data (5, 11, 12) and recent modeling of TWD1-ABC interfaces (54). More severe disruption, probably caused by BUM binding to NBD1-NBD2 interfaces, suggests that BUM achieves TWD1-ABCB1 disruption either by long range, intramolecular movements proposed for ABCBs (53, 55) or by binding to TWD1 in analogy to NPA (11). Although *twd1* is gravacin-insensitive (23), gravacin does not disrupt TWD1-ABCB1 interaction. Therefore, TWD1 is apparently not a direct target of gravacin as has been proposed recently (23).

DISCUSSION

Recent analyses of PIN and ABCB transport mechanisms suggest independent (or sometimes even opposite) and at certain domains additive and synergistic actions (9, 10). In this study, we have identified by means of chemical genomics a novel ATI that efficiently blocks auxin-related plant physiology and development. Quantification of physiological parameters, drug binding, and transport data indicates that ABCBs, primarily ABCB1, are direct BUM/NPA targets, whereas PINs are apparently less affected, which is in agreement with previous findings on NPA (14, 22, 23). This makes BUM a valuable tool for auxin research, allowing differentiation between ABCB- and PIN-mediated efflux systems. On the other hand, our work also suggests that pin-formed inflorescences, which are caused by BUM and NPA and that phenocopy *PIN1* loss-of-function mutations are primarily caused by ABCB transport inhibition of the functional ABCB-PIN efflux complex.

Our findings also demonstrate that BUM inhibition, like NPA inhibition, is light-dependent. This leads to the suggestion that ABCBs, obviously the cellular targets of BUM- and NPA-induced inhibition in *Arabidopsis*, are part of a light-controlled developmental pathway, which is in agreement with the concept that auxin has a more important role in elongation and bending responses in the light (44, 45). This concept was recently genetically supported by demonstrating that the photoreceptors, phytochromes and cryptochromes, regulate differential growth of *Arabidopsis* hypocotyls in an ABCB-dependent manner (45).

In many physiological respects and partially also structurally, BUM resembles NPA functionality. Based on our transport and drug binding data, both have a stronger effect on ABCB1 than on ABCB19 (Figs. 5 and 6). However, BUM has the advantage of not showing activation of plant growth at lower concentrations and acting roughly a factor of 30 stronger than NPA, which seems to be mainly caused by apically shifted root influx maxima. This again might be the result of altered binding preferences or affinities to the ABCBs. An alternative, simpler explanation that we cannot rule out at the moment is that BUM, being less hydrophobic compared with NPA, has a higher solubility. BUM shares this higher apparent solubility with the phytotropin l-(2′-carboxyphenyl)-3-phenylpropane-1,3-dione, which competes for the same binding site and does affect the same processes of auxin transport and geotropic curvature as NPA (56). However, based on our binding, the primary BUM target seems to be ABCB1. This makes BUM complementary to NPA that has been shown to affect besides ABCB19 also other ABCBs (5, 22, 57). Most interestingly, BUM reveals a more drastic effect (even at lower concentrations) on root transport (Fig. 5) and root elongation (Fig. 2) than found in the hypocotyl in comparison with NPA, which shows an inverse behavior. The molecular reasons are unknown and under current investigation. However, this finding is in agreement with higher ABCB19 expression in the hypocotyl (9) and a lower inhibition ABCB19 by BUM compared with ABCB1.

BUM apparently also acts differently compared with the recently identified ATI, gravacin, which primarily inhibits ABCB19 (23). However, as shown by BRET analysis, BUM, unlike gravacin, also alters TWD1 function, suggesting that BUM might indirectly also regulate ABCB19 activity by disrupting TWD1-ABCB19 interaction. Another advantage is that BUM, unlike gravacin, apparently does not interfere with ABCB trafficking.

Besides its academic usage as an ATI and its obvious potential as powerful weed herbicide, BUM might have a direct clinical impact because multidrug resistance toward many anticancer drugs is largely caused by human ABCB1, leading often to chemotherapy ineffectiveness. Interestingly, human and plant ABCBs share broad inhibitor sensitivities, which was demonstrated for the flavonol quercetin, which acts both as modulator of auxin transport and as inhibitor of mammalian

Downloaded from www.jbc.org at SMAC Consortium - University of ZÃƒÂ¼rich, on October 25, 2010

and plant ABCBs, and for clinically relevant ABCB inhibitors, like cyclosporine A and verapamil (5, 12). Based on our findings, plant ABCB inhibitors, such as BUM and NPA, are therefore *bona fide* human ABCB inhibitors that might suppress multidrug resistance when co-administered with anti-cancer drugs.

Acknowledgments—We thank A. Murphy for gravacin, S. pombe strains, and expression plasmids, E. Martinoia for discussion and support, and the Korean Chemical Bank for the chemical library donation.

REFERENCES

1. Blakeslee, J. J., Peer, W. A., and Murphy, A. S. (2005) *Curr. Opin. Plant Biol.* **8,** 494–500
2. Kepinski, S., and Leyser, O. (2005) *Curr. Biol.* **15,** R208–R210
3. Vieten, A., Sauer, M., Brewer, P. B., and Friml, J. (2007) *Trends Plant Sci.* **12,** 160–168
4. Benjamins, R., and Scheres, B. (2008) *Annu. Rev. Plant. Biol.* **59,** 443–465
5. Geisler, M., Blakeslee, J. J., Bouchard, R., Lee, O. R., Vincenzetti, V., Bandyopadhyay, A., Titapiwatanakun, B., Peer, W. A., Bailly, A., Richards, E. L., Ejendal, K. F., Smith, A. P., Baroux, C., Grossniklaus, U., Müller, A., Hrycyna, C. A., Dudler, R., Murphy, A. S., and Martinoia, E. (2005) *Plant J.* **44,** 179–194
6. Geisler, M., and Murphy, A. S. (2006) *FEBS Lett.* **580,** 1094–1102
7. Petrásek, J., Mravec, J., Bouchard, R., Blakeslee, J. J., Abas, M., Seifertová, D., Wisniewska, J., Tadele, Z., Kubes, M., Covanová, M., Dhonukshe, P., Skupa, P., Benková, E., Perry, L., Krecek, P., Lee, O. R., Fink, G. R., Geisler, M., Murphy, A. S., Luschnig, C., Zazímalová, E., and Friml, J. (2006) *Science* **312,** 914–918
8. Blilou, I., Xu, J., Wildwater, M., Willemsen, V., Paponov, I., Friml, J., Heidstra, R., Aida, M., Palme, K., and Scheres, B. (2005) *Nature* **433,** 39–44
9. Blakeslee, J. J., Bandyopadhyay, A., Lee, O. R., Mravec, J., Titapiwatanakun, B., Sauer, M., Makam, S. N., Cheng, Y., Bouchard, R., Adamec, J., Geisler, M., Nagashima, A., Sakai, T., Martinoia, E., Friml, J., Peer, W. A., and Murphy, A. S. (2007) *Plant Cell* **19,** 131–147
10. Mravec, J., Kubes, M., Bielach, A., Gaykova, V., Petrásek, J., Skůpa, P., Chand, S., Benková, E., Zazímalová, E., and Friml, J. (2008) *Development* **135,** 3345–3354
11. Bailly, A., Sovero, V., Vincenzetti, V., Santelia, D., Bartnik, D., Koenig, B. W., Mancuso, S., Martinoia, E., and Geisler, M. (2008) *J. Biol. Chem.* **283,** 21817–21826
12. Bouchard, R., Bailly, A., Blakeslee, J. J., Oehring, S. C., Vincenzetti, V., Lee, O. R., Paponov, I., Palme, K., Mancuso, S., Murphy, A. S., Schulz, B., and Geisler, M. (2006) *J. Biol. Chem.* **281,** 30603–30612
13. Cox, D. N., and Muday, G. K. (1994) *Plant Cell* **6,** 1941–1953
14. Luschnig, C. (2001) *Curr. Biol.* **11,** R831–833
15. Michalke, W., Katekar, G. F., and Geissler, A. E. (1992) *Planta* **187,** 254–260
16. Petrásek, J., Cerná, A., Schwarzerová, K., Elckner, M., Morris, D. A., and Zazímalová, E. (2003) *Plant Physiol.* **131,** 254–263
17. Sussman, M. R., and Gardner, G. (1980) *Plant Physiol.* **66,** 1074–1078
18. Bernasconi, P., Patel, B. C., Reagan, J. D., and Subramanian, M. V. (1996) *Plant Physiol.* **111,** 427–432
19. Lomax, T. L., Muday, G. K., and Rubery, P. H. (1995) in *Plant Hormones: Physiology, Biochemistry, and Molecular Biology* (Davies, P. J., ed) pp. 509–530, Kluwer, Dordrecht, The Netherlands
20. Okada, K., Ueda, J., Komaki, M. K., Bell, C. J., and Shimura, Y. (1991) *Plant Cell* **3,** 677–684
21. Geldner, N., Friml, J., Stierhof, Y. D., Jürgens, G., and Palme, K. (2001) *Nature* **413,** 425–428
22. Nagashima, A., Uehara, Y., and Sakai, T. (2008) *Plant Cell Physiol.* **49,** 1250–1255
23. Rojas-Pierce, M., Titapiwatanakun, B., Sohn, E. J., Fang, F., Larive, C. K., Blakeslee, J., Cheng, Y., Cutler, S. R., Peer, W. A., Murphy, A. S., and Raikhel, N. V. (2007) *Chem. Biol.* **14,** 1366–1376
24. Murphy, A. S., Hoogner, K. R., Peer, W. A., and Taiz, L. (2002) *Plant Physiol.* **128,** 935–950
25. Noh, B., Murphy, A. S., and Spalding, E. P. (2001) *Plant Cell* **13,** 2441–2454
26. Armstrong, J. I., Yuan, S., Dale, J. M., Tanner, V. N., and Theologis, A. (2004) *Proc. Natl. Acad. Sci. U.S.A.* **101,** 14978–14983
27. Zhao, Y., Dai, X., Blackwell, H. E., Schreiber, S. L., and Chory, J. (2003) *Science* **301,** 1107–1110
28. Norambuena, L., Hicks, G. R., and Raikhel, N. V. (2009) *Methods in Molecular Biology* **495,** 133–143
29. Robert, S., Chary, S. N., Drakakaki, G., Li, S., Yang, Z., Raikhel, N. V., and Hicks, G. R. (2008) *Proc. Natl. Acad. Sci. U.S.A.* **105,** 8464–8469
30. Surpin, M., Rojas-Pierce, M., Carter, C., Hicks, G. R., Vasquez, J., and Raikhel, N. V. (2005) *Proc. Natl. Acad. Sci. U.S.A.* **102,** 4902–4907
31. Savaldi-Goldstein, S., Baiga, T. J., Pojer, F., Dabi, T., Butterfield, C., Parry, G., Santner, A., Dharmasiri, N., Tao, Y., Estelle, M., Noel, J. P., and Chory, J. (2008) *Proc. Natl. Acad. Sci. U.S.A.* **105,** 15190–15195
32. Luschnig, C., Gaxiola, R. A., Grisafi, P., and Fink, G. R. (1998) *Genes Dev.* **12,** 2175–2187
33. Lewis, D. R., and Muday, G. K. (2009) *Nat. Protoc.* **4,** 437–451
34. Mancuso, S., Marras, A. M., Magnus, V., and Baluska, F. (2005) *Anal. Biochem.* **341,** 344–351
35. Santelia, D., Vincenzetti, V., Azzarello, E., Bovet, L., Fukao, Y., Düchtig, P., Mancuso, S., Martinoia, E., and Geisler, M. (2005) *FEBS Lett.* **579,** 5399–5406
36. Yang, H., and Murphy, A. S. (2009) *Plant J.* **59,** 179–191
37. Morris, D. A. (2000) *Plant Growth Regul.* **32,** 161–172
38. Santelia, D., Henrichs, S., Vincenzetti, V., Sauer, M., Bigler, L., Klein, M., Bailly, A., Lee, Y., Friml, J., Geisler, M., and Martinoia, E. (2008) *J. Biol. Chem.* **283,** 31218–31226
39. Benková, E., Michniewicz, M., Sauer, M., Teichmann, T., Seifertová, D., Jürgens, G., and Friml, J. (2003) *Cell* **115,** 591–602
40. Bhalerao, R. P., Eklöf, J., Ljung, K., Marchant, A., Bennett, M., and Sandberg, G. (2002) *Plant J.* **29,** 325–332
41. Casimiro, I., Beeckman, T., Graham, N., Bhalerao, R., Zhang, H., Casero, P., Sandberg, G., and Bennett, M. J. (2003) *Trends Plant Sci.* **8,** 165–171
42. Rashotte, A. M., DeLong, A., and Muday, G. K. (2001) *Plant Cell* **13,** 1683–1697
43. Achard, P., Vriezen, W. H., Van Der Straeten, D., and Harberd, N. P. (2003) *Plant Cell* **15,** 2816–2825
44. Jensen, P. J., Hangarter, R. P., and Estelle, M. (1998) *Plant Physiol.* **116,** 455–462
45. Nagashima, A., Suzuki, G., Uehara, Y., Saji, K., Furukawa, T., Koshiba, T., Sekimoto, M., Fujioka, S., Kuroha, T., Kojima, M., Sakakibara, H., Fujisawa, N., Okada, K., and Sakai, T. (2008) *Plant J.* **53,** 516–529
46. Rashotte, A. M., Brady, S. R., Reed, R. C., Ante, S. J., and Muday, G. K. (2000) *Plant Physiol.* **122,** 481–490
47. Swarup, R., Kramer, E. M., Perry, P., Knox, K., Leyser, H. M., Haseloff, J., Beemster, G. T., Bhalerao, R., and Bennett, M. J. (2005) *Nat. Cell Biol.* **7,** 1057–1065
48. Ottenschläger, I., Wolff, P., Wolverton, C., Bhalerao, R. P., Sandberg, G., Ishikawa, H., Evans, M., and Palme, K. (2003) *Proc. Natl. Acad. Sci. U.S.A.* **100,** 2987–2991
49. Peer, W. A., Bandyopadhyay, A., Blakeslee, J. J., Makam, S. N., Chen, R. J., Masson, P. H., and Murphy, A. S. (2004) *Plant Cell* **16,** 1898–1911
50. Vieten, A., Vanneste, S., Wisniewska, J., Benková, E., Benjamins, R., Beeckman, T., Luschnig, C., and Friml, J. (2005) *Development* **132,** 4521–4531
51. Wu, G., Lewis, D. R., and Spalding, E. P. (2007) *Plant Cell* **19,** 1826–1837
52. Titapiwatanakun, B., Blakeslee, J. J., Bandyopadhyay, A., Yang, H., Mravec, J., Sauer, M., Cheng, Y., Adamec, J., Nagashima, A., Geisler, M., Sakai, T., Friml, J., Peer, W. A., and Murphy, A. S. (2009) *Plant J.* **57,** 27–44
53. Dawson, R. J., and Locher, K. P. (2006) *Nature* **443,** 180–185
54. Granzin, J., Eckhoff, A., and Weiergräber, O. H. (2006) *J. Mol. Biol.* **364,** 799–809
55. Locher, K. P. (2009) *Philos. Trans. R. Soc. Lond. B. Biol. Sci.* **364,** 239–245
56. Katekar, G. F., and Geissler, A. E. (1980) *Plant Physiol.* **66,** 1190–1195
57. Terasaka, K., Blakeslee, J. J., Titapiwatanakun, B., Peer, W. A., Bandyopadhyay, A., Makam, S. N., Lee, O. R., Richards, E. L., Murphy, A. S., Sato, F., and Yazaki, K. (2005) *Plant Cell* **17,** 2922–2939

Downloaded from www.jbc.org at SMAC Consortium - University of ZÃƒÂ¼rich, on October 25, 2010

Chapter 4:

TWISTED DWARF1 regulates auxin transport by interfering with the ACTIN7 cytoskeleton

Chapter 4

Personal Contributions

Figure 2: Growth measurements and imaging

Figure 3: Trichome branching evaluation

Figure 4: Auxin transport assays, gravitropism, and apical hook measurement

Figure 5: Drug binding and plant growth evaluation

Figure 6: IAA levels and localization, and starch accumulation assays

Figure 7B: Actin imaging

Figure 8: ABCB19 and PIN2 imaging

Figure S2: Growth assays

Figure S3: Lateral root evaluation

Figure S4: Root gravitropism assays

Figure S5: Plant growth evaluation

Figure S6: Lateral root evaluation

Title page

TWISTED DWARF1 regulates auxin transport by interfering with the ACTIN7 cytoskeleton

Valpuri Sovero[1], Yoichiro Fukao[2], Markus Schlicht[3,5], Frantisek Baluska[3], Flora Moreau[4], Clément Thomas[4], Stephan Pollmann[6,7], Stefano Mancuso[8] and Markus Geisler[1,9]

[1] Zurich-Basel Plant Science Center and University of Zurich, Institute of Plant Biology, Zurich, Switzerland
[2] Laboratory of Cell Dynamics, Graduate School of Bioagricultural Sciences Nagoya University, Nagoya, Japan.
[3] IZMB; Rheinische Friedrich-Wilhelms-Universität; Bonn, Germany
[4] Plant Molecular Biology, CRP-Sante, Batiment modulaire, L-1526 Luxembourg
[5] Max Planck Institute for Plant Breeding Research, Carl-von-Linné-Weg 10, D-50829 Köln, Germany
[6] Ruhr-Universität Bochum, Lehrstuhl für Pflanzenphysiologie, Germany
[7] Centro de Biotecnología y Genómica de Plantas, Campus de Montegancedo, 28223 Pozuelo de Alarcón, Madrid, Spain
[8] Department of Horticulture, University of Firenze, Sesto Fiorentino, Italy
[9] to whom correspondence should be addressed: markus.geisler@ botinst.uzh.ch

Key words: actin, ACTIN7, cytoskeleton, auxin transport inhibitor, TWD1

Abstract

ABCB-mediated long-range transport of auxin has been shown to be dependent on physical interaction with the FKBP42, TWISTED DWARF1 (TWD1), documented by a close overlap between *twd1* and *abcb1 abcb19* dwarf phenotypes. However, *abcb1abcb19* organs lack an undirected helical rotation of epidermal layers that is diagnostic for *twd1*.
Here, by means of co-immunoprecipitation and mass spectrometry we have identified ACTIN7 as a physical interactor of the auxin efflux complex characterized by TWD1. *Twd1* and *act7* single mutants share overlapping auxin-related growth phenotypes, like di-branched trichomes and reduced root lengths. The latter is over-exaggerated in the *twd1 act7* double mutant that shows extreme dwarfism. These defects are most likely caused by elevated auxin efflux from *act7* cells enhancing basipetal root transport and thus resulting in elevated auxin levels.
Twd1 roots show unevenly labeled cross-ends but strong actin bundling in the *twd1* stele absent in the wild type and *abcb1 abcb19,* suggesting that either de-regulated actin bundling and/or mistargeted actin filaments might be the primary cause of the cellular twist. Interestingly, and in agreement with previous work showing high-affinity NPA binding proteins to interact with the actin cytoskeleton, *twd1,* like *act7,* bears reduced NPA binding and is widely insensitive toward NPA. In summary, our data provide evidence that TWD1 functions as an integrator of NPA action effecting actin stability and thus downstream dynamics of auxin efflux transporter vesicles.

Introduction

The cell-to-cell or polar transport of the plant hormone auxin (PAT) is one of the primary determinants of plant architecture and functionality (Friml and Sauer, 2008)Due to the chemical properties of the major relevant auxin, IAA, PAT is controlled on the efflux level, which is catalyzed by members of the PIN- (PIN-FORMED) and the B subfamily of ABC transporters, called ABCBs/PGPs/MDRs. PINs and ABCBs export auxin in an independent and interactive fashion (Bandyopadhyay et al., 2007; Blakeslee et al., 2007). ABCB1/PGP1 and ABCB19/PGP19/MDR1-mediated long-range transport of auxin has been shown to be dependent on physical interaction with the FKBP42 (FK506-binding protein), TWISTED DWARF1 (TWD1) (Bouchard et al., 2006; Bailly et al., 2008), which is documented by a close overlap between *twd1* and *abcb1abcb19* dwarf phenotypes and undirected helical disorientation of growth at later stages. However, *abcb1,19* does not show any twisted organization of the epidermal layer at the cellular level. Most of the twisted mutants with fixed handedness have been shown to have defects in microtubule functions whereas mutants that twist in non-fixed handedness appear to be defective in auxin signaling or transport (Ishida et al., 2007). However, the molecular reasons underlying this handed helical rotation in *twd1* is unknown.

Our knowledge on the mechanisms of PAT was broadly enlarged by the usage of synthetic auxin transport inhibitors (ATIs), such as 1-N-naphtylphtalamic acid (NPA), a non-competitive auxin efflux inhibitor (Cox and Muday, 1994; Butler et al., 1998). High NPA concentrations cause inhibition of auxin efflux catalyzed by ABCB1 and ABCB19 (Geisler et al., 2005; Bouchard et al., 2006; Geisler and Murphy, 2006). Independently, ABCB1 and ABCB19 have been identified as NPA targets (Geisler et al., 2005; Rojas-Pierce et al., 2007; Nagashima et al., 2008) while NPA obviously has no effect on the activity of members of the PIN family (Rojas-Pierce et al., 2007; Kim et al., 2010). Importantly, interaction of ABCB1 with its positive regulatory protein, TWD1, is disrupted by nM NPA concentrations resulting in loss of ABCB1 activation (Bailly et al., 2008). Beside ABCB1, TWD1 itself also binds NPA, which is inline with the identification of two different NPA-binding affinities on the plasma membrane (Michalke et al., 1992), the transporter itself and the NPA-binding regulatory subunit.
Although the exact number and the identity of the NPA binding proteins (NBPs) is still controversial (Luschnig, 2001), several *in vitro* and *in vivo* lines of evidence support the concept that the peripheral NBP is associated with the cytoskeleton: First, extraction of plasma membrane vesicles with Triton X-100 resulted in retention of NPA binding activity in the detergent-insoluble cytoskeletal pellet, but the chaotropic reagent KI released NPA binding activity and actin. Second, treatment of a cytoskeletal pellet with cytochalasin D doubled NPA binding activity in the resulting supernatant (Cox and Muday, 1994). Third, phalloidin, altering actin polymerization, increased both filamentous actin (F-actin) and NPA-binding activity, while cytochalasin D decreased both F-actin and NPA-binding activity in cytoskeletal pellets. Fourth, the microtubule stabilizing drug taxol increased pelletable tubulin, but did not alter either the amount of pelletable actin or NPA-binding activity,

excluding an involvement of microtubuli. Fifth, treatment of etiolated zucchini hypocotyls with cytochalasin D decreased the amount of auxin transport and its regulation by NPA (Dixon et al., 1996). These experimental results are consistent with an actin cytoskeletal association of the NBP and with the requirement of an intact actin cytoskeleton for maximal polar auxin transport *in vivo.*

Several lines of evidence support the concept that the machinery for transporting auxin is facilitated by actin dynamics. All auxin transporters have been shown to be constitutively recycled between the plasma membrane and endosomal compartments. The endocytosis step of PIN1 seems to depend on actin filaments as cytochalasin D was shown to prevent PIN1 mislocalization caused by brefeldin A (BFA) treatment (Geldner et al., 2001). Moreover, auxin transport inhibitors, like TIBA, interfere with this trafficking, although neither cytochalasin D nor NPA alone were efficient (Geldner et al., 2001; Dhonukshe et al., 2008). IAA blocks endocytotic recycling resulting in enhances in export in line with the canalization hypothesis (Paciorek et al., 2005)
A recent study revealed that ATIs TIBA and PBA blocked auxin transport by stabilizing actin bundles and thus cell dynamics. This action was surprisingly conserved among plants, yeast and mammalian cells (Dhonukshe et al., 2008). Surprisingly, NPA had no actin stabilizing effect, suggesting a distinct mode of action (Dhonukshe et al., 2008). However, these findings are in conflict with older data showing an association of NPA with the cytoskeleton (Cox and Muday, 1994) and others showing that actin bundling enhances the sensitivity toward NPA (Maisch and Nick, 2007).

The cytoskeleton, which consists primarily of microtubules and actin filaments, has been studied in detail because of its primary role in determining essential processes such as the division, shape, and expansion of cells (Blancaflor et al., 2006). Several lines of evidence support the concept that the actin cytoskeleton functionally or physically directly interferes with the auxin efflux machinery: First, as described above, the NPA-binding protein that is a part of the auxin efflux complex is associated with the actin cytoskeleton. Second, the cycling of efflux catalysts that forms the basis for their polar expression is guided by actin filaments. Third, auxin responses are defective in ROP GTPase mutants, known to be implicated in actin polymerization (Xu and Scheres, 2005). And, fourth, actin isoform ACTIN7 (ACT7) is auxin responsive, required for callus formation, germination and root growth (Gilliland et al., 2003; Kandasamy et al., 2009).
These findings in summary suggest a role for the actin cytoskeleton in determining cell polarity, a key feature of auxin-controlled plant development. However, the mechanism underlying actin cytoskeleton stabilization triggered by ATIs remains unknown.

Results and Discussion

Identification of ACTIN7 as an interactor of the auxin efflux complex characterized by TWD1

Recently we have identified the AGC kinase PINOID as a relevant TWD1 interactor using a co-IP approach followed by shotgun mass spectrometry analysis using TAPa-tagged TWD1 (TAPa-TWD1). One of the specific interactors that was not further considered was ACTIN8 because its score was below chosen the cut-off of 30 (Henrichs et al. submitted). In a modified assay using, in contrast to the original protocol, MS analysis of individual, size-selected bands were cut out of the silver-stained gel prior to MS analysis (Fig. S1A). In combination with vector control subtraction we were thus further able to reduce background and gain specificity. Beside TWD1 as an obvious dominant pulled-down protein (protein score of 92, 15% coverage; Fig. 1), we found an translocon of the chloroplast inner envelope, TIC110, and the large subunit of RuBisCo, a common Co-IP contamination, that were both considered as being unspecific. Of major interest were the Rab GTPase RabE1b/Rab8D (protein score of 212) and ACT7 (protein score of 39, 6% coverage) that was chosen for this analysis as, of the actin isoforms, it is the most strongly expressed in young plant tissues, induced by auxin and required for normal callus formation (Kandasamy et al., 2001). Further, *act7* alleles show a dramatic reduction in root growth, increased root twisting and waving, resembling *twd1*. Also, *act7*-4 root apical cells were not in straight files but contained oblique junctions (Gilliland et al., 2003).
Arabidopsis thaliana encodes 10 actin genes of which 8 gene products have been studied in detail. Three vegetative actins, ACT2, ACT7, and ACT8, build two ancient and highly divergent subclasses, while *ACT1, 3, 4, 11* and *ACT12* are reproductive actins (Kandasamy et al., 2009). Double *ACT7* mutant combinations were extremely dwarfed, with altered cell and organ morphology while *act2* crosses were totally root-hairless (e.g., *act2-1 act8-2*) suggesting that ACT7 was involved in root growth, epidermal cell specification, cell division, and root architecture, while ACT2 and ACT8 were essential for root hair tip growth (Kandasamy et al., 2009).

Identification of ACT7 as TAPa-TWD1 interactor does not necessarily imply direct physical interaction. In order to test this possibility and to verify the TAP data, we performed *in vitro* co-sedimentation assays using rabbit skeletal muscle actin and TWD1$^{1-337}$ protein (Henrichs et al. submitted). Using different salt and pH conditions and actin-TWD1 stoichiometries, only a very faint portion of TWD1 protein was pulled-down by actin. However, as this portion was also found in the absence of actin, we consider it as being unspecific. Moreover, TWD1 had no obvious impact on actin filament polymerization and depolymerization in classical fluorimetric assays (not shown).
This suggests that the PID-TWD1 interaction might be mediated via a third TWD1 interacting protein or a component that is absent in the in vitro assay.
However, using an identical protocol but root material instead of entire seedlings, we identified ACTIN7 and ACTIN8 with scores above 30 by shotgun mass spectrometry. Moreover, we identified independently ACTIN7 when we used entire seedlings that were exposed to a 2h gravistimulus.

Interestingly, ACT7 was also found with ABCB1-MYC (Mravec et al., 2008) but never with ABCB19-HA (Mravec et al., 2008) or PIN2-GFP (Xu and Scheres, 2005), the latter not shown to be a TWD1 interactor, suggesting that ACT7 interaction might be specific to the TWD1-ABCB1 complex.

Twd1 and _act7_ alleles show overlapping and opposite auxin related phenotypes

TWD1-ACT7 interaction, auxin-responsiveness together with the fact that *act7* seedlings resembled in some respects those of *twd1* prompted us to compare *act7* and *twd1* growth phenotypes and development in more detail. For this we used the strong *act7-4* allele (Gilliland et al., 2003; Kandasamy et al., 2009) and *twd1-1*, both in the Wassilewskija (Ws) ecotype throughout this study.

Both alleles share shorter roots under light (Fig. 1B, C). However, while *twd1* roots are longer in the dark (Fig. 1C; (Geisler et al., 2003)), this is obviously not the case for *act7*, suggesting no direct involvement in auxin transport. *Act7* roots were reported to show a twisting (Gilliland et al., 2003). When we quantified root twisting under our conditions, we found that act7 revealed essentially wt twisting (Fig. 2D) but owned a higher waving frequency (not shown) that might have led to this misinterpretation.

While *twd1* hypocotyls are extremely shortened (Fig. 1A-C, (Geisler et al., 2003)), *act7-4* hypocotyls are significantly longer at 8h light but not in the dark (Fig. 1B-C). Quantification of development revealed that the overall development was slightly reduced for root and shoot tissues (Fig. S2). In order to understand this discrepancy we measured cell lengths and cell numbers. While for roots we did not detect any significant differences, we found that *act7* hypocotyls had a factor 2 longer cells than *twd1* that itself showed 68% reduction compared to the wild type. This finding is also reflected by the adult plant that shows longer inflorescences under an 8h light cycle (not shown).

Next we investigated lateral root (LR) development, another hallmark of auxin-triggered development. In contrast to *twd1* showing roughly 130% more LRs (Fig. S3, S6; (Geisler et al., 2003)), *act7* produced significantly less LRs while LR emergence was only slightly effected (Fig. S3, S6).

Further we analyzed trichome branching as *Arabidopsis* trichomes that are unicellular structures that have been established as an ideal system in which to study actin-dependent growth in plant cells (Schellmann and Hülskamp, 2005). While wild type trichomes show a natural variation between one and four branches, both *act7* alleles showed a significant shift toward di-branched trichomes leading to a reduction of tri- and four-branched trichome appearance (Fig. 3) as reported before only for act8 act7 double mutants (Kandasamy et al., 2009). Strikingly, *act7-4* and *twd1-1* show widely identical trichome branching patterns.

To gain further genetic insight into the functional relationship between *TWD1* and *ACT7*, we crossed *twd1-1* and *act7-4* alleles. Homozygous *twd1 act7* plants were extremely stunted and difficult to propagate. Both root and shoots (hypocotyls) were shorter than their parent alleles, while root twisting was surprisingly exaggerated compared to *twd1*, suggesting in summary additive effects.

Twd1 and *act7* alleles show overlapping defects in auxin transport and auxin-regulated physiology

Overlapping auxin-related growth phenotypes of gene products linking auxin transport and the cytoskeleton and additive defects of the *twd1 act7* double mutant prompted us to quantify auxin transport in *act7*.

First, we quantified auxin efflux capacities from leaf protoplasts that has become a standard system for measuring cellular auxin efflux (Geisler et al., 2005). Loss-of *ACT7* function resulted in a significant 30-130% increase in auxin efflux shown for native IAA and synthetic NAA assayed in parallel and for both *act7* alleles tested (Fig. 4A). This was surprising as *twd1* was shown to have greatly reduced efflux capacities (Bouchard et al., 2006). However, this finding is inline with current models suggesting a tight mechanistic link between actin dynamics and auxin efflux (Muday, 2000; Blancaflor et al., 2006; Dhonukshe et al., 2008).

Second we measured basipetal PAT in the root (shoot-ward) and shoot (root-ward in hypocotyl) of *twd1* and *act7* alleles. In agreement with our unicellular system, we found significantly enhanced basipetal PAT (for both IAA and NAA) in the root *for act7-4* and *twd1* while the effect for the weaker *act7-1* allele was subtler (Fig. 4B). Surprisingly, we found the opposite for *act7* hypocotyls, which is in agreement with previous measurements using *twd1* (Geisler et al., 2003) and the finding that actin disruption inhibits PAT in the shoot (Muday and Murphy, 2002).

These defects in shoot and root auxin transport motivated us to assay apical hook opening and root gravitropism, both hallmarks of auxin-controlled plant physiology. Interestingly, neither hook opening nor root gravitropism were significantly affected in *act7* alleles, while *twd1* was agravitrope (Fig. 4D; (Bouchard et al., 2006; Bailly et al., 2008)). The first is in agreement with the pharmacological usage of actin-disrupting drugs that do not appear to have a significant effect on either root nor shoot gravitropism (reviewed in (Blancaflor et al., 2006)). However, we found that in analogy to *twd1* (Bailly et al., 2008) both *act7* alleles were significantly less sensitive toward the ATIs NPA and TIBA, compared to the wild type (Fig. 4D), also found with lateral root formation (Fig. S3).

ATIs and auxin partially rescue *act7* and *twd1* growth defects

Reduced sensitivities found for *twd1* and *act7* alleles toward ATIs prompted us to test ATI binding to microsomal fractions prepared from mutant alleles. As shown in (Bailly et al., 2008), specific NPA binding was slightly reduced in *twd1-1* but likewise in *act7-4* (Fig. 5A). This difference - although not significant - was specific, as it was not found with negative control benzoic acid (not shown). Also the flavonol and ATI, quercetin, did not bind to TWD1 or ACT7 as no significant difference was found with *twd1* or *act7* microsomes. This might reflect kingdom-wide differences between plant and mammalian actin isoforms and functionality as quercetin was found to tightly bind to mammalian actin (Böhl et al., 2005).

Therefore, we measured the impact of ATIs and auxins. Interestingly, IAA but

not synthetic auxins, NAA and 2.4-D, was able to partialy rescue hypocotyl and root growth reduction of *twd1* and *act7* alleles. Moreover, this rescue was found for 16h light but not found for seedlings grown in the dark or 8h light (Fig. S5). Interestingly, TIBA was mostly able to phenocopy this rescue as was found for *twd1* hypocotyls and *act7* roots while NPA and 2.4-D had mostly opposite effects (Fig. 5B). Finally, partial rescue with IAA and TIBA was also found for *act7* LR development (Fig. S6).
IAA and TIBA were recently suggested to regulate auxin transport by enhancing actin filament bundling while NPA and 2.4-D had a debundling effect (Dhonukshe et al., 2008). In order to test this concept, we employed actin cytoskeleton-stabilizing and -destabilizing drugs, jaspakinolide and latrunculin B, respectively. While latrunculin B used at 1 µM had only mild effects on hypocotyl elongation, root elongation was drastically blocked but showed no significant differences between genotypes. Jasplakinolide had only mild effects on wt and *act7-4* but drastically blocked *twd1* root elongation. Interestingly, this inhibition could be phenocopied by addition of microtubuli-stabilizing agent, paclitaxel (taxol), suggesting functional actin and microtubuli cytoskeleton interaction in regulation of auxin transport (Hasenstein et al., 1999).

Loss-of ACT7 alters auxin levels and responses
Defects in auxin transport on one hand and plant development and performance on the other motivated us to analyze free IAA levels in *act7* seedlings. Both root (70%) and shoot IAA levels (26%) were significantly elevated in *act7-4* alleles, while this was only found for *twd1* roots (Fig. 6A; (Bouchard et al., 2006)). In agreement, activation of the auxin-responsive DR5-GFP element was slightly enhanced in the *act7-4* root tip but unchanged in *act7-1* (Fig. 6B; (Bouchard et al., 2006)).
Disruption of the F-actin cytoskeleton limits statolith movement in *Arabidopsis* hypocotyls (Palmieri and Kiss, 2005). In order to investigate if this would be the case also for *act7*, we decorated columella statoliths using Lugol stain. While *act7-1* showed only a subtle reduction, we were unable to detect any statolits in the *act7-4* columella cells but instead found a strong starch stain in the root tip above. This pattern mimics a Lugol stain after IAA treatment and is inline with highly elevated auxin levels in *act7-4* roots (Fig. 6A).

***Twd1* roots show altered actin cytoskeleton patterns**
Our findings so far suggest that TWD1 might be the ATI (and auxin) target that physically links the effect of ATIs on actin cytoskeleton bundling and auxin transport. In this model, loss-of-*TWD1* would result in either de-regulated actin bundling and/or mistargeted actin filaments finally resulting in a cellular twist.
Our assumption is supported by actin imaging of *twd1* roots. First, whole-mount immunolocalizations using polyclonal anti-actin (Schlicht et al., 2006). While *twd1* meristematic and transition zones on the first view revealed no major differences in actin labeling, however, 3D projections of epidermal cells in the transition zone mark uniformly labeled cross-end poles in wild-type and *abcb1 abcb19* but unevenly labeled cross-ends of *twd1* cells (arrows in Fig. 7A). Median section of early elongation zones again show unevenly labeled cross-ends of *twd1* cells but strong actin bundling in the *twd1* stele (asterisks)

absent in the wild type and *abcb1 abcb19.* Moreover, epidermal cells of *twd1* early elongation and transition zones show the presence of strong actin-spots of unclear function.
Second, in order to further substantiate these cytoskeletal defects in *twd1*, we imaged the actin cytoskeleton using the mouse talin-GFP (mTn-GFP; (Kost et al., 1998)). As found with whole-mount ILs, the stele of *twd1* roots revealed a higher actin bundling. Third, due to the fact that the mTn-GFP has received some criticism (Ketelaar et al., 2004; Thomas et al., 2009), we backed up these findings using the well-established fimbrin derived actin marker ABD2-GFP (fABD2-GFP; (Sheahan et al., 2004)). As reported before (Gilliland et al., 2003; Kandasamy et al., 2009) we found reduced actin labeling in columella and stele cells of *act7-4* roots. More interestingly, and in analogy to previous imaging techniques we again found more dense actin bundling in the *twd1* stele.

Conclusion

In summary, by means of co-IP and mass spectrometry we have identified ACT7 as a physical interactor of the auxin efflux complex characterized by TWD1 (Fig. 1). *Twd1* and *act7* single mutants share overlapping auxin-related growth phenotypes, like di-branched trichomes (Fig. 3) and reduced root lengths (Fig. 2). The later is over-exaggerated in the *twd1 act7* double mutant that shows an extreme dwarf phenotype. In contrast to *twd1, act7* hypocotyls are longer, which is caused by enhanced cell elongation (Fig. 2). Shorter roots but elongated hypocotyls are probably the result of inhibition of root- but enhancement of shoot cell elongation, respectively, caused by elevated free auxin levels in *act7* roots and hypocotyls (Fig. 6). These are most likely the result of higher basipetal root but reduced hypocotyl PAT (Fig. 6).
The question that arises is how genetic disruption of a component of the actin cytoskeleton can interfere with auxin transport. The most obvious answer might come from the finding that cellular auxin efflux is elevated from *act7* cells (Fig. 4). This leaves essentially two possibilities: either efflux transporters of the ABCB- or PIN subclass are up-regulated in *act7* or stabilized on the plasma membrane. The first option could be ruled out as expression of ABCB19 and PIN2 are even slightly reduced in *act7* or essentially unchanged (Fig. 8), suggesting that exporters are trapped on the PM.
As members of both exporter families have been shown to constantly cycle between the PM and internal compartments, the most likely mechanism how this might happen is that disruption of the actin cytoskeleton either chemically or genetically results in block of endocytotic recycling. Indeed, F-actin disruption was shown to alter PIN cycling (Geldner et al., 2001; Friml et al., 2002). Although the function of actin in endocytosis is far from being understood, our data support the concept that TWD1 as positive regulator of ABCB-mediated auxin efflux is a key component in linking auxin transport and actin (here: ACT7) cytoskeleton action.

Another important question is, how ATIs (and auxin) interfere with auxin cytoskeleton dynamics. The effect of ATIs on the actin cytoskeleton bundling does not seem to be direct because the amount of polymerized actin at the

steady state was found to be unaffected by TIBA or PBA *in vitro* (Dhonukshe et al., 2008) supporting a model where ATIs function either by activating an actin filament stabilizer or by deactivating an actin filament-destabilizing factor. Potential targets include actin-binding proteins, whose activities directly regulate actin cytoskeleton organization and dynamics (Winder and Ayscough, 2005). Previous work suggested that high-affinity NPA binding proteins interact with the actin cytoskeleton (Butler et al., 1998; Hu et al., 2000; Muday, 2000).

Although at the current state we cannot exclude that ACT7-TWD1 interaction is indirect, TWD1 fulfills in principle both criteria: ACT7 was isolated as a valid TWD interactor and is an NPA-binding protein (Bailly et al., 2008). Recent binding analysis using highly pure protein suggests an apparent k*D* of around 10 nM (Bailly and Wang, in prep.), qualifying it as a high-affinity NPA binding protein. As a result, *twd1* reveals reduced NPA binding and is widely insensitive toward NPA as shown here (Fig. 5, S3, S6), while the *twd1 act7* double mutant is hypersensitive.

In agreement, we here show that the weak auxin and ATI TIBA as well as IAA (but not 2.4-D and NAA) are able to partially rescue the growth defects of *twd1* and *act7*. TWD1 itself most likely has no direct effect on exporter endocytosis as PIN1,2 locations are unchanged in *twd1* (Bouchard et al., 2006). Therefore, in our current model we see TWD1 as an integrator of ATIs (and potentially also auxins) affecting actin stability and thus downstream endocytosis of auxin efflux transporter vesicles. This is of relevance beyond the plant kingdom as ATIs were shown to impair vesicle motility and actin cytoskeleton dynamics in diverse eukaryotes (Dhonukshe et al., 2008).

Methods

Tandem affinity purification of TAP-TWD1 interacting proteins and mass spectrometric analysis

Co-immuniprecipitation analyses were carried out as described recently (Henrichs et al submitted) except that in some cased root materail or entire seedlings exposed to a 2h gravistimulus prior to membrane extraction were used. Moreover, bands of interest were size selcetd by silver stain and manually cut out of the gel prior to trypson digest (Fig. S1). LC-MS/MS analyses were performed by using an LTQ-Orbitrap XL-HTC-PAL system as described (Henrichs et al submitted). MS/MS spectra were analyzed using the MASCOT server (version 2.2) searching the TAIR9 database (The Arabidopsis Information Resource). The mascot search parameters were as follows: set off the threshold at 0.05 in the ion-score cut off, peptide tolerance at 10 ppm, MS/MS tolerance at ± 0.8Da, peptide charge of 2+ or 3+, trypsin as enzyme allowing up to 1 missed cleavage, carboxymethylation on cysteines as a fixed modification and oxidation on methionine as a variable modification. Mascot identified vector control proteins were subtracted manually from TAP-TWD1 proteins, and proteins with a score above 30 were considered as significant interactors (Fig. 1).

In vitro interaction analyses

Bnding of TWD1 and FKBD proteins to actin filaments was assessed in high-speed co-sedimentation assays. Briefly, increasing amounts (0.2 - 8µM) of TWD1 or FKBD protein were incubated with pre-polymerized F-actin (4 µM) and centrifuged at 150.000*g.* The resulting pellet and supernatant fractions were analyzed by SDS-PAGE and Coomasie Blue staining. Direct interaction will be indicated by the presence of TWD1 or FKBD in the pellet fraction.
The influence of TWD1 on actin filament polymerization and depolymerization kinetics was investigated in classical fluorimetric assays (Michelot et al., 2005).

Analysis of plant growth

Seedlings were grown if not indicated otherwise for 5 dag on vertical plates containing 0.5× Murashige and Skoog medium, 1% sucrose, 1% phytoagar in the dark, at 8h or at 16 h of light/day. For growth quantification, seeds were germinated and grown on drug-containing plates (NPA, Quer, TIBA, Latrunculin B, Oryzalin 1µM; IAA and 2,4-D 1nM; Jasplakinolide 100nM), plates were scanned, and root and hypocotyl lengths, and lateral root numbers were measured using Photoshop 10.0.1 (Adobe Systems). All experiments were performed at a minimum as triplicates with 20–30 seedlings per experiment.
For agarose imprints, 9dag seedlings were transferred to microscope slides freshly coated with 3% agarose, then removed. The imprint was photographed at a 10X magnification and images were processed and measured as above.

Auxin transport assays

IAA export from Arabidopsis mesophyll protoplasts was analyzed as in (Mravec et al., 2008b). Relative IAA/NAA export is calculated from effluxed radioactivity as follows: ((radioactivity in the medium at time t) - (radioactivity in the medium at time t=0)) * (100%)/ (radioactivity in the medium at t=0). Presented are average values from 4 independent experiments.

For measurements of basipetal root and hypocotyl (shoot) transport, seedlings were grown for 7 dag on vertical plates containing 0.5× Murashigge and Skoog medium, 1% sucrose, 1% phytoagar at 16 h of light/day at 100 microeinsteins (root) or 10 microeinsteins (hypocotyl), respectively. Measurements were performed as described in (Lewis and Muday, 2009) using radiolabeled IAA that was applied by placing solidified agar droplets next to the seedlings root tips or at the apical (cut) end of the hypocotyls. Data are means of three independent experiments with each four replica of 10 seedlings each.

A platinum microelectrode was used to monitor IAA fluxes in *Arabidopsis* roots as described previously (Bouchard et al., 2006; Bailly et al., 2008). For measurements, Was wild-type plants or *act7-4* were grown in hydroponic cultures and used at 5 dag. Differential current from an IAA-selective microelectrode was recorded in the absence and presence of 5 µM brefeldin A, jasplakinolide or latrunculin B.

Drug binding studies

Drug binding assays using *Arabidopsis* microsomes were performed as described elsewhere (Bailly et al., 2008). Four replicates of each 20 *µ*g of protein were incubated with 10 nM radiolabelled drugs (30-60 Ci/mmol) in the presence and absence of the corresponding 10 *µ*M non-radiolabelled drug. [^{3}H](G)quercetin (10 Ci/mmol; 1.0 mCi/ml) was custom-synthetized by ARC Inc.(St. Louis, USA). Reported values are the means of specific radiolabeled drug bound in the absence of cold drug (total) minus radiolabelled drug bound in the presence of cold drug (unspecific) from at least three independent experiments with four replicates each.

***In planta* analysis of auxin contents and responses**

Endogenous free IAA was quantified from shoot and root segments of MeOH extracted seedlings by using gas chromatography-mass spectrometry (GC-MS) as described in (Bouchard et al., 2006b). Data are means of four independent lots of 30–50 seedlings each, and equivalent to ca. 30 mg root and 60 mg shoot material, respectively.

Homozygous F4 generations of *A. thaliana* seedlings expressing the maximal auxin-inducible reporter Pro_{DR5}:GFP (Ottenschläger et al., 2003) were grown vertically for 5 dag and analyzed by confocal laser-scanning microscopy (Leica; DMIRE2). For histological signal localization, differential interference contrast and GFP images were merged electronically using Photoshop 10.0.1 (Adobe Systems).

Starch granules in the *Arabidopsis* root cap were visualised by Lugol staining (Friml et al., 2002b) after clearing.

Quantitative Analysis of Root Gravitropism
Root gravitropism in the dark of wild type, *twd1-1* (At3g21640), *act7-1* (At5g09810), act7-4 and *abcb1/pgp1* (At2G36910) or *abcb19/pgp19* (At3G28860) mutant combinations (all ecotype Was (Was Wt) in the presence of drugs (NPA, TIBA, Latrunculin B, BFA 1µM; Jasplakinolide 100nM) was performed as described previously (Santelia et al., 2008). Helical wheels were plotted using PolarBar software.

Actin cytoskeletal and auxin transporter imaging
F-actin was imaged by using whole-mount anti-actin (maize) immunolocalizations as described in Schlicht et al. (2006). For non-invasive imaging wild type and mutant alleles were transformed with *GFP-fABD2* (Wang et al. 2004) and *mTn-GFP* constructs. Act7-4 aleles were transformed with *ABCB19:ABCB19-GFP* and *PIN2:PIN2-GFP*.
Independent homozygpus F4 generations were analyzed by confocal laser scanning microscopy (Leica, DMIRE2).

Data Analysis
Data were analyzed using Prism 4.0b (GraphPad Software, San Diego, CA).

Acknowledgments
We thank V. Vincenzetti for outstanding technical support, Youngsook Lee for *mTn-GFP*, M. Weiwad for recombinant TWD1 protein, B. Scheres for *PIN2-GFP* and E. Martinoia for continous support. This work was supported by grants from the Swiss National Funds (to M.G.)

Author contributions
M.G. and V.S. designed the research; V.S. performed auxin transport-, root gravitropism-, confocal- and drug binding- analyses; M.S. performed whole-mount ILs, S.M. analyzed root IAA fluxes; S.P. analyzed free auxins; Y.F. performed Co-IP and MS analysis and M.G. wrote the manuscript.

Abbreviations
IAA, indole-3-acetic acid; PAT, polar auxin transport; ABCB, ATP-binding cassette protein subfamily B; PIN, pin-formed; MDR, multidrug resistance; PGP, phosphoglycoprotein; PID, PINOID;

Figure Legends

Figure 1: TWD1 interactors identified by Co-IP followed by size-selected proteomic analysis using TAPa-TWD1 as bait.
Mascot identified vector control proteins were subtracted manually from TAPa-TWD1 proteins, and proteins with a score above 30 were considered as significant interactors (see Table S1 for complete listing).

Figure 2: Morphological analysis of *twd1* and *act7* mutant alleles
(A) Growth phenotypes of 9dag seedlings.
(B) Agarose imprints of shoot (hypocotyl) and root sections.
(C) Quantification of hypocotyl and root lengths (mean ± SE; n = 4).
(D) Quantification of hypocotyl) and root cell lengths, cell number and epidermal twisting analyzed by microscopy of agarose imprints (mean ± SE; n = 4).
Significant differences (unpaired *t* test with Welch's correction, $p < 0.05$) between wild type are indicated by asterisks.

Figure 3: *twd1* and *act7* alleles show a higher frequency of 2-branched trichomes
(A) Microscopical analysis of leaf trichomes
(B) Quantification of leaf trichomes frequences (mean ± SE; n = 4).

Figure 4: Comparison of auxin transport, apical hook opening and root gravitropism of *twd1* and *act7* alleles.
(A) Cellular efflux from act7 leaf protoplasts is enhanced.
(B) Basipetal auxin transport is enhanced in the root but reduced in the shoot.
(C) Apical hook formation is not altered in *act7* and sensitive to auxin transport inhinitors.
(D) Root gravitropism is not significantly altered in *act7* but less sensitive to auxin ransport inhibitors. The length of each bar represents the mean percentages ± S.D. of seedlings showing the same direction of root growth of at least three independent experiments; numbers correspond to the mean percent occurrence of 60 and 90° bending (sum of 60 and 90° sectors).
Significant differences (unpaired *t* test with Welch's correction, $p < 0.05$) between wild type are indicated by asterisks (mean ± SE; n = 4).

Figure 5: Analysis of drug binding and sensitivity in *twd1* and *act7*
(A) Specific NPA but not quercetin binding to *twd1* and *act7* micrososmes is reduced.
(B) Quantification of hypocotyl and root lengths upon drug treatment under 16h light cycle.
Significant differences (unpaired *t* test with Welch's correction, $p<0.05$) between wild-type and mutant alleles are indicated by asterisks (means ± SE; n = 4).

Figure 6: Auxin levels and responses are altered in *act7*
(A) Free IAA levels are significantly elevated in the roots and shoot of act7

alleles. Data are mean ± SE (n = 4 with each 40-50 seedlings); absolute wild-type values were .084 ± .02 and .077 ± .005 pmol/mg (fresh weight) for roots and shoots, respectively.
(B) Expression of the auxin-responsive reporter DR5-GFP (green) is reduced in *twd1-1* and enhanced in *act7-4* root tips.
(C) Cleared and Lugol-stained *Arabidopsis* root tips. Note slightly reduced stain of columella cells in *twd1-1* and *act7-4* but absence of columella stain and highly enhanced stain of the stele in *act7-4.*

Figure 7: Actin imaging in *twd1.*
(A) Whole-mount anti actin (maize) immunolocalization of *twd1* and *abcb1 abcb19* alleles. Median section of early elongation zones (**i.-iii.**). Arrowheads mark uniformly labeled cross-end poles in wild-type and *abcb1 abcb19* but uneven labeled cross-ends of *twd1* cells. Note actin bundling in the *twd1* stele (marked by an asterisk) absent in the wild-type and *abcb1 abcb19.* 3D projections of epidermal cells in the transition zone (**iv.-vi.**). Arrowheads mark uniformely labelled cross-end poles in wild-type and *abcb1 abcb19* but uneven labelled cross-ends of *twd1* cells. Note the presence of actin-spots both in the *twd1* epidermal cells of early elongation and transition zones.
(B) The actin-reporter mTn-GFP (green) lables actin bundles in the stele of the *twd1* elongation zone (marked by an asterisk).
(C) GFP-fABD2 labeling is reduced in *act7* but shows also higher acting bundling in the stele (marked by an asterisk).

Figure 8: Expression of ABCB19 and PIN2 in *act7*
Expression of ABCB19-GFP is reduced in *act7-4* roots while PIN2-GFP expression and location beside some morphological abnormalities is not significantly altered.

Supplementary Figure Legends

Figure S1: TWD1-actin interaction is either indirect or requires aditional components.
(A) Silver-stain of TAP-purified vector control and TAP-TWD1 proteins after PAGE. Arrows mark excised samples used for MS analysis.
(B, C) Co-sedimentation analysis using purified TWD1 and polymerized rabbit actin using either pH 6.8 **(B)** or pH 6.0 or pH 7.4 **(C).**

Figure S2: Developmental analysis of *twd1* and *act7* seedlings.
Note slight delay in root development for *twd1* and *act7* allels under 8h light and for leaves and root under 16h light (mean ± SE; n = 4).

Figure S3: Analysis of lateral root number and emergence in *twd1* and *act7* single and double mutant alleles.
(A) The number of lateral roots is elvated in twd1 but reduced in *act7*. Note hypersensitivity of the *twd1 act7* dounble mutant toward NPA (mean ± SE; n = 4).
(B) Lateral root emergence is not significantly altered in *twd1* and *act7* alleles and not affected by NPA (mean ± SE; n = 4).

Figure S4: Latrunculin B rescues partially the agravitropic phenotype of *twd1* while *act7* is hypersensitive.
The length of each bar represents the mean percentages ± S.D. of seedlings showing the same direction of root growth of at least three independent experiments; numbers correspond to the mean percent occurrence of 60 and 90° bending (sum of 60 and 90° sectors; mean ± SE; n = 4).

Figure S5: Drug sensitivity of *twd1* and *act7* hypocotyl and root lengths.
Quantification of hypocotyl **(A)** and root lengths **(B)** upon drug treatment at 0h and 8h light; 16h light is shown in Fig. 5B. Significant differences (unpaired *t* test with Welch's correction, $p<0.05$) between wild-type and mutant alleles are indicated by asterisks (means ± SE; n = 4).

Figure S6: Drug sensitivity of *twd1* and *act7* lateral root development.
(A) The number of lateral roots is elvated in *twd1* but reduced in *act7*. Note insensitivity of *twd1* toward jasplakinolide (mean ± SE; n = 4).
(B) Lateral root emergence is not significantly altered in *twd1* and *act7* alleles Note reduced sensitivities of *twd1* and *act7* toward NPA and TIBA (mean ± SE; n = 4).

References

Bailly, A., Sovero, V., Vincenzetti, V., Santelia, D., Bartnik, D., Koenig, B.W., Mancuso, S., Martinoia, E., and Geisler, M. (2008). Modulation of P-glycoproteins by Auxin Transport Inhibitors Is Mediated by Interaction with Immunophilins. J Biol Chem **283,** 21817-21826.

Bandyopadhyay, A., Blakeslee, J.J., Lee, O.R., Mravec, J., Sauer, M., Titapiwatanakun, B., Makam, S.N., Bouchard, R., Geisler, M., Martinoia, E., Friml, J., Peer, W.A., and Murphy, A.S. (2007). Interactions of PIN and PGP auxin transport mechanisms. Biochem. Soc. Trans **35,** 137-141.

Blakeslee, J.J., Bandyopadhyay, A., Lee, O.R., Mravec, J., Titapiwatanakun, B., Sauer, M., Makam, S.N., Cheng, Y., Bouchard, R., Adamec, J., Geisler, M., Nagashima, A., Sakai, T., Martinoia, E., Friml, J., Peer, W.A., and Murphy, A.S. (2007). Interactions among PIN-FORMED and P-glycoprotein auxin transporters in Arabidopsis. Plant Cell **19,** 131-147.

Blancaflor, E.B., Wang, Y.-S., and Motes, C.M. (2006). Organization and function of the actin cytoskeleton in developing root cells. Int Rev Cytol **252,** 219-264.

Böhl, M., Czupalla, C., Tokalov, S.V., Hoflack, B., and Gutzeit, H.O. (2005). Identification of actin as quercetin-binding protein: an approach to identify target molecules for specific ligands. Anal Biochem **346,** 295-299.

Bouchard, R., Bailly, A., Blakeslee, J.J., Oehring, S.C., Vincenzetti, V., Lee, O.R., Paponov, I.A., Palme, K., Mancuso, S., Murphy, A.S., Schulz, B., and Geisler, M. (2006). Immunophilin-like TWISTED DWARF1 modulates auxin efflux activities of Arabidopsis P-glycoproteins. J Biol Chem **281,** 30603-30612.

Butler, J.H., Hu, S., Brady, S.R., Dixon, M.W., and Muday, G.K. (1998). In vitro and in vivo evidence for actin association of the naphthylphthalamic acid-binding protein from zucchini hypocotyls. Plant J **13,** 291-301.

Cox, D.N., and Muday, G.K. (1994). NPA binding activity is peripheral to the plasma membrane and is associated with the cytoskeleton. Plant Cell **6,** 1941-1953.

Dhonukshe, P., Grigoriev, I., Fischer, R., Tominaga, M., Robinson, D.G., Hasek, J., Paciorek, T., Petrásek, J., Seifertová, D., Tejos, R., Meisel, L.A., Zazímalová, E., Gadella, T.W.J., Stierhof, Y.-D., Ueda, T., Oiwa, K., Akhmanova, A., Brock, R., Spang, A., and Friml, J. (2008). Auxin transport inhibitors impair vesicle motility and actin cytoskeleton dynamics in diverse eukaryotes. Proc Natl Acad Sci USA **105,** 4489-4494.

Dixon, M., Jacobson, J., Cady, C., and Muday, G.K. (1996). Cytoplasmic

Orientation of the Naphthylphthalamic Acid-Binding Protein in Zucchini Plasma Membrane Vesicles. Plant Physiol **112,** 421-432.

Friml, J., and Sauer, M. (2008). Plant biology: in their neighbour's shadow. Nature **453,** 298-299.

Friml, J., Wiśniewska, J., Benková, E., Mendgen, K., and Palme, K. (2002). Lateral relocation of auxin efflux regulator PIN3 mediates tropism in Arabidopsis. Nature **415,** 806-809.

Geisler, M., and Murphy, A.S. (2006). The ABC of auxin transport: the role of p-glycoproteins in plant development. FEBS Lett **580,** 1094-1102.

Geisler, M., Kolukisaoglu, U., Bouchard, R., Billion, K., Berger, J., Saal, B., Frangne, N., Koncz-Kalman, Z., Koncz, C., Dudler, R., Blakeslee, J.J., Murphy, A.S., Martinoia, E., and Schulz, B. (2003). TWISTED DWARF1, a unique plasma membrane-anchored immunophilin-like protein, interacts with Arabidopsis multidrug resistance-like transporters AtPGP1 and AtPGP19. Mol Biol Cell **14,** 4238-4249.

Geisler, M., Blakeslee, J.J., Bouchard, R., Lee, O.R., Vincenzetti, V., Bandyopadhyay, A., Titapiwatanakun, B., Peer, W.A., Bailly, A., Richards, E.L., Ejendal, K.F.K., Smith, A.P., Baroux, C., Grossniklaus, U., Müller, A., Hrycyna, C.A., Dudler, R., Murphy, A.S., and Martinoia, E. (2005). Cellular efflux of auxin catalyzed by the Arabidopsis MDR/PGP transporter AtPGP1. Plant J **44,** 179-194.

Geldner, N., Friml, J., Stierhof, Y.-D., Jürgens, G., and Palme, K. (2001). Auxin transport inhibitors block PIN1 cycling and vesicle trafficking. Nature **413,** 425-428.

Gilliland, L.U., Pawloski, L.C., Kandasamy, M.K., and Meagher, R.B. (2003). Arabidopsis actin gene ACT7 plays an essential role in germination and root growth. Plant J **33,** 319-328.

Hasenstein, K.H., Blancaflor, E.B., and Lee, J.S. (1999). The microtubule cytoskeleton does not integrate auxin transport and gravitropism in maize roots. Physiol Plantarum **105,** 729-738.

Hu, S., Brady, S.R., Kovar, D.R., Staiger, C.J., Clark, G.B., Roux, S.J., and Muday, G.K. (2000). Technical advance: identification of plant actin-binding proteins by F-actin affinity chromatography. Plant J **24,** 127-137.

Ishida, T., Thitamadee, S., and Hashimoto, T. (2007). Twisted growth and organization of cortical microtubules. J Plant Res **120,** 61-70.

Kandasamy, M., McKinney, E., and Meagher, R. (2009). A Single Vegetative Actin Isovariant Overexpressed under the Control of Multiple Regulatory Sequences Is Sufficient for Normal Arabidopsis Development. Plant Cell.

Kandasamy, M.K., Gilliland, L.U., McKinney, E.C., and Meagher, R.B. (2001). One plant actin isovariant, ACT7, is induced by auxin and required for normal callus formation. Plant Cell **13,** 1541-1554.

Ketelaar, T., Anthony, R.G., and Hussey, P.J. (2004). Green fluorescent protein-mTalin causes defects in actin organization and cell expansion in Arabidopsis and inhibits actin depolymerizing factor's actin depolymerizing activity in vitro. Plant Physiol **136,** 3990-3998.

Kim, J.-Y., Henrichs, S., Bailly, A., Vincenzetti, V., Sovero, V., Mancuso, S., Pollmann, S., Kim, D., Geisler, M., and Nam, H.-G. (2010). Identification of an ABCB/P-glycoprotein-specific inhibitor of auxin transport by chemical genomics. The Journal of biological chemistry.

Kost, B., Spielhofer, P., and Chua, N.H. (1998). A GFP-mouse talin fusion protein labels plant actin filaments in vivo and visualizes the actin cytoskeleton in growing pollen tubes. Plant J **16,** 393-401.

Luschnig, C. (2001). Auxin transport: why plants like to think BIG. Curr Biol **11,** R831-833.

Maisch, J., and Nick, P. (2007). Actin is involved in auxin-dependent patterning. Plant Physiol **143,** 1695-1704.

Michalke, W., Katekar, G.F., and Geissler, A.E. (1992). Phytotropin-binding sites and auxin transport in Cucurbita pepo: evidence for two recognition sites Planta **187,** 254-260.

Mravec, J., Kubes, M., Bielach, A., Gaykova, V., Petrásek, J., Skupa, P., Chand, S., Benková, E., Zazímalová, E., and Friml, J. (2008). Interaction of PIN and PGP transport mechanisms in auxin distribution-dependent development. Development.

Muday, G.K. (2000). Maintenance of asymmetric cellular localization of an auxin transport protein through interaction with the actin cytoskeleton. J Plant Growth Regul **19,** 385-396.

Muday, G.K., and Murphy, A.S. (2002). An emerging model of auxin transport regulation. Plant Cell **14,** 293-299.

Nagashima, A., Uehara, Y., and Sakai, T. (2008). The ABC subfamily B auxin transporter AtABCB19 is involved in the inhibitory effects of N-1-naphthyphthalamic acid on the phototropic and gravitropic responses of Arabidopsis hypocotyls. Plant Cell Physiol **49,** 1250-1255.

Paciorek, T., Zazímalová, E., Ruthardt, N., Petrásek, J., Stierhof, Y.-D., Kleine-Vehn, J., Morris, D.A., Emans, N., Jürgens, G., Geldner, N., and Friml, J. (2005). Auxin inhibits endocytosis and promotes its own efflux from cells. Nature **435,** 1251-1256.

Palmieri, M., and Kiss, J.Z. (2005). Disruption of the F-actin cytoskeleton limits statolith movement in Arabidopsis hypocotyls. J Exp Bot **56,** 2539-2550.

Rojas-Pierce, M., Titapiwatanakun, B., Sohn, E.J., Fang, F., Larive, C.K., Blakeslee, J.J., Cheng, Y., Cuttler, S., Peer, W.A., Murphy, A.S., and Raikhel, N.V. (2007). Arabidopsis P-glycoprotein19 participates in the inhibition of gravitropism by gravacin. Chem Biol **14,** 1366-1376.

Schellmann, S., and Hülskamp, M. (2005). Epidermal differentiation: trichomes in Arabidopsis as a model system. The International Journal of Developmental Biology **49,** 579-584.

Schlicht, M., Strnad, M., Scanlon, M.J., Mancuso, S., Hochholdinger, F., Palme, K., Volkmann, D., Menzel, D., and Baluska, F. (2006). Auxin immunolocalization implicates vesicular neurotransmitter-like mode of polar auxin transport in root apices. Plant Signaling & Behavior **1,** 122-133.

Sheahan, M.B., Staiger, C.J., Rose, R.J., and McCurdy, D.W. (2004). A green fluorescent protein fusion to actin-binding domain 2 of

Arabidopsis fimbrin highlights new features of a dynamic actin cytoskeleton in live plant cells. Plant Physiol **136,** 3968-3978.

Thomas, C., Tholl, S., Moes, D., Dieterle, M., Papuga, J., Moreau, F., and Steinmetz, A. (2009). Actin bundling in plants. Cell Motil Cytoskeleton.

Winder, S.J., and Ayscough, K.R. (2005). Actin-binding proteins. J Cell Sci **118,** 651-654.

Xu, J., and Scheres, B. (2005). Cell polarity: ROPing the ends together. Curr Opin Plant Biol **8,** 613-618.

sample no.	protein identity	AGI Code	score	assigned sequence	cover
2	ATTIC110/TIC110	At1g06950	152	AYVTDALSGGR EAEAISVDVTSK QQAEVILADGQLTK QVGLPQPQAEKVIK DAISSGVDGYDAETR LANAVSSGDLEAQDSK LSDELAEDLFREHTR	9
4	TWD1 (Twisted Dwarf11)	At3g21640	92	SDMTVEER YQDMALAVK KMDGNSLFK AELGQMDSAR VDSEAEVLDEK YSTCFLHYR	15
8	ribulose-1,5-bisphosphate carboxylase/ oxygenase, large subunit	ArthCp030	386	IPPAYTK AVYECLR AMHAVIDR SQAETGEIK DLAVEGNEIIR LTYYTPEYETK LSGGDHIHAGTVVGK DDENVNSQPFMR TFQGPPHGIQVER YGRPLLGCTIKPK GGLDFTKDDENVNSQPFMR	24
10	AtRABE1b/AtRab8D	At4g20360	212	SYTVTGVEMFQK GITINTATVEYETENR	5
11	ACT7 (Actin7)	At5g09810	39	AGFAGDDAPR SEYDESGPSIVHR	6

Figure 1

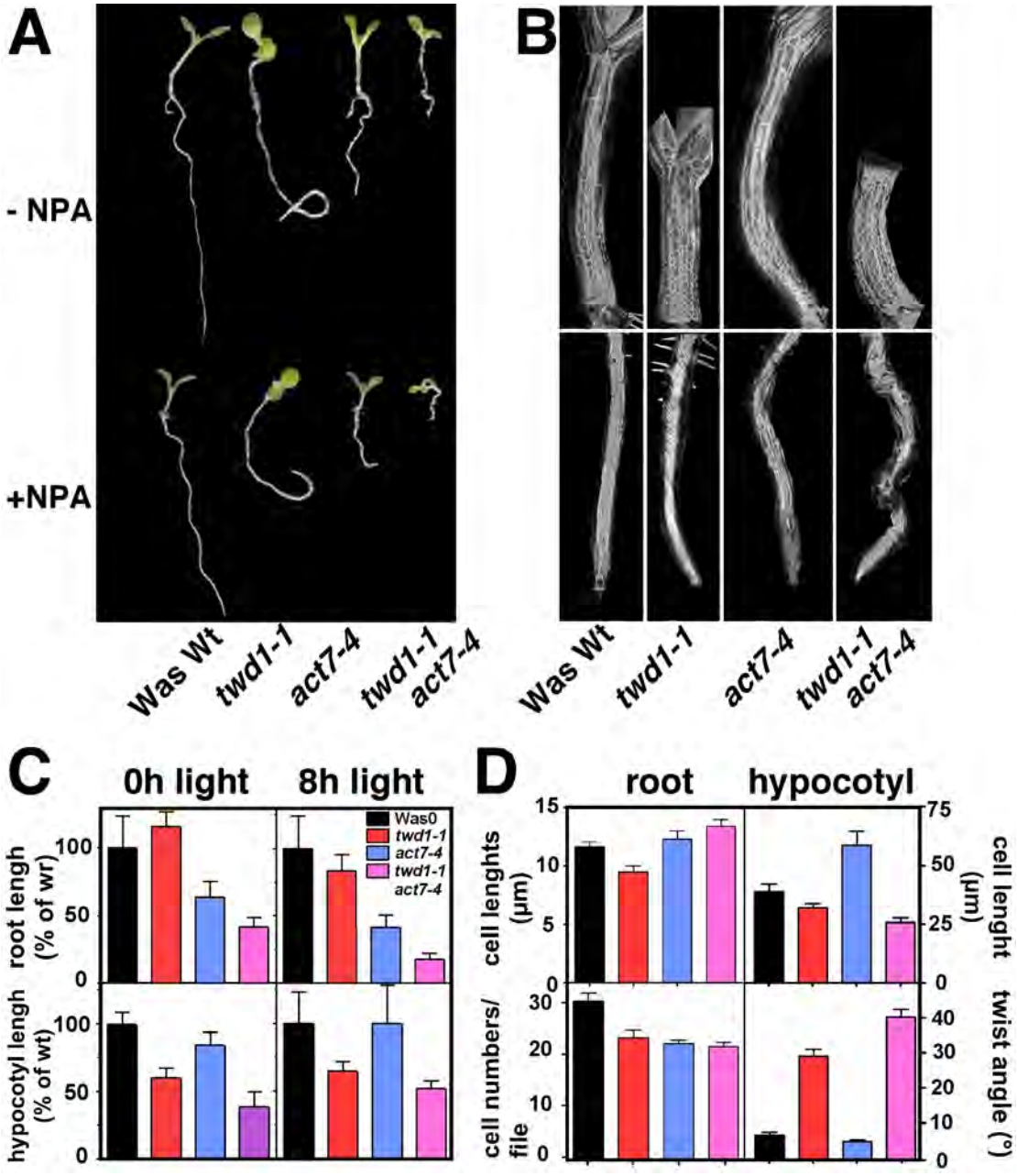
A
- NPA
+NPA
Was Wt
twd1-1
act7-4
twd1-1
act7-4
B
Was Wt
twd1-1
act7-4
twd1-1
act7-4
C
0h light
8h light
root lengh (% of wr)
hypocotyl lengh (% of wt)
Was0
twd1-1
act7-4
twd1-1
act7-4
D
root
hypocotyl
cell lenghts (µm)
cell numbers/ file
cell lenght (µm)
twist angle (°)

Figure 2

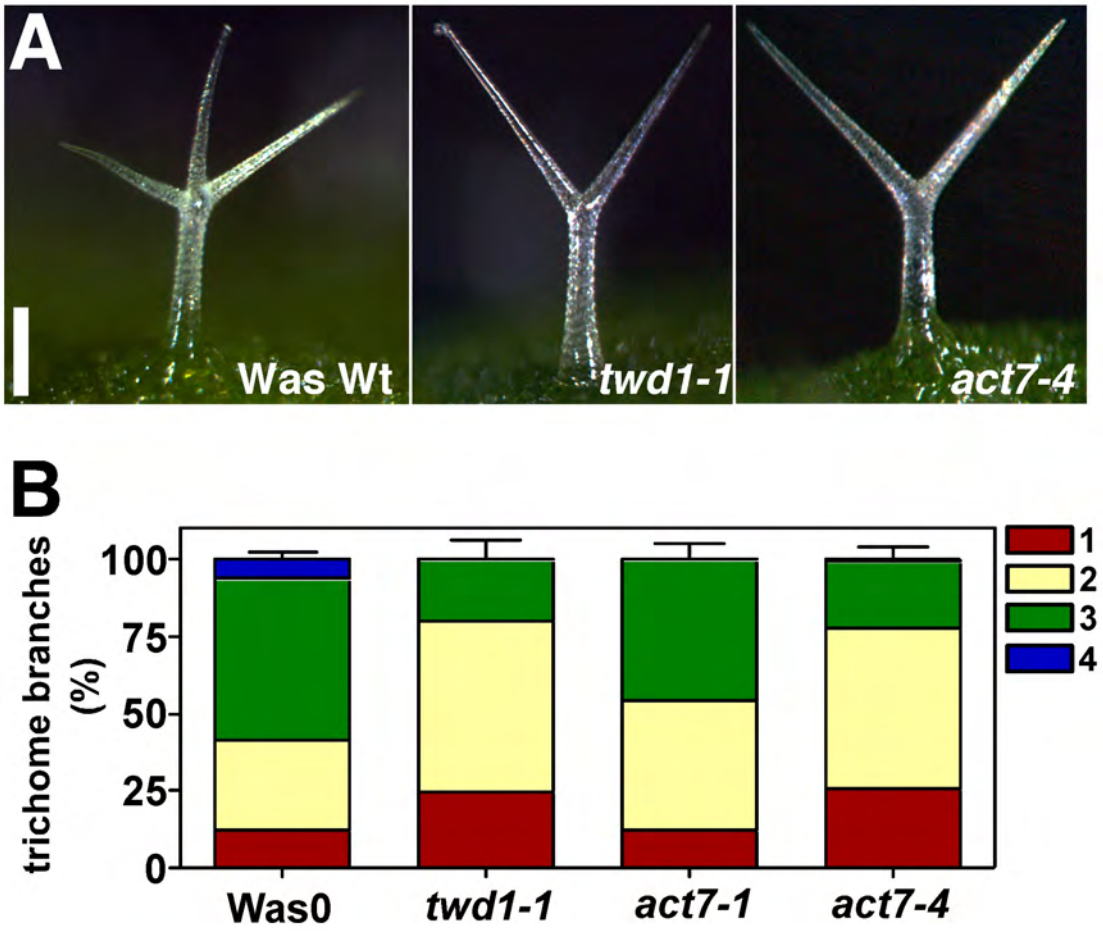
A
Was Wt
twd1-1
act7-4
B
trichome branches (%)
100
75
50
25
0
Was0
twd1-1
act7-1
act7-4
1
2
3
4

Figure 3

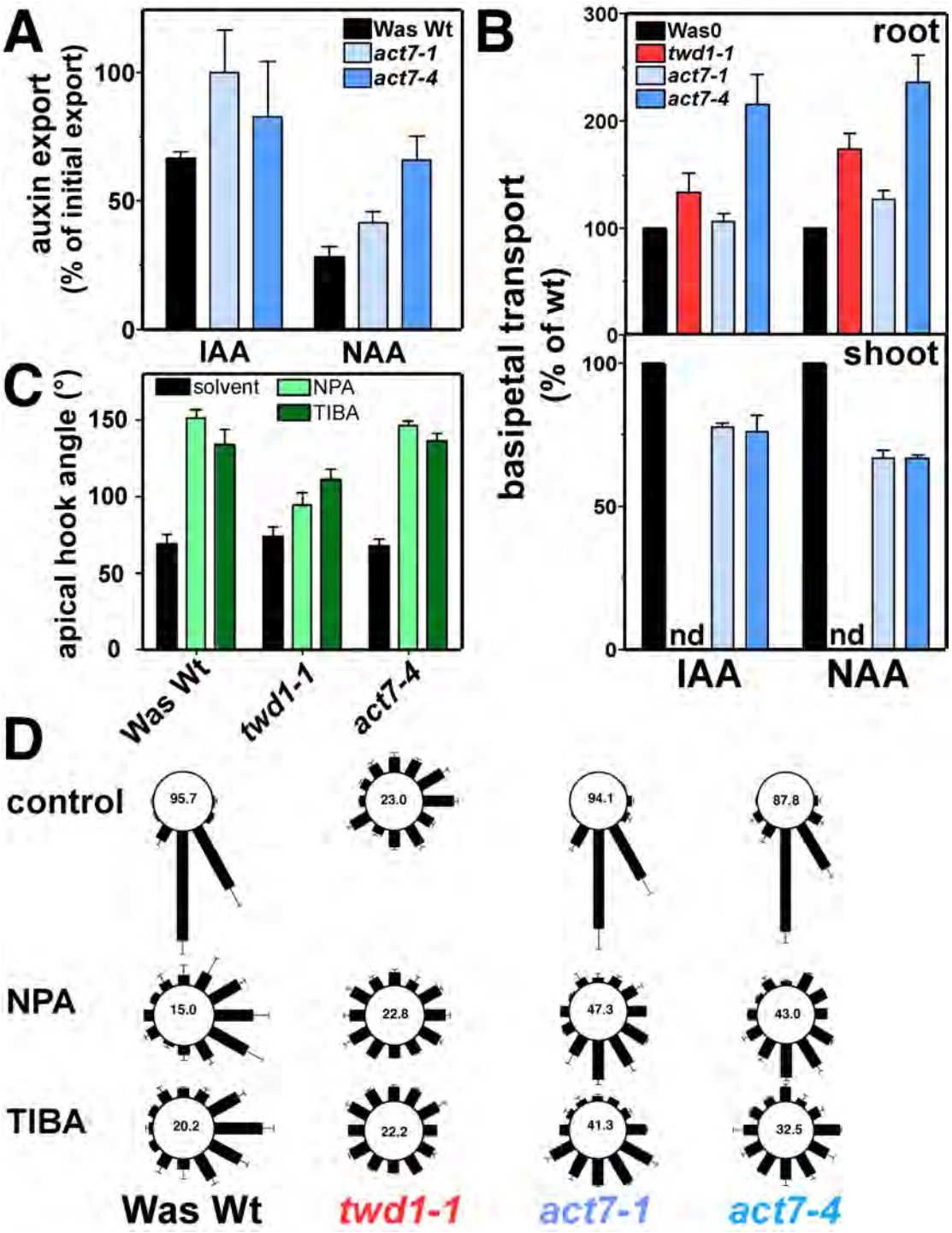
A
auxin export
(% of initial export)
Was Wt
act7-1
act7-4
IAA
NAA
B
basipetal transport
(% of wt)
Was0
twd1-1
act7-1
act7-4
root
shoot
nd
nd
IAA
NAA
C
apical hook angle (°)
solvent
NPA
TIBA
Was Wt
twd1-1
act7-4
D
control
NPA
TIBA
95.7
23.0
94.1
87.8
15.0
22.8
47.3
43.0
20.2
22.2
41.3
32.5
Was Wt
twd1-1
act7-1
act7-4

Figure 4

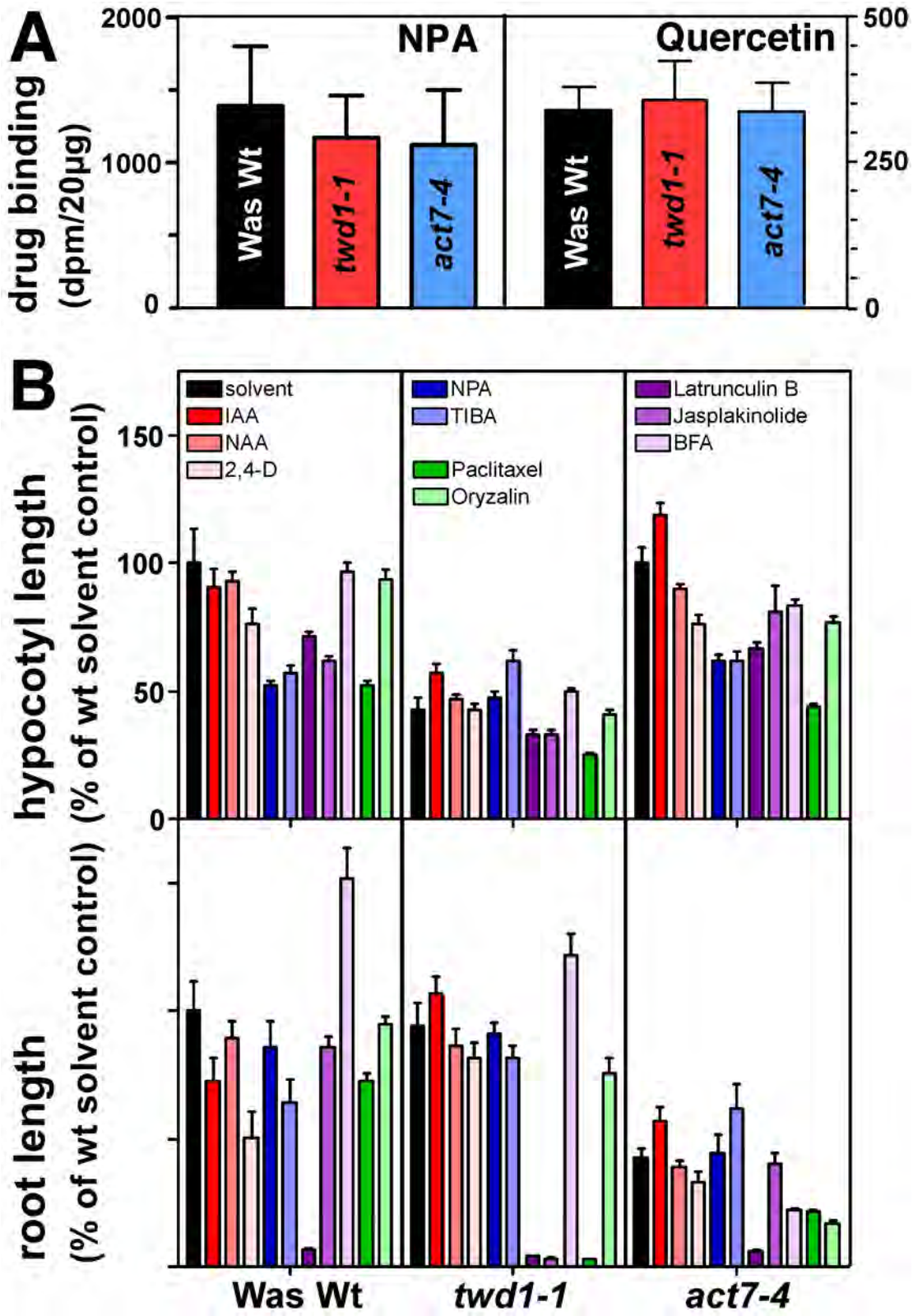
A
drug binding
(dpm/20µg)
2000
1000
0
NPA
Quercetin
500
250
0
Was Wt
twd1-1
act7-4
Was Wt
twd1-1
act7-4
B
hypocotyl length
(% of wt solvent control)
root length
(% of wt solvent control)
150
100
50
0
solvent
IAA
NAA
2,4-D
NPA
TIBA
Paclitaxel
Oryzalin
Latrunculin B
Jasplakinolide
BFA
Was Wt
twd1-1
act7-4

Figure 5

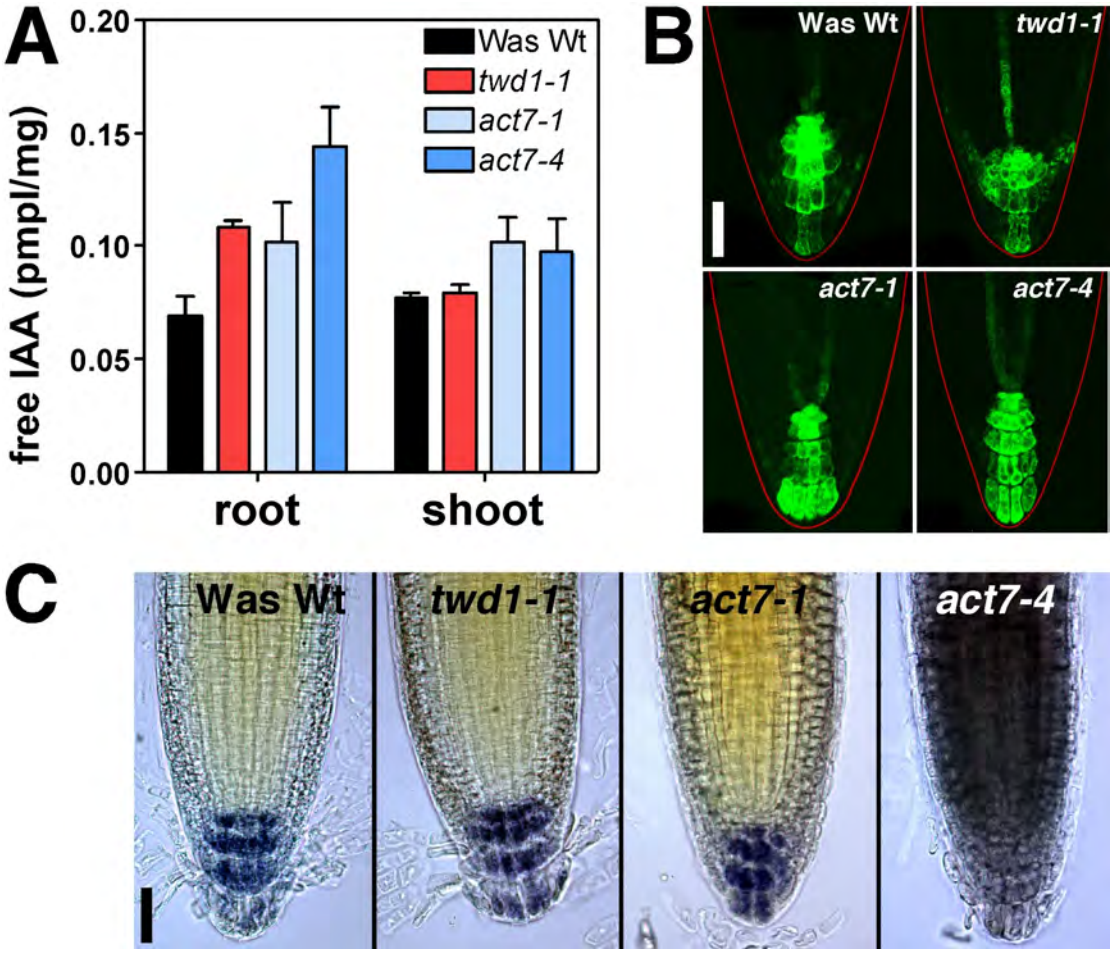
A
0.20
0.15
0.10
0.05
0.00
free IAA (pmpl/mg)
Was Wt
twd1-1
act7-1
act7-4
root
shoot
B
Was Wt
twd1-1
act7-1
act7-4
C
Was Wt
twd1-1
act7-1
act7-4

Figure 6

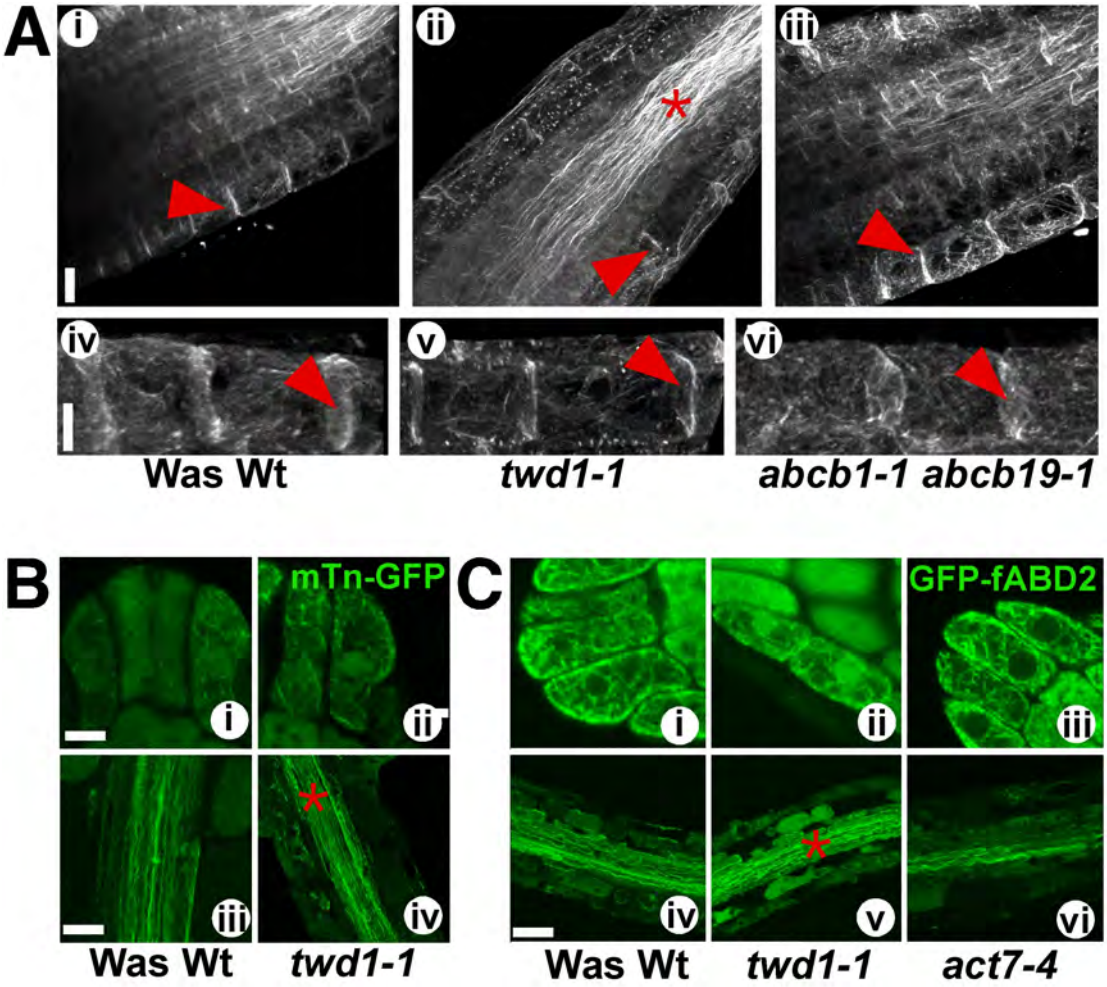
A
i
ii
iii
iv
v
vi
Was Wt
twd1-1
abcb1-1 abcb19-1
B
mTn-GFP
i
ii
iii
iv
Was Wt
twd1-1
C
GFP-fABD2
i
ii
iii
iv
v
vi
Was Wt
twd1-1
act7-4

Figure 7

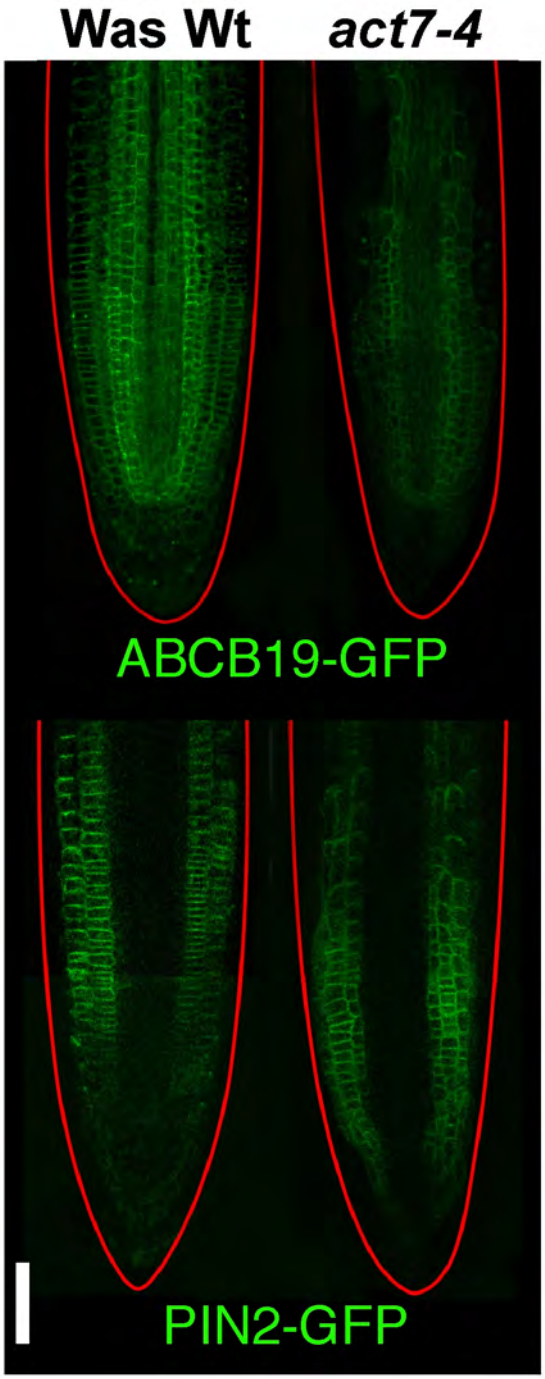

Figure 8

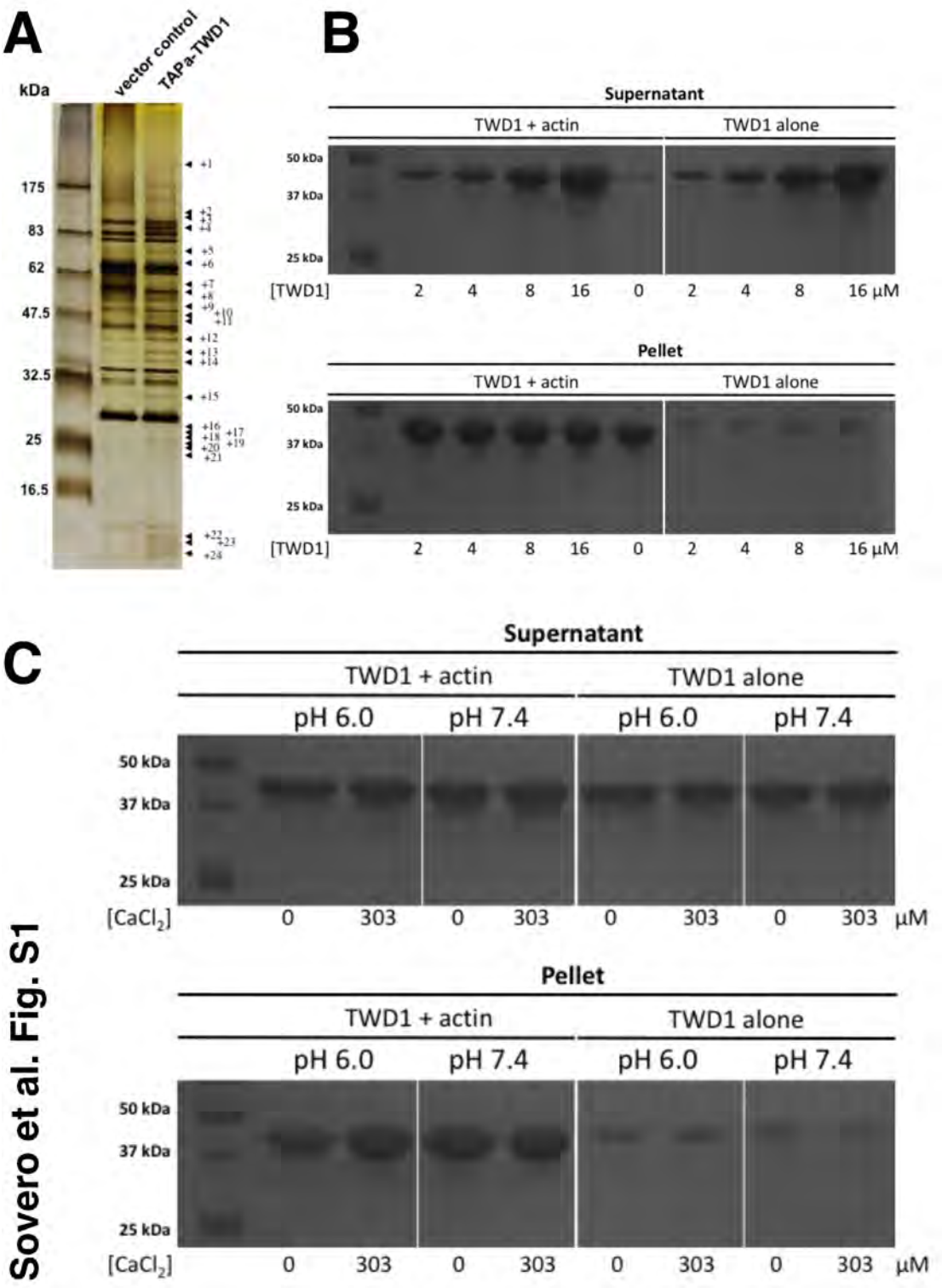

Sovero et al. Fig. S1

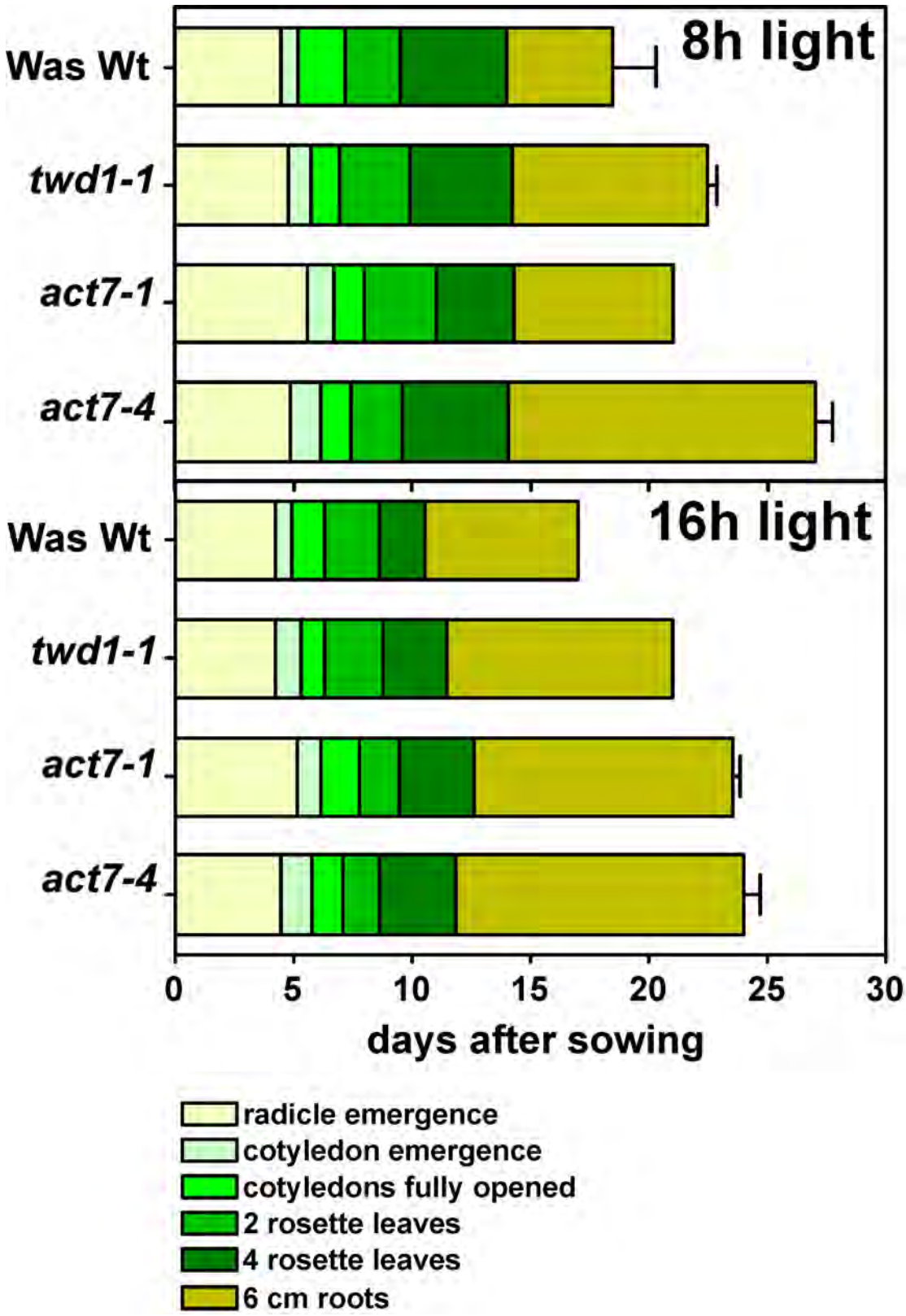
8h light
Was Wt
twd1-1
act7-1
act7-4
16h light
Was Wt
twd1-1
act7-1
act7-4
0
5
10
15
20
25
30
days after sowing
radicle emergence
cotyledon emergence
cotyledons fully opened
2 rosette leaves
4 rosette leaves
6 cm roots

Figure S2

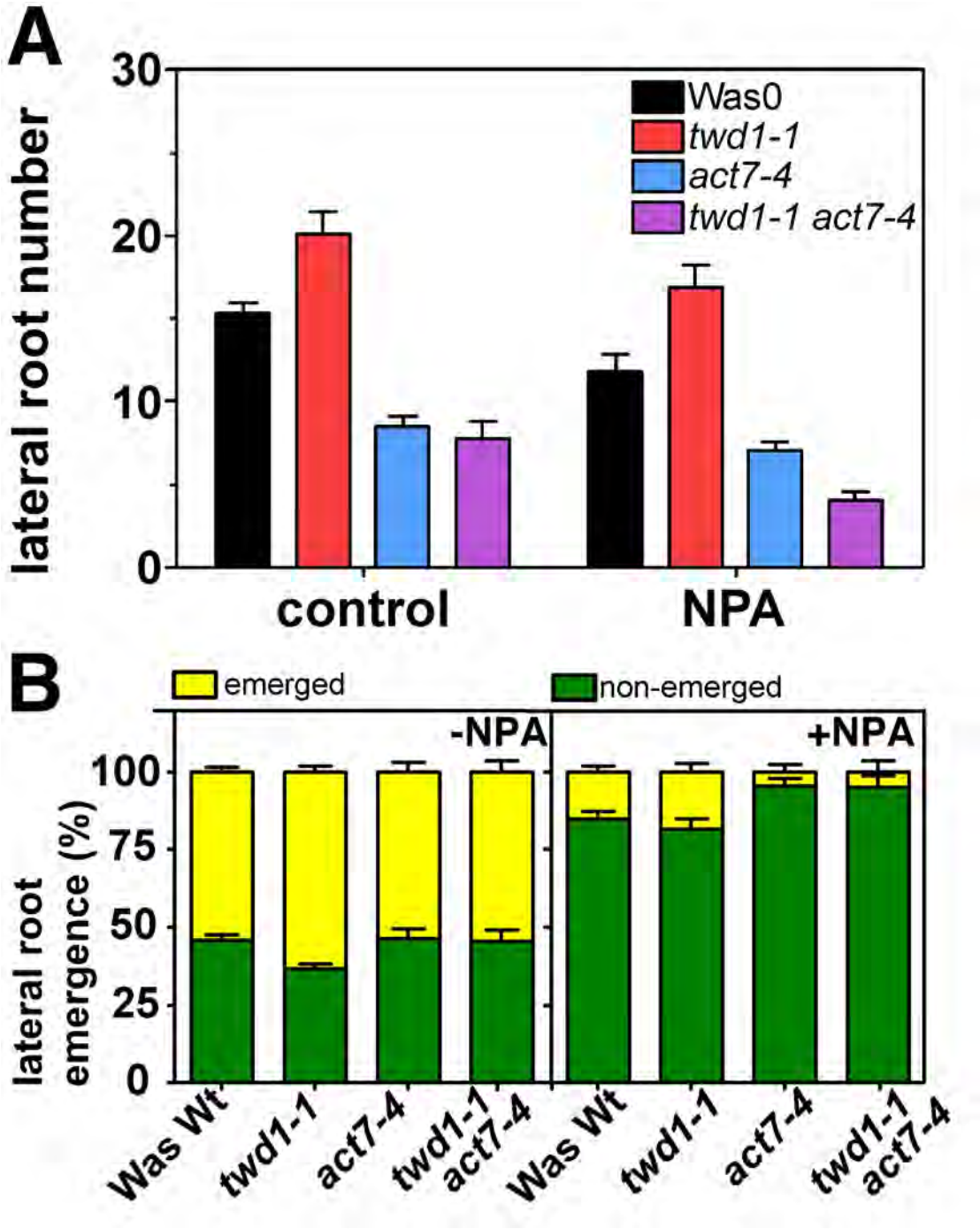
A
lateral root number
30
20
10
0
Was0
twd1-1
act7-4
twd1-1 act7-4
control
NPA
B
emerged
non-emerged
-NPA
+NPA
lateral root emergence (%)
100
75
50
25
0
Was Wt
twd1-1
act7-4
twd1-1 act7-4
Was Wt
twd1-1
act7-4
twd1-1 act7-4

Figure S3

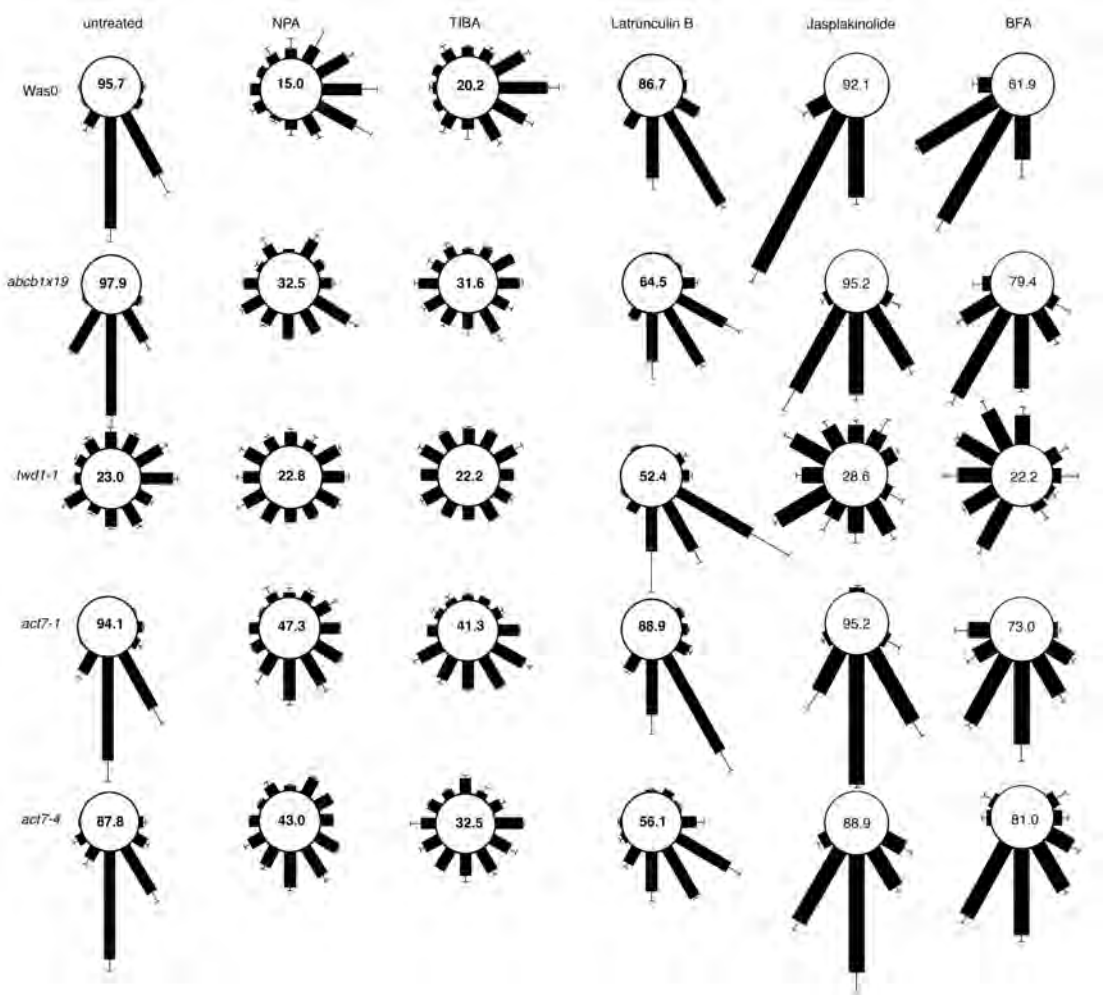
untreated
NPA
TIBA
Latrunculin B
Jasplakinolide
BFA
Was0
95.7
15.0
20.2
86.7
92.1
61.9
abcb1x19
97.9
32.5
31.6
64.5
95.2
79.4
twd1-1
23.0
22.8
22.2
52.4
28.6
22.2
act7-1
94.1
47.3
41.3
88.9
95.2
73.0
act7-4
87.8
43.0
32.5
56.1
88.9
81.0

Figure S4

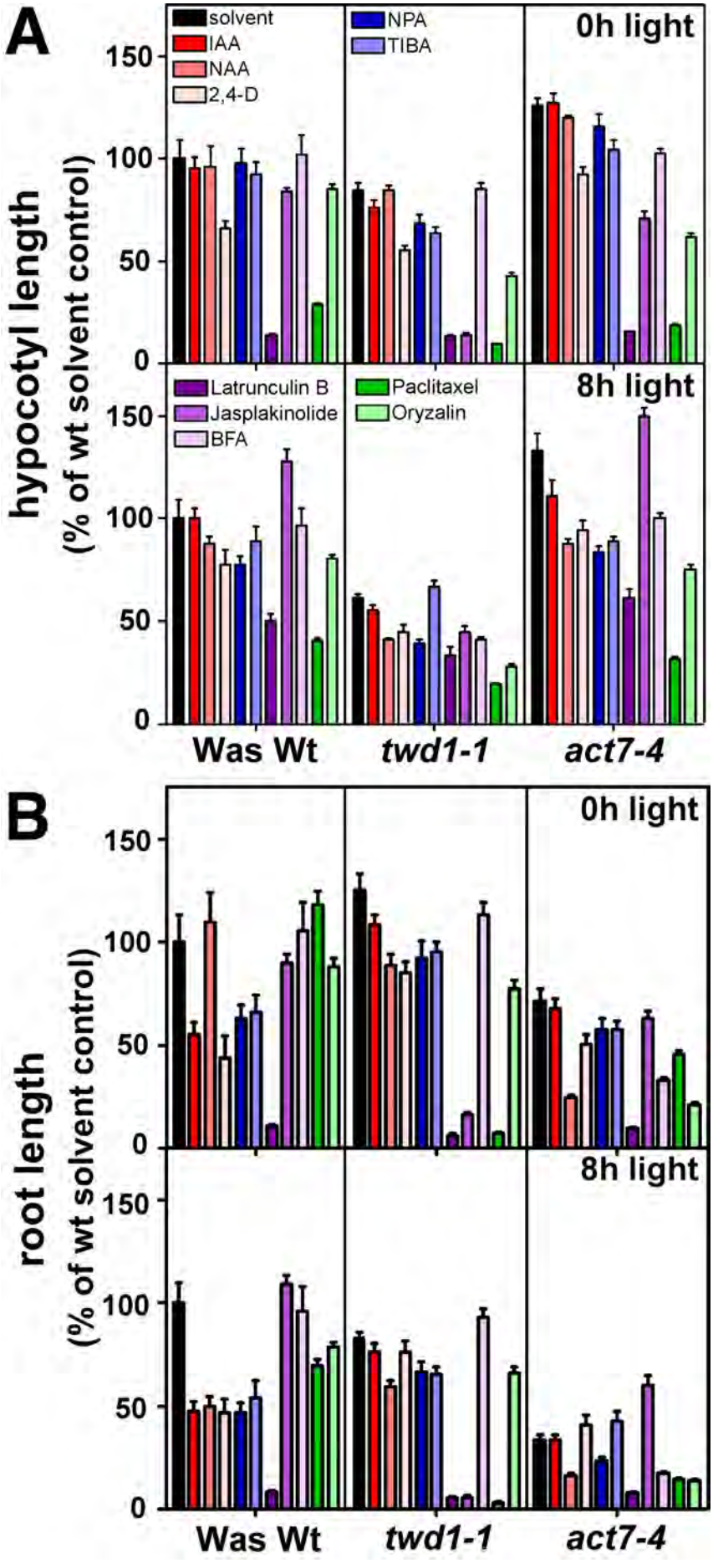
A
solvent
IAA
NAA
2,4-D
NPA
TIBA
0h light
Latrunculin B
Jasplakinolide
BFA
Paclitaxel
Oryzalin
8h light
hypocotyl length
(% of wt solvent control)
150
100
50
0
Was Wt
twd1-1
act7-4
B
0h light
8h light
root length
(% of wt solvent control)
150
100
50
0
Was Wt
twd1-1
act7-4

Figure S5

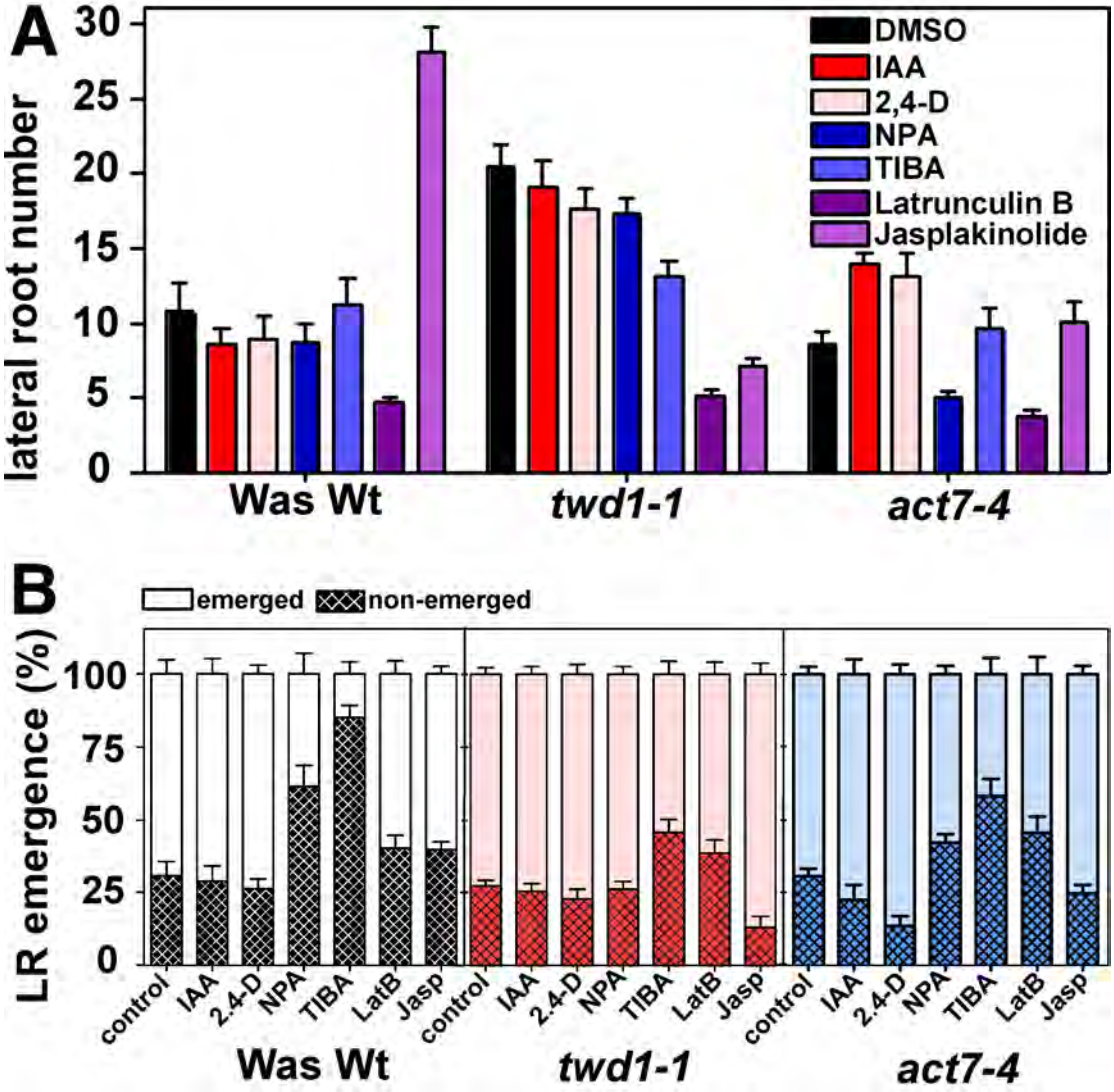
A
lateral root number
30
25
20
15
10
5
0
DMSO
IAA
2,4-D
NPA
TIBA
Latrunculin B
Jasplakinolide
Was Wt
twd1-1
act7-4
B
LR emergence (%)
emerged
non-emerged
100
75
50
25
0
control
IAA
2,4-D
NPA
TIBA
LatB
Jasp
Was Wt
twd1-1
act7-4

Figure S6

Chapter 5:

Discussion

Discussion

The aim of this thesis was to investigate the mechanism of NPA-mediated inhibition of auxin transport and the twisting phenotype of the *twd1* loss-of-function mutation. Based on previous studies, the theory was formulated that TWD1 directly interacted with the actin cytoskeleton, and through its further interaction with ABCBs, contributed to the activity and/or stabilization of the auxin-efflux complex at the correct place in the plasma membrane. NPA binding to ABCBs and TWD1 would destabilize the interaction and the complex, and this reduction would result in a reduction of polar auxin transport.

NPA

To understand why and how the twisting phenotype and NPA inhibition of auxin transport intersect, it is first important to discuss the importance of NPA in auxin transport research.

Polar auxin transport (PAT) is a key defining feature of auxin and auxin action. Therefore, finding tools to study it has been an important part of auxin research. One of these tools is the chemical inhibition of transport. Early on, several compounds were found that could specifically enhance accumulation of auxin by blocking its efflux, and one of the most important ones of these is naphthylphthalmic acid (NPA). The regular use of NPA in plant research has proven to be very beneficial. For example, the comparison of NPA efflux inhibition capability with other inhibitors such as TIBA, as well as more general metabolic decreases of PAT was a key in the elucidation of the overall mechanism of auxin transport (as in Goldsmith, 1977). NPA specifically enhanced IAA accumulation without increasing the accumulation of benzoic acid or other indoles (Sussman and Goldsmith, 1981). Unlike TIBA, NPA is not polarly transported, and does not act like a weak auxin, competing with IAA for its active site. Therefore, it must have a completely different and

specific mode of action (Thomson et al., 1973). Additionally, the similarity of the *pin1* mutant to wild-type plants treated with high concentrations of NPA led its being identified as the first auxin-efflux catalyser. Now we have used this tool to look at the regulation of auxin transport by protein-protein interactions and the cytoskeleton, as well as identifying a new ATI to further break down the individual components of the auxin efflux complex.

NPA-binding proteins

Over the years, many approaches to discovering the NPA-binding protein or proteins have been taken, and many clues have been thus uncovered. Although there is still debate about the number of actual binding sites, at least one has been found to be peripheral to the membrane and associated to the cytoskeleton (Cox and Muday, 1994). The other suggested NPA binding protein has been found to be an integral membrane protein (Bernasconi et al., 1996). Since ABCBs have been shown to bind NPA (Murphy et al., 2002), they could be this integral membrane protein component.

Could it then be possible that TWD1 would be the membrane-peripheral NBP? More evidence that the ABCBs and TWD1 could be the main NPA targets in the cell comes from the iconic *pin1* loss-of-function mutation. The mutation shows striking pin-shaped inflorescences, which looks

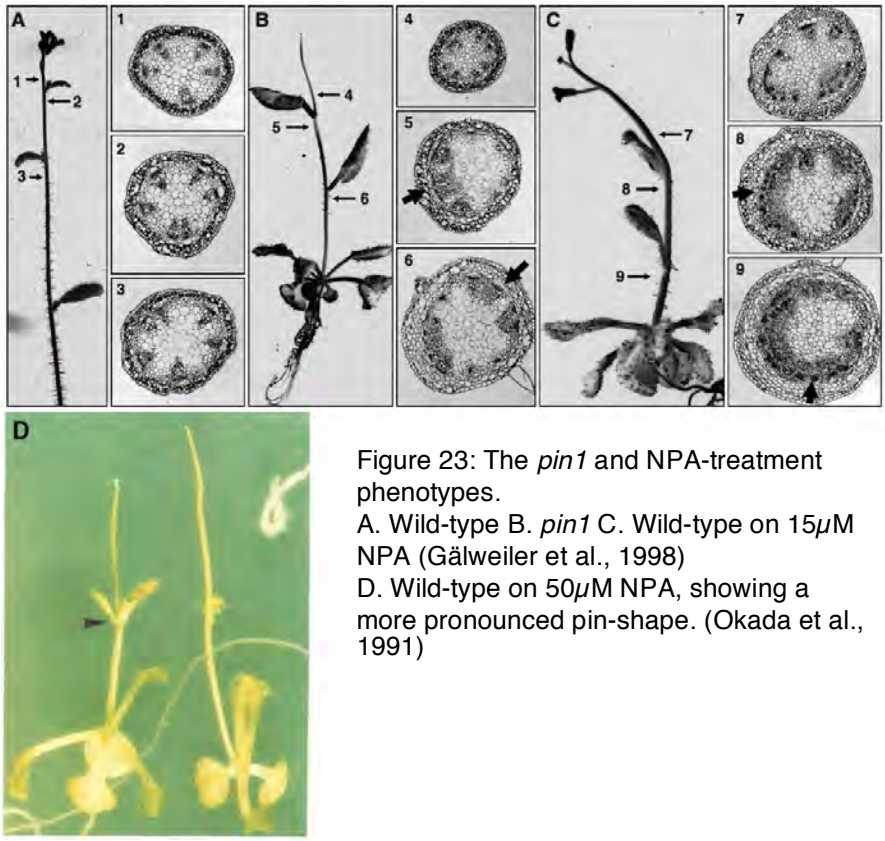

Figure 23: The *pin1* and NPA-treatment phenotypes.
A. Wild-type B. *pin1* C. Wild-type on 15μM NPA (Gälweiler et al., 1998)
D. Wild-type on 50μM NPA, showing a more pronounced pin-shape. (Okada et al., 1991)

outwardly similar to the phenotype one gets when applying large concentrations of NPA. Interestingly, despite this similarity of phenotype, PIN proteins do not seem to show NPA binding activity (Kim et al., 2010) indicating that it must be the loss of function of a protein that works with PIN1 that causes the pin shape. This reinforces the idea that the auxin efflux complex must consist of at least two components, the efflux carrier and an NPA-binding regulator, or that another, NPA-sensitive family of proteins that interact and co-regulate auxin transport, must be involved to bring about the phenotype.

Our research has characterized a new auxin transport inhibitor, BUM, that also creates this classic pin phenotype in plants grown on it (Kim et al., 2010). Notably, BUM seems to mainly affect ABCB1-related auxin transport while NPA mainly affects ABCB19. ABCB1 and 19 have overlapping, but not identical, function and localization which makes it very difficult to decipher their roles. More importantly, BUM has no significant effect on PIN-mediated auxin transport. This is more proof that the pin phenotype is not solely a result of malfunctioning auxin transport by PINs, but rather that PINs regulate or control in some way the NPA/BUM binding proteins. BUM will be useful in further separating out the individual roles not only of protein families, but the individual proteins themselves, and also, by comparison of the subtle differences, in finally discovering the mystery of NPA.

ABCB1 NPA binding and transport activity

At the start of this thesis, one of the aims was to investigate the NPA-binding properties of the auxin-transport protein ABCB1 as well as its interacting partner TWD1, and to further explain the mechanics of NPA inhibition of the transport. As mentioned above, a search for NPA-binding proteins had come up with ABCBs as candidates (Murphy et al., 2002). Investigations had then shown that TWD1 interacted with ABCB1 and ABCB19 (Geisler et al., 2003). Significantly, this interaction was through the PPIase domain of TWD1, instead of the more common FKBP hub for protein-protein interaction, the

TPR domain, and at the ABCBs' nucleotide binding domain. Even more importantly, TWD1 interaction modulated the auxin efflux capacity of ABCB1, with interaction enhancing the rate of efflux (Bouchard et al., 2006). This could have been indication that TWD1 interferes with ATP binding to the ABCBs, and thus influences their activity. But what was the role of NPA? Here, building on work completed earlier, it was found that the binding of NPA disrupted the interaction between ABCB1 and TWD1. In fact, it is precisely this disruption that forms the basis of the reduction of auxin transport of ABCB1 by NPA (Brunn et al., 1992; Murphy et al., 2002; Bailly et al., 2008). Interestingly, several other compounds were also able to have this effect, most significantly, plant-endogenous flavonoids such as quercetin, but not TIBA, which, as discussed previously, has an entirely different mode of operation. As NPA is not naturally found in plants, it has been questioned what the natural substrate for the NPA binding site might be. It had been speculated that flavonoids played this role (Brunn et al., 1992; Murphy et al., 2002). This is further evidence of the natural auxin-transport regulating function of TWD1 in plants. Manipulation of the FKBD/PPIase domain in TWD1, which is the site of interaction with the ABCBs, through site-directed mutagenesis gave further insight into the mechanism of the disruption (Bailly et al., 2008). Changes in only a few amino acids at a time are able to individually change TWD1 interaction with the ABCBs and the transmission of the NPA inhibitory effect. This level of subtle variation suggests that there is a high level of regulation of and by TWD1 on the auxin efflux complex, indicating its key role in plant growth. The importance of TWD1 is also evident in the severity of its loss-of-function mutant.

twd1 twisting

Understanding the role of TWD1 in mediating the effect of NPA on ABCB1-regulated auxin efflux unfortunately does not give an answer to the most striking part of the *twd1* loss-of-function phenotype, namely, the twist. If reducing the overall level of auxin transport was all that the loss of TWD1 brought about, one would expect the knockout plants to look like the

abcb1/abcb19 double mutants, merely dwarfed and with other auxin-related phenotypes, such as epinastic hypocotyls. However much *twd1* plants do look like *abcb1/abcb19* plants, the twist indicates that there must be an additional level of control by TWD1. Of course, this could simply relate to the many other interacting partners that TWD1 has. The ABCBs are known to interact with the N-terminal FKBD, or PPIase domain, but TWD1 also has a TPR domain, which is often a hub for protein-protein interactions. In TWD1, this

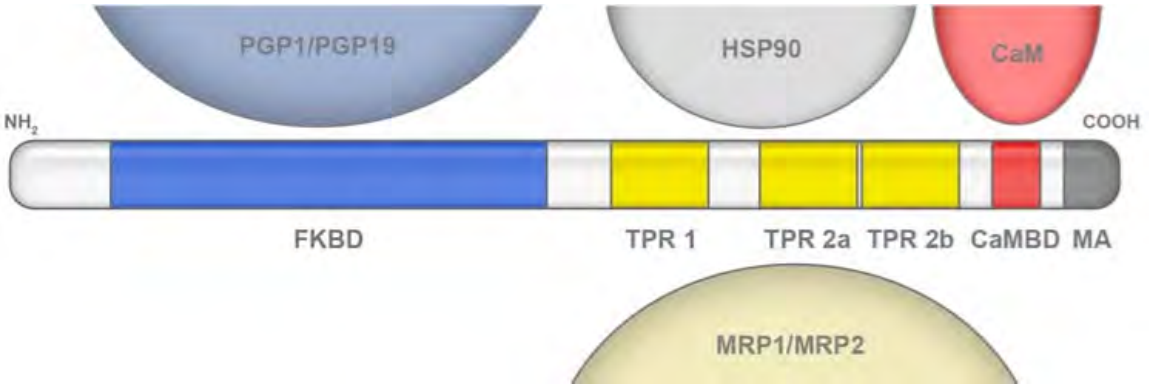

Figure 24: TWD1 domains and interacting partners. (Bailly et al., 2006)

domain interacts with heat shock protein HSP90, an abundant molecular chaperone, which has been found, in mammals, to be involved in coordinating cytoplasmic trafficking along cytoskeletal elements via interaction with immunophilins (Pratt et al., 1999). The TPR domain also interacts with the ABCCs MRP1 and 2, which are localized to the vacuolar membrane (Geisler et al., 2004). In addition, TWD1 has a calmodulin binding domain. Calmodulin integrates many of the cell's calcium signaling pathways, and therefore this domain might indicate TWD1's involvement in auxin and calcium signaling crosstalk. Most of these interactions have played only a very peripheral role in our research thus far, and may prove to be the key to the difference between simply knocking out the transporter or the one that controls them all.

While many twisted mutants with a fixed handedness have been found to have a specific mutation that is somehow related to the microtubule cytoskeleton, other twisted mutants with no fixed handedness have been found to have deficiencies in normal auxin distribution (Ishida et al., 2007).

These points are both relevant to this work. Obviously we know that TWD1 participates in the regulation of correct auxin flow. So how does disruption of this regulation lead to random twisting? And why in *twd1* when not in *abcb1/abcb19?* One idea is that the specific localization of TWD1 within the plant could be a factor. For example, in the shoot, if the loss of TWD1 is in certain zones, the elongation of these zones could be differentially affected. Then, if the epidermal layer cells elongate at a faster rate than those below them, the added strain would lead to twisting. A similar mechanism would work in the root. As individual *twd1* cells such as trichomes do not show much evidence of twisting, this could be a cause. However, it is not clear if it is the only mechanism, or indeed a mechanism at all. Further experiments on the nature of individual cells or possible differentia elongation rates would shed light on this theory.

Despite these, one point which bears repeating is the putative NPA-bindng site that is actin associated. The various components of the cytoskeleton play an important role in determining cell shape, cell shape could be the key to the twist, and TWD1 could be the actin-associated NPA binding protein. Could the cytoskeleton play a role despite the lack of handedness?

ATIs and actin

Besides serving as a structural element, actin is an important part of regulating the proper auxin transport pathway. One direct mechanism is by influencing the rate of cytoplasmic streaming, by which auxin can move from one end of the cell to the other (Holweg, 2007). Also, actin can provide a path to targeting the auxin efflux components correctly (Muday et al., 2000). One way this has been examined is by the effect of ATIs on actin. Some ATIs, such as TIBA, have been directly shown to affect vesicle trafficking (Dhonukshe et al., 2008). The relationship between NPA and actin is still disputed. NPA has been shown to remove actin and thereby slow down cytoplasmic streaming (Rahman et al., 2007), and actin bundling seems to enhance sensitivity to NPA (Maisch and Nick, 2007), but it does not seem to have the same kind of auxin-related actin interaction as TIBA (Dhonukshe et al., 2008). Significantly,

mammalian actin was found to bind quercetin (Böhl et al., 2005), and it can be speculated that it retains this function in plants, but the specific effect of quercetin binding to actin in auxin transport remains to be elucidated.

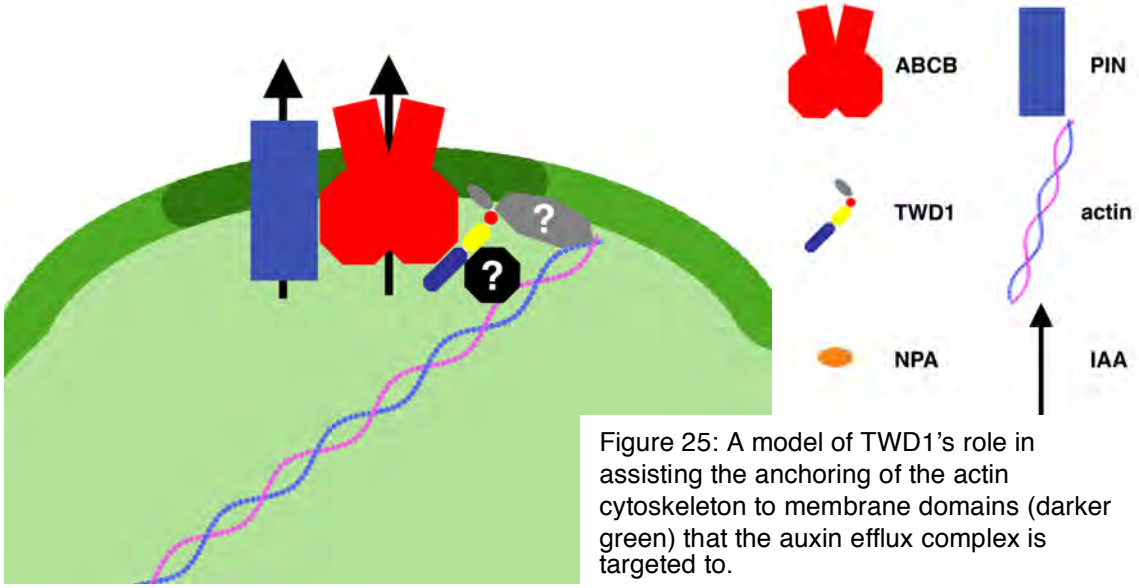

Figure 25: A model of TWD1's role in assisting the anchoring of the actin cytoskeleton to membrane domains (darker green) that the auxin efflux complex is targeted to.

TWD1 and actin

As mentioned previously, one of the features that was looked for in an NPA-binding protein was an interaction with the actin cytoskeleton. Considering the ATI-integrating function of TWD1, a large part of the work for this thesis was based on the hypothesis that TWD1 might be the actin interacting NPA-binding protein. Its membrane peripheral location was a further indication in this direction. Protein pull-down assay were in fact able to identify ACT7 as a part of the TWD1-ABCB1 auxin efflux complex. However, based on *in vitro* assays, this interaction may be indirect (Sovero et al., in preparation). Biochemical evidence leans strongly in the direction of an intersection between the two. The *act7* loss-of-function mutant shows marked auxin transport deficiency phenotypes, such as reduced root length and increased shoot length. The phenotype is caused by enhanced levels of free auxin, correlating with enhanced basipetal transport in each, as it is known that high auxin will stimulate hypocotyls elongation while inhibiting the same in roots. Also, members of the auxin efflux complex (especially PIN2) were slightly mis-localized, with more signal non-polarly localized than in wild type, and DR5-GFP expression in root tips showed a loss of focus, with broader

expression in the very tip-most cell layers when compared to the wild type. Besides this, NPA binding was similarly reduced in *act7-4* and *twd1*, and both showed similarly deficient trichome building, with a striking increase in two-branched trichomes. On the *twd1* side, the mutant plant showed enhanced actin bundles. These all hint to an interaction between TWD1 and the actin cytoskeleton, both working together though not explicitly to regulate the correct location and activation of the export complex. The loss of the auxin-responsive actin variation could affect the proper cycling of the proteins to and from the plasma membrane. In this case, the enhanced efflux of auxin observed would seem to indicate that there are more transporters stuck on the plasma membrane. A simple model of interaction at the site of the main auxin efflux complex might look like below, with unknown proteins, either cytoplasmic or membrane-associated leading to actin association with the complex, through TWD1.

A model

What kind of general model can we draw from the information we have gathered here? It is a complex picture, with many parts, and not easy to decipher. The loss of one, actin-responsive actin isoform lead to a greater rate of auxin efflux from single cells, and in shoots and roots. We can infer two possibilities from this. Either there are more efflux proteins at the plasma membrane, or the ones that are there stay there for a longer time. Considering what we know about the importance of actin to protein trafficking (Kim et al., 2005), and the importance of protein trafficking to correct PIN localization (Friml 2010), we can conclude that faulty actin might lead to faulty protein trafficking. This would lead to auxin efflux proteins being trapped at the plasma membrane for longer than normal (Figure 26B), which would raise the rate of export, but not necessarily a change in its direction. The elevated rate leads to higher amounts of auxin in cells over time, as more auxin could be made to make up for it leaving the site of synthesis too quickly. Higher auxin levels explain both the longer shoots and shorter roots of the *act-4* loss-of-function mutations.

The loss of TWD1 could lead to a looser interaction between components of the efflux complex. BUM treatment can lead to partial mislocalization of PIN proteins (Kim et al., 2010), and this could also be evidence the lack of focus generated by the loss of TWD1 activity on the ABCBs. A slight decrease in

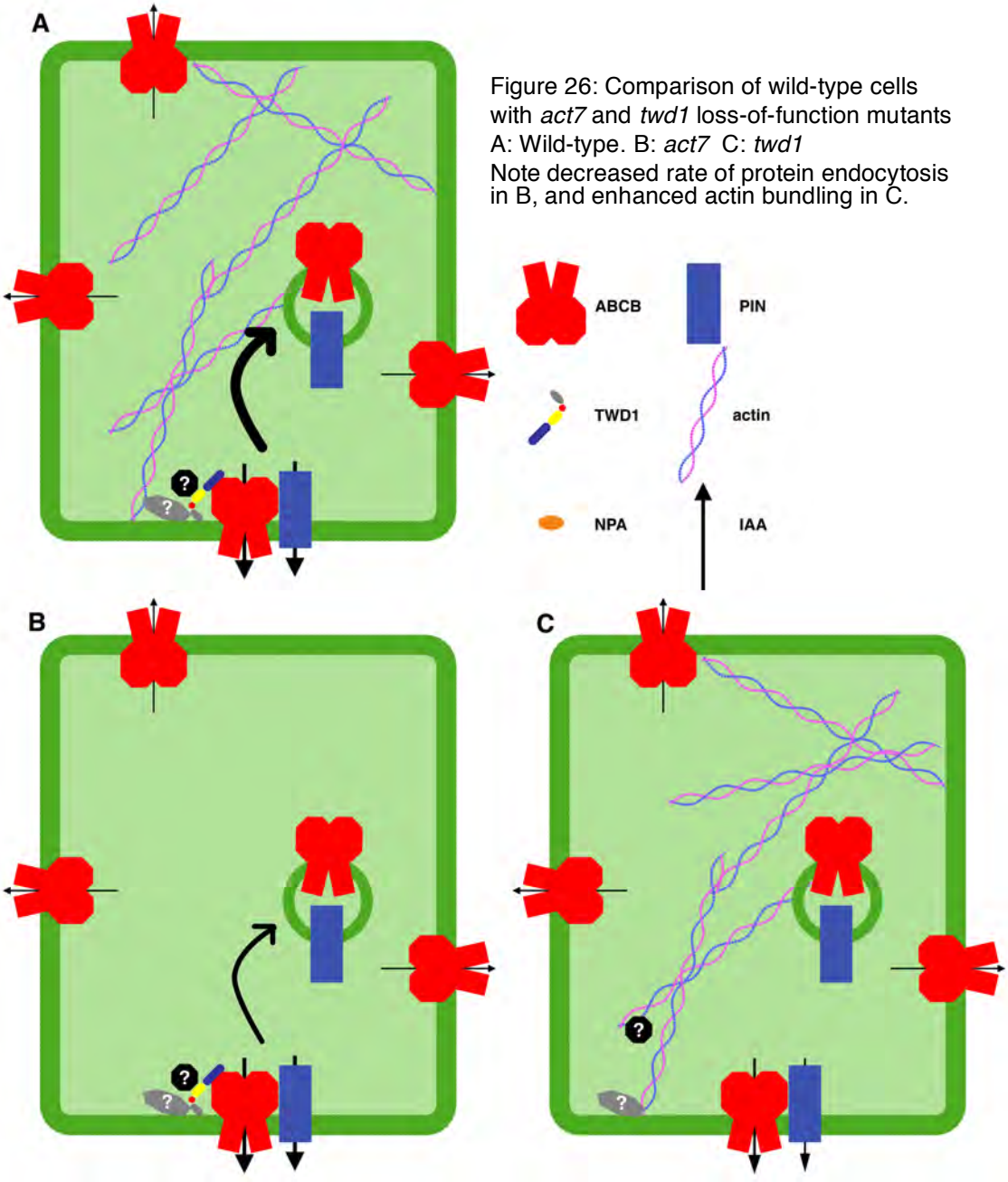

Figure 26: Comparison of wild-type cells with *act7* and *twd1* loss-of-function mutants
A: Wild-type. B: *act7* C: *twd1*
Note decreased rate of protein endocytosis in B, and enhanced actin bundling in C.

flow in one direction, coupled with a slight increase in flow towards another, could lead to cells growing in unusual shapes or at varying rates, either of which could lead to the twisting phenotype. Of course, this is an oversimplified model that does not take into account the many other interactors of both TWD1 and actin. Any of these could provide the key to the

twist. Of key relevance to this study is the effect that the loss of TWD1 has on actin. The *twd1* mutants show brighter actin signals, indicating enhanced actin bundling resulting from actin losing a PM anchor. Without the TWD1 interaction anchoring certain actin filaments in their correct paths, auto-assembly mechanisms are over-emphasized, leading to excessive bundling (Figure 26C). Over-bundling has been shown to result in impaired gravitropism and reduced longitudinal auxin transport (Nick 2009). Alternately, mis-targeted actin filaments could produce and effect in this aspect similar to the loss of one actin isoform, that is, a reduction in protein trafficking, or at least correctly localized protein trafficking. This could lead to differences in auxin transport in discrete zones of the plant or plant organs, perhaps some zones demonstrating reduced auxin transport, as *twd1* isolated mesophyll protoplasts (Bouchard et al., 2006) do, while basipetal transport in roots is enhanced (Sovero et al., in preparation). These differences could lead to the mis-regulated cellular elongation that could lead to the twisting phenotype.

But what about NPA? Although *twd1* plants show reduced sensitivity to NPA, clearly the phenotypes are not the same. NPA likely has a more specialized role than TWD1. Although NPA has been shown to bind to at least two proteins, TWD1 interacts with many protein families, with multiple interaction zones on one fairly small protein (Geisler and Bailly, 2007). That is, while the loss of TWD1 leads to drastic phenotypes due to the many processes it touches, treatment with NPA only influences one of these, the TWD1-ABCB1/19 interaction and their effect on the directionality caused by the PINs. It is likely that it is this loss of polarity in transport that causes the pin phenotype, rather than an overall reduction of auxin efflux, since the loss of ABCB1 and/or 19 does not cause it.

Future work on the topic should focus on the other interacting partners of TWD1. Calmodulin and HSP90 are particularly interesting, as both are well know integrators of signaling pathways and are therefore likely to play interesting roles in regulating TWD1, the regulator.

References

Alpi, A., Amrhein, N., Bertl, A., Blatt, M.R., Blumwald, E., Cervone, F., Dainty, J., De Michelis, M.I., Epstein, E., Galston, A.W., Goldsmith, M.H., Hawes, C., Hell, R., Hetherington, A., Hofte, H., Juergens, G., Leaver, C.J., Moroni, A., Murphy, A., Oparka, K., Perata, P., Quader, H., Rausch, T., Ritzenthaler, C., Rivetta, A., Robinson, D.G., Sanders, D., Scheres, B., Schumacher, K., Sentenac, H., Slayman, C.L., Soave, C., Somerville, C., Taiz, L., Thiel, G., and Wagner, R. (2007). Plant neurobiology: no brain, no gain? Trends Plant Sci **12,** 135-136.

Bailly, A., Sovero, V., and Geisler, M. (2006). The TWISTED DWARF's ABC: How Immunophilins Regulate Auxin Transport. Plant Signaling & Behavior, 4.

Bailly, A., Sovero, V., Vincenzetti, V., Santelia, D., Bartnik, D., Koenig, B.W., Mancuso, S., Martinoia, E., and Geisler, M. (2008). Modulation of P-glycoproteins by Auxin Transport Inhibitors Is Mediated by Interaction with Immunophilins. J Biol Chem **283,** 21817-21826.

Baker, D.B., and Ray, P.M. (1965). Relation between Effects of Auxin on Cell Wall Synthesis and Cell Elongation. Plant Physiol **40,** 360-368.

Baluska, F., Jasik, J., Edelmann, H.G., Salajová, T., and Volkmann, D. (2001). Latrunculin B-induced plant dwarfism: Plant cell elongation is F-actin-dependent. Dev Biol **231,** 113-124.

Baluška, F., Samaj, J., and Menzel, D. (2003). Polar transport of auxin: carrier-mediated flux across the plasma membrane or neurotransmitter-like secretion? Trends Cell Biol **13,** 282-285.

Baluška, F., Volkmann, D., and Menzel, D. (2005). Plant synapses: actin-based domains for cell-to-cell communication. Trends Plant Sci **10,** 106-111.

Bandyopadhyay, A., Blakeslee, J.J., Lee, O.R., Mravec, J., Sauer, M., Titapiwatanakun, B., Makam, S.N., Bouchard, R., Geisler, M., Martinoia, E., Friml, J., Peer, W.A., and Murphy, A.S. (2007). Interactions of PIN and PGP auxin transport mechanisms. Biochem. Soc. Trans **35,** 137-141.

Barik, S. (2006). Immunophilins: for the love of proteins. Cell Mol Life Sci **63,** 2889-2900.

Benjamins, R., Quint, A., Weijers, D., Hooykaas, P., and Offringa, R. (2001). The PINOID protein kinase regulates organ development in Arabidopsis by enhancing polar auxin transport. Development **128,** 4057-4067.

Benková, E., Ivanchenko, M., Friml, J., Shishkova, S., and Dubrovsky, J. (2009). A morphogenetic trigger: is there an emerging concept in plant developmental biology? Trends Plant Sci.

Bennett, M.J., Marchant, A., Green, H.G., May, S.T., Ward, S.P., Millner, P.A., Walker, A.R., Schulz, B., and Feldmann, K.A. (1996).

Arabidopsis AUX1 gene: a permease-like regulator of root gravitropism. Science **273,** 948-950.

Berleth, T., Scarpella, E., and Prusinkiewicz, P. (2007). Towards the systems biology of auxin-transport-mediated patterning. Trends Plant Sci **12,** 151-159.

Bernasconi, P., Patel, B., Reagan, J., and Subramanian, M. (1996). The N-1-Naphthylphthalamic Acid-Binding Protein Is an Integral Membrane Protein. Plant Physiol **111,** 427-432.

Blakeslee, J.J., Bandyopadhyay, A., Lee, O.R., Mravec, J., Titapiwatanakun, B., Sauer, M., Makam, S.N., Cheng, Y., Bouchard, R., Adamec, J., Geisler, M., Nagashima, A., Sakai, T., Martinoia, E., Friml, J., Peer, W.A., and Murphy, A.S. (2007). Interactions among PIN-FORMED and P-glycoprotein auxin transporters in Arabidopsis. Plant Cell **19,** 131-147.

Blancaflor, E.B., and Masson, P.H. (2003). Plant gravitropism. Unraveling the ups and downs of a complex process. Plant Physiol **133,** 1677-1690.

Blancaflor, E.B., Wang, Y.-S., and Motes, C.M. (2006). Organization and function of the actin cytoskeleton in developing root cells. Int Rev Cytol **252,** 219-264.

Böhl, M., Czupalla, C., Tokalov, S.V., Hoflack, B., and Gutzeit, H.O. (2005). Identification of actin as quercetin-binding protein: an approach to identify target molecules for specific ligands. Anal Biochem **346,** 295-299.

Bouchard, R., Bailly, A., Blakeslee, J.J., Oehring, S.C., Vincenzetti, V., Lee, O.R., Paponov, I.A., Palme, K., Mancuso, S., Murphy, A.S., Schulz, B., and Geisler, M. (2006). Immunophilin-like TWISTED DWARF1 modulates auxin efflux activities of Arabidopsis P-glycoproteins. J Biol Chem **281,** 30603-30612.

Brenner, E.D., Stahlberg, R., Mancuso, S., Baluska, F., and Van Volkenburgh, E. (2007). Response to Alpi et al.: plant neurobiology: the gain is more than the name. Trends Plant Sci **12,** 285-286.

Brenner, E.D., Stahlberg, R., Mancuso, S., Vivanco, J.M., Baluška, F., and Van Volkenburgh, E. (2006). Plant neurobiology: an integrated view of plant signaling. Trends Plant Sci **11,** 413-419.

Brunn, S., Muday, G.K., and Haworth, P. (1992). Auxin Transport and the Interaction of Phytotropins: Probing the Properties of a Phytotropin Binding Protein. Plant Physiol **98,** 101-107.

Bubb, M.R., Spector, I., Beyer, B.B., and Fosen, K.M. (2000). Effects of jasplakinolide on the kinetics of actin polymerization. An explanation for certain in vivo observations. J Biol Chem **275,** 5163-5170.

Chandler, J. (2009). Auxin as compère in plant hormone crosstalk. Planta.

Chen, J.G., Ullah, H., Young, J.C., Sussman, M.R., and Jones, A.M. (2001). ABP1 is required for organized cell elongation and division in Arabidopsis embryogenesis. Genes Dev **15,** 902-911.

Cho, M., Lee, S., and Cho, H. (2007). P-Glycoprotein4 Displays Auxin Efflux Transporter Like Action in Arabidopsis Root Hair Cells and Tobacco Cells. Plant Cell.

Christian, M., Steffens, B., Schenck, D., Burmester, S., Böttger, M., and Lüthen, H. (2006). How does auxin enhance cell elongation? Roles of auxin-binding proteins and potassium channels in growth control. Plant Biol (Stuttg) **8,** 346-352.
Cox, D.N., and Muday, G.K. (1994). NPA binding activity is peripheral to the plasma membrane and is associated with the cytoskeleton. Plant Cell **6,** 1941-1953.
Darwin, C. (1880). The Power of Movement in Plants. (London: John Murray).
Dawson, R.J.P., and Locher, K.P. (2006). Structure of a bacterial multidrug ABC transporter. Nature **443,** 180-185.
Dawson, R.J.P., and Locher, K.P. (2007). Structure of the multidrug ABC transporter Sav1866 from Staphylococcus aureus in complex with AMP-PNP. FEBS Lett **581,** 935-938.
Dharmasiri, N., Dharmasiri, S., and Estelle, M. (2005). The F-box protein TIR1 is an auxin receptor. Nature **435,** 441-445.
Dhonukshe, P., Grigoriev, I., Fischer, R., Tominaga, M., Robinson, D.G., Hasek, J., Paciorek, T., Petrásek, J., Seifertová, D., Tejos, R., Meisel, L.A., Zazímalová, E., Gadella, T.W.J., Stierhof, Y.-D., Ueda, T., Oiwa, K., Akhmanova, A., Brock, R., Spang, A., and Friml, J. (2008). Auxin transport inhibitors impair vesicle motility and actin cytoskeleton dynamics in diverse eukaryotes. Proc Natl Acad Sci USA **105,** 4489-4494.
Dixon, M., Jacobson, J., Cady, C., and Muday, G.K. (1996). Cytoplasmic Orientation of the Naphthylphthalamic Acid-Binding Protein in Zucchini Plasma Membrane Vesicles. Plant Physiol **112,** 421-432.
Faure, J.D., Gingerich, D., and Howell, S.H. (1998). An Arabidopsis immunophilin, AtFKBP12, binds to AtFIP37 (FKBP interacting protein) in an interaction that is disrupted by FK506. Plant J **15,** 783-789.
Fleming, A.J. (2006). Plant signalling: the inexorable rise of auxin. Trends Cell Biol **16,** 397-402.
Friml, J., Yang, X., Michniewicz, M., Weijers, D., Quint, A., Tietz, O., Benjamins, R., Ouwerkerk, P.B.F., Ljung, K., Sandberg, G., Hooykaas, P.J.J., Palme, K., and Offringa, R. (2004). A PINOID-dependent binary switch in apical-basal PIN polar targeting directs auxin efflux. Science **306,** 862-865.
Galván-Ampudia, C.S., and Offringa, R. (2007). Plant evolution: AGC kinases tell the auxin tale. Trends Plant Sci **12,** 541-547.
Gälweiler, L., Guan, C., Müller, A., Wisman, E., Mendgen, K., Yephremov, A., and Palme, K. (1998). Regulation of polar auxin transport by AtPIN1 in Arabidopsis vascular tissue. Science **282,** 2226-2230.
Ganguly, A., Lee, S.H., Cho, M., Lee, O.R., Yoo, H., and Cho, H.-T. (2010). Differential Auxin-Transporting Activities of PIN-FORMED Proteins in Arabidopsis Root Hair Cells. Plant Physiol.
Geisler, M., and Bailly, A. (2007). Tête-à-tête: the function of FKBPs in plant development. Trends Plant Sci **12,** 465-473.
Geisler, M., Girin, M., Brandt, S., Vincenzetti, V., Plaza, S., Paris, N., Kobae, Y., Maeshima, M., Billion, K., Kolukisaoglu, U., Schulz, B., and Martinoia, E. (2004). Arabidopsis immunophilin-like TWD1

functionally interacts with vacuolar ABC transporters. Mol Biol Cell **15,** 3393-3405.

Geisler, M., Kolukisaoglu, U., Bouchard, R., Billion, K., Berger, J., Saal, B., Frangne, N., Koncz-Kalman, Z., Koncz, C., Dudler, R., Blakeslee, J.J., Murphy, A.S., Martinoia, E., and Schulz, B. (2003). TWISTED DWARF1, a unique plasma membrane-anchored immunophilin-like protein, interacts with Arabidopsis multidrug resistance-like transporters AtPGP1 and AtPGP19. Mol Biol Cell **14,** 4238-4249.

Geisler, M., Blakeslee, J.J., Bouchard, R., Lee, O.R., Vincenzetti, V., Bandyopadhyay, A., Titapiwatanakun, B., Peer, W.A., Bailly, A., Richards, E.L., Ejendal, K.F.K., Smith, A.P., Baroux, C., Grossniklaus, U., Müller, A., Hrycyna, C.A., Dudler, R., Murphy, A.S., and Martinoia, E. (2005). Cellular efflux of auxin catalyzed by the Arabidopsis MDR/PGP transporter AtPGP1. Plant J **44,** 179-194.

Geldner, N., Friml, J., Stierhof, Y.-D., Jürgens, G., and Palme, K. (2001). Auxin transport inhibitors block PIN1 cycling and vesicle trafficking. Nature **413,** 425-428.

Geldner, N., Anders, N., Wolters, H., Keicher, J., Kornberger, W., Muller, P., Delbarre, A., Ueda, T., Nakano, A., and Jurgens, G. (2003). The Arabidopsis GNOM ARF-GEF mediates endosomal recycling, auxin transport, and auxin-dependent plant growth. Cell **112,** 219-230.

Gibbon, B.C., Kovar, D.R., and Staiger, C.J. (1999). Latrunculin B has different effects on pollen germination and tube growth. Plant Cell **11,** 2349-2363.

Gilliland, L.U., Kandasamy, M.K., Pawloski, L.C., and Meagher, R.B. (2002). Both vegetative and reproductive actin isovariants complement the stunted root hair phenotype of the Arabidopsis act2-1 mutation. Plant Physiol **130,** 2199-2209.

Gilliland, L.U., Pawloski, L.C., Kandasamy, M.K., and Meagher, R.B. (2003). Arabidopsis actin gene ACT7 plays an essential role in germination and root growth. Plant J **33,** 319-328.

Goldsmith, M.H. (1977). The Polar Transport of Auxin. Annual Review of Plant Physiology **28,** 439-478.

Granzin, J., Eckhoff, A., and Weiergräber, O.H. (2006). Crystal structure of a multi-domain immunophilin from Arabidopsis thaliana: a paradigm for regulation of plant ABC transporters. J Mol Biol **364,** 799-809.

Grunewald, W., and Friml, J. (2010). The march of the PINs: developmental plasticity by dynamic polar targeting in plant cells. EMBO J **29,** 2700-2714.

Gurdon, J.B., and Bourillot, P.Y. (2001). Morphogen gradient interpretation. Nature **413,** 797-803.

Harding, M.W., Galat, A., Uehling, D.E., and Schreiber, S.L. (1989). A receptor for the immunosuppressant FK506 is a cis-trans peptidyl-prolyl isomerase. Nature **341,** 758-760.

Harrar, Y., Bellini, C., and Faure, J.D. (2001). FKBPs: at the crossroads of folding and transduction. Trends Plant Sci **6,** 426-431.

Hasenstein, K.H., Blancaflor, E.B., and Lee, J.S. (1999). The microtubule cytoskeleton does not integrate auxin transport and gravitropism in maize roots. Physiol Plantarum **105,** 729-738.
He, Z., Li, L., and Luan, S. (2004). Immunophilins and parvulins. Superfamily of peptidyl prolyl isomerases in Arabidopsis. Plant Physiol **134,** 1248-1267.
Holmes, K.C., and Kabsch, W. (1991). Muscle proteins: actin. Current Opinion in Structural Biology **1,** 270-280.
Holmes, K.C., Popp, D., Gebhard, W., and Kabsch, W. (1990). Atomic model of the actin filament. Nature **347,** 44-49.
Holweg, C., and Nick, P. (2004). Arabidopsis myosin XI mutant is defective in organelle movement and polar auxin transport. Proc Natl Acad Sci USA **101,** 10488-10493.
Holweg, C.L. (2007). Acto-Myosin motorises the flow of auxin. Plant Signal Behav **2,** 247-248.
Hou, G., Mohamalawari, D.R., and Blancaflor, E.B. (2003). Enhanced gravitropism of roots with a disrupted cap actin cytoskeleton. Plant Physiol **131,** 1360-1373.
Hou, G., Kramer, V.L., Wang, Y.-S., Chen, R., Perbal, G., Gilroy, S., and Blancaflor, E.B. (2004). The promotion of gravitropism in Arabidopsis roots upon actin disruption is coupled with the extended alkalinization of the columella cytoplasm and a persistent lateral auxin gradient. Plant J **39,** 113-125.
Ishida, T., Thitamadee, S., and Hashimoto, T. (2007). Twisted growth and organization of cortical microtubules. J Plant Res **120,** 61-70.
Kabsch, W., Mannherz, H.G., Suck, D., Pai, E.F., and Holmes, K.C. (1990). Atomic structure of the actin:DNase I complex. Nature **347,** 37-44.
Kaksonen, M., Toret, C.P., and Drubin, D.G. (2006). Harnessing actin dynamics for clathrin-mediated endocytosis. Nat Rev Mol Cell Biol **7,** 404.
Kamphausen, T., Fanghänel, J., Neumann, D., Schulz, B., and Rahfeld, J.-U. (2002). Characterization of Arabidopsis thaliana AtFKBP42 that is membrane-bound and interacts with Hsp90. Plant J **32,** 263-276.
Kandasamy, M.K., Gilliland, L.U., McKinney, E.C., and Meagher, R.B. (2001). One plant actin isovariant, ACT7, is induced by auxin and required for normal callus formation. Plant Cell **13,** 1541-1554.
Kang, C.B., Feng, L., Chia, J., and Yoon, H.S. (2005). Molecular characterization of FK-506 binding protein 38 and its potential regulatory role on the anti-apoptotic protein Bcl-2. Biochem Biophys Res Commun **337,** 30-38.
Keitt, G.W., and Baker, R.A. (1966). Auxin Activity of Substituted Benzoic Acids and Their Effect on Polar Auxin Transport. Plant Physiol **41,** 1-10.
Kepinski, S., and Leyser, O. (2005). The Arabidopsis F-box protein TIR1 is an auxin receptor. Nature **435,** 446-451.
Ketelaar, T., and Emons, A.M.C. (2001). The cytoskeleton in plant cell growth: lessons from root hairs New Phytologist **152,** 409-418.

Ketelaar, T., Allwood, E.G., and Hussey, P.J. (2007). Actin organization and root hair development are disrupted by ethanol-induced overexpression of Arabidopsis actin interacting protein 1 (AIP1). New Phytol **174,** 57-62.

Kim, H., Park, M., Kim, S.J., and Hwang, I. (2005). Actin filaments play a critical role in vacuolar trafficking at the Golgi complex in plant cells. Plant Cell **17,** 888-902.

Kim, J.-Y., Henrichs, S., Bailly, A., Vincenzetti, V., Sovero, V., Mancuso, S., Pollmann, S., Kim, D., Geisler, M., and Nam, H.-G. (2010). Identification of an ABCB/P-glycoprotein-specific inhibitor of auxin transport by chemical genomics. The Journal of biological chemistry.

Kleine-Vehn, J., and Friml, J. (2008). Polar targeting and endocytic recycling in auxin-dependent plant development. Annu Rev Cell Dev Biol **24,** 447-473.

Kleine-Vehn, J., Dhonukshe, P., Swarup, R., Bennett, M.J., and Friml, J. (2006). Subcellular trafficking of the Arabidopsis auxin influx carrier AUX1 uses a novel pathway distinct from PIN1. Plant Cell **18,** 3171-3181.

Kleine-Vehn, J., Huang, F., Naramoto, S., Zhang, J., Michniewicz, M., Offringa, R., and Friml, J. (2009). PIN auxin efflux carrier polarity is regulated by PINOID kinase-mediated recruitment into GNOM-independent trafficking in Arabidopsis. Plant Cell **21,** 3839-3849.

Kleine-Vehn, J., Dhonukshe, P., Sauer, M., Brewer, P.B., Wi□niewska, J., Paciorek, T., Benková, E., and Friml, J. (2008). ARF GEF-Dependent Transcytosis and Polar Delivery of PIN Auxin Carriers in Arabidopsis. Curr Biol **18,** 526-531.

Kotchoni, S.O., Zakharova, T., Mallery, E.L., Le, J., El-Assal, S.E.-D., and Szymanski, D.B. (2009). The association of the Arabidopsis actin-related protein2/3 complex with cell membranes is linked to its assembly status but not its activation. Plant Physiol **151,** 2095-2109.

Kramer, E.M., and Bennett, M.J. (2006). Auxin transport: a field in flux. Trends Plant Sci **11,** 382-386.

Lloyd, C. (1988). Actin in plants. Journal of cell science **90,** 185-188.

Maher, E.P., and Martindale, S.J. (1980). Mutants of Arabidopsis thaliana with altered responses to auxins and gravity. Biochem Genet **18,** 1041-1053.

Maisch, J., and Nick, P. (2007). Actin is involved in auxin-dependent patterning. Plant Physiol **143,** 1695-1704.

Marchant, A., Kargul, J., May, S.T., Muller, P., Delbarre, A., Perrot-Rechenmann, C., and Bennett, M.J. (1999). AUX1 regulates root gravitropism in Arabidopsis by facilitating auxin uptake within root apical tissues. EMBO J **18,** 2066-2073.

Mathur, J., Spielhofer, P., Kost, B., and Chua, N.-H. (1999). The actin cytoskeleton is required to elaborate and maintain spatial patterning during trichome cell morphogenesis in Arabidopsis thaliana. Development **126,** 5559-5568.

McDowell, J.M., An, Y.Q., Huang, S., McKinney, E.C., and Meagher, R.B. (1996). The arabidopsis ACT7 actin gene is expressed in rapidly

developing tissues and responds to several external stimuli. Plant Physiol **111,** 699-711.
McKinney, E.C., and Meagher, R.B. (1998). Members of the Arabidopsis actin gene family are widely dispersed in the genome. Genetics **149,** 663-675.
Merks, R.M.H., Van de Peer, Y., Inzé, D., and Beemster, G.T.S. (2007). Canalization without flux sensors: a traveling-wave hypothesis. Trends Plant Sci **12,** 384-390.
Michalke, W., Katekar, G.F., and Geissler, A.E. (1992). Phytotropin-binding sites and auxin transport in Cucurbita pepo: evidence for two recognition sites Planta **187,** 254-260.
Michniewicz, M., Zago, M.K., Abas, L., Weijers, D., Schweighofer, A., Meskiene, I., Heisler, M.G., Ohno, C., Zhang, J., Huang, F., Schwab, R., Weigel, D., Meyerowitz, E.M., Luschnig, C., Offringa, R., and Friml, J. (2007). Antagonistic regulation of PIN phosphorylation by PP2A and PINOID directs auxin flux. Cell **130,** 1044-1056.
Mravec, J., Sk□pa, P., Bailly, A., Hoyerová, K., K□e□ek, P., Bielach, A., Petrášek, J., Zhang, J., Gaykova, V., Stierhof, Y.-D., Dobrev, P.I., Schwarzerová, K., Rol□ík, J., Seifertová, D., Luschnig, C., Benková, E., Za□ímalová, E., Geisler, M., and Friml, J. (2009). Subcellular homeostasis of phytohormone auxin is mediated by the ER-localized PIN5 transporter. Nature, 1-7.
Muday, G.K. (2000). Maintenance of asymmetric cellular localization of an auxin transport protein through interaction with the actin cytoskeleton. J Plant Growth Regul **19,** 385-396.
Muday, G.K., and DeLong, A. (2001). Polar auxin transport: controlling where and how much. Trends Plant Sci **6,** 535-542.
Muday, G.K., Hu, S., and Brady, S.R. (2000). The actin cytoskeleton may control the polar distribution of an auxin transport protein. Gravitational and space biology bulletin : publication of the American Society for Gravitational and Space Biology **13,** 75-83.
Muday, G.K., Peer, W.A., and Murphy, A.S. (2003). Vesicular cycling mechanisms that control auxin transport polarity. Trends Plant Sci **8,** 301-304.
Muday, G.K., Brunn, S., Haworth, P., and Subramanian, M. (1993). Evidence for a Single Naphthylphthalamic Acid Binding Site on the Zucchini Plasma Membrane. Plant Physiol **103,** 449-456.
Müller, A., Guan, C., Gälweiler, L., Tänzler, P., Huijser, P., Marchant, A., Parry, G., Bennett, M., Wisman, E., and Palme, K. (1998). AtPIN2 defines a locus of Arabidopsis for root gravitropism control. EMBO J **17,** 6903-6911.
Multani, D.S., Briggs, S.P., Chamberlin, M.A., Blakeslee, J.J., Murphy, A.S., and Johal, G.S. (2003). Loss of an MDR transporter in compact stalks of maize br2 and sorghum dw3 mutants. Science **302,** 81-84.
Murphy, A.S., Peer, W.A., and Taiz, L. (2000). Regulation of auxin transport by aminopeptidases and endogenous flavonoids. Planta **211,** 315-324.
Murphy, A.S., Hoogner, K.R., Peer, W.A., and Taiz, L. (2002). Identification, purification, and molecular cloning of N-1-naphthylphthalmic acid-

binding plasma membrane-associated aminopeptidases from Arabidopsis. Plant Physiol **128,** 935-950.
Nick, P., Han, M., and An, G. (2009). Auxin stimulates its own transport by shaping actin filaments. Plant Physiol.
Noh, B., Murphy, A.S., and Spalding, E.P. (2001). Multidrug resistance-like genes of Arabidopsis required for auxin transport and auxin-mediated development. Plant Cell **13,** 2441-2454.
Okada, K., Ueda, J., Komaki, M., Bell, C., and Shimura, Y. (1991). Requirement of the Auxin Polar Transport System in Early Stages of Arabidopsis Floral Bud Formation. Plant Cell **3,** 677-684.
Paciorek, T., Zazímalová, E., Ruthardt, N., Petrásek, J., Stierhof, Y.-D., Kleine-Vehn, J., Morris, D.A., Emans, N., Jürgens, G., Geldner, N., and Friml, J. (2005). Auxin inhibits endocytosis and promotes its own efflux from cells. Nature **435,** 1251-1256.
Parry, G., Marchant, A., May, S., Swarup, R., Swarup, K., James, N., Graham, N., Allen, T., Martucci, T., Yemm, A., Napier, R., Manning, K., King, G., and Bennett, M. (2001). Quick on the Uptake: Characterization of a Family of Plant Auxin Influx Carriers. J Plant Growth Regul **20,** 217-225.
Pennazio, S. (2002). The discovery of the chemical nature of the plant hormone auxin. Riv Biol **95,** 289-308.
Pérez-Pérez, J.M., Ponce, M.R., and Micol, J.L. (2004). The ULTRACURVATA2 gene of Arabidopsis encodes an FK506-binding protein involved in auxin and brassinosteroid signaling. Plant Physiol **134,** 101-117.
Petrásek, J., and Friml, J. (2009). Auxin transport routes in plant development. Development **136,** 2675-2688.
Petrásek, J., Mravec, J., Bouchard, R., Blakeslee, J.J., Abas, M., Seifertová, D., Wi□niewska, J., Tadele, Z., Kubes, M., Covanová, M., Dhonukshe, P., Skupa, P., Benková, E., Perry, L., Krecek, P., Lee, O.R., Fink, G.R., Geisler, M., Murphy, A.S., Luschnig, C., Zazímalová, E., and Friml, J. (2006). PIN proteins perform a rate-limiting function in cellular auxin efflux. Science **312,** 914-918.
Phillips, I.D.J. (1971). Introduction to the Biochemistry and Physiology of Plant Growth Hormones. (New York: McGraw-Hill Book Company).
Pollard, T.D., and Cooper, J.A. (1986). Actin and actin-binding proteins. A critical evaluation of mechanisms and functions. Annu Rev Biochem **55,** 987-1035.
Pratt, W.B., Silverstein, A.M., and Galigniana, M.D. (1999). A model for the cytoplasmic trafficking of signalling proteins involving the hsp90-binding immunophilins and p50cdc37. Cell Signal **11,** 839-851.
Quint, M., and Gray, W.M. (2006). Auxin signaling. Curr Opin Plant Biol **9,** 448-453.
Rahman, A., Bannigan, A., Sulaman, W., Pechter, P., Blancaflor, E.B., and Baskin, T.I. (2007). Auxin, actin and growth of the Arabidopsis thaliana primary root. Plant J **50,** 514-528.

Rashotte, A.M., DeLong, A., and Muday, G.K. (2001). Genetic and chemical reductions in protein phosphatase activity alter auxin transport, gravity response, and lateral root growth. Plant Cell **13,** 1683-1697.
Raven, J. (1975). Transport of Indoleacetic Acid in Plant Cells in Relation to pH and Electrical Potential Gradients, and its Significance for Polar IAA Transport. New Phytologist **74,** 163-172.
Rea, P.A. (2007). Plant ATP-binding cassette transporters. Annual review of plant biology **58,** 347-375.
Rubery, P., and Sheldrake, A. (1974). Carrier-mediated Auxin Transport. Planta **118,** 101-121.
Sachs, T. (1991). Cell polarity and tissue patterning in plants. Development **91(Suppl.),** 83-93.
Samaj, J., Baluska, F., Voigt, B., Schlicht, M., Volkmann, D., and Menzel, D. (2004). Endocytosis, actin cytoskeleton, and signaling. Plant Physiol **135,** 1150-1161.
Sangster, T.A., and Queitsch, C. (2005). The HSP90 chaperone complex, an emerging force in plant development and phenotypic plasticity. Curr Opin Plant Biol **8,** 86-92.
Santelia, D., Vincenzetti, V., Azzarello, E., Bovet, L., Fukao, Y., Duchtig, P., Mancuso, S., Martinoia, E., and Geisler, M. (2005). MDR-like ABC transporter AtPGP4 is involved in auxin-mediated lateral root and root hair development. FEBS Lett **579,** 5399-5406.
Santelia, D., Henrichs, S., Vincenzetti, V., Sauer, M., Bigler, L., Klein, M., Bailly, A., Lee, Y., Friml, J., Geisler, M., and Martinoia, E. (2008). Flavonoids redirect PIN-mediated polar auxin fluxes during root gravitropic responses. J Biol Chem.
Santner, A., Calderon-Villalobos, L.I.A., and Estelle, M. (2009). Plant hormones are versatile chemical regulators of plant growth. Nat Chem Biol **5,** 301-307.
Sarkadi, B., Price, E.M., Boucher, R.C., Germann, U.A., and Scarborough, G.A. (1992). Expression of the human multidrug resistance cDNA in insect cells generates a high activity drug-stimulated membrane ATPase. J Biol Chem **267,** 4854-4858.
Scheidt, H.A., Vogel, A., Eckhoff, A., Koenig, B.W., and Huster, D. (2007). Solid-state NMR characterization of the putative membrane anchor of TWD1 from Arabidopsis thaliana. Eur Biophys J **36,** 393-404.
Serrani, J.C., Carrera, E., Ruiz-Rivero, O., Gallego-Giraldo, L., Peres, L.E.P., and Garcia-Martinez, J.L. (2010). Inhibition of Auxin Transport from the Ovary or from the Apical Shoot Induces Parthenocarpic Fruit-Set in Tomato Mediated by Gibberellins. Plant Physiol.
Smyczynski, C., Roudier, F., Gissot, L., Vaillant, E., Grandjean, O., Morin, H., Masson, T., Bellec, Y., Geelen, D., and Faure, J.-D. (2006). The C terminus of the immunophilin PASTICCINO1 is required for plant development and for interaction with a NAC-like transcription factor. J Biol Chem **281,** 25475-25484.
Sukumar, P., Edwards, K., Rahman, A., DeLong, A., and Muday, G. (2009). PINOID kinase regulates root gravitropism through modulation of

PIN2-dependent basipetal auxin transport in Arabidopsis thaliana. Plant Physiol.

Sussman, M.R., and Gardner, G. (1980). Solubilization of the Receptor for N-1-Naphthylphthalamic Acid. Plant Physiol **66,** 1074-1078.

Sussman, M.R., and Goldsmith, M.H.M. (1981). Auxin Uptake and Action of N-1-Naphthylphthalamic Acid in Corn Coleoptiles. Planta **150,** 15-25.

Swarup, K., Benková, E., Swarup, R., Casimiro, I., Péret, B., Yang, Y., Parry, G., Nielsen, E., De Smet, I., Vanneste, S., Levesque, M.P., Carrier, D., James, N., Calvo, V., Ljung, K., Kramer, E.M., Roberts, R., Graham, N., Marillonnet, S., Patel, K., Jones, J.D.G., Taylor, C.G., Schachtman, D.P., May, S., Sandberg, G., Benfey, P., Friml, J., Kerr, I.D., Beeckman, T., Laplaze, L., and Bennett, M.J. (2008). The auxin influx carrier LAX3 promotes lateral root emergence. Nat Cell Biol **10,** 946-954.

Swarup, R., Friml, J., Marchant, A., Ljung, K., Sandberg, G., Palme, K., and Bennett, M. (2001). Localization of the auxin permease AUX1 suggests two functionally distinct hormone transport pathways operate in the Arabidopsis root apex. Genes Dev **15,** 2648-2653.

Taiz, L., and Zeiger, E. (2006). Plant Physiology. (Sunderland, Massachusetts: Sinauer Associates, Inc.).

Tanaka, H., Dhonukshe, P., Brewer, P.B., and Friml, J. (2006). Spatiotemporal asymmetric auxin distribution: a means to coordinate plant development. Cell Mol Life Sci **63,** 2738-2754.

Teale, W.D., Paponov, I.A., and Palme, K. (2006). Auxin in action: signalling, transport and the control of plant growth and development. Nat Rev Mol Cell Biol **7,** 847-859.

Terasaka, K., Blakeslee, J.J., Titapiwatanakun, B., Peer, W.A., Bandyopadhyay, A., Makam, S.N., Lee, O.R., Richards, E.L., Murphy, A.S., Sato, F., and Yazaki, K. (2005). PGP4, an ATP binding cassette P-glycoprotein, catalyzes auxin transport in Arabidopsis thaliana roots. Plant Cell **17,** 2922-2939.

Thomas, C., Tholl, S., Moes, D., Dieterle, M., Papuga, J., Moreau, F., and Steinmetz, A. (2009). Actin bundling in plants. Cell Motil Cytoskeleton.

Thomson, K.-S., Hertel, R., and Müller, S. (1973). 1-N-Naphthylphthalamic Acid and 2,3,5-Triiodobenzoic Acid: In-vitro Binding to Particulate Cell Fractions and Action on Auxin Transport in Corn Coleoptiles Planta **109,** 337-352.

Titapiwatanakun, B., Blakeslee, J.J., Bandyopadhyay, A., Yang, H., Mravec, J., Sauer, M., Cheng, Y., Adamec, J., Nagashima, A., Geisler, M., Sakai, T., Friml, J., Peer, W.A., and Murphy, A.S. (2008). ABCB19/PGP19 stabilises PIN1 in membrane microdomains in Arabidopsis. Plant J.

Trewavas, A. (2007). Response to Alpi et al.: Plant neurobiology--all metaphors have value. Trends Plant Sci **12,** 231-233.

Turing, A.M. (1952). The chemical basis of morphogenesis. . Philosophical Transactions of the Royal Society of London **237,** 37-72.

Ueda, H., Yokota, E., Kutsuna, N., Shimada, T., Tamura, K., Shimmen, T., Hasezawa, S., Dolja, V.V., and Hara-Nishimura, I. (2010). Myosin-dependent endoplasmic reticulum motility and F-actin organization in plant cells. Proc Natl Acad Sci USA **107,** 6894-6899.

Vespa, L., Vachon, G., Berger, F., Perazza, D., Faure, J.-D., and Herzog, M. (2004). The immunophilin-interacting protein AtFIP37 from Arabidopsis is essential for plant development and is involved in trichome endoreduplication. Plant Physiol **134,** 1283-1292.

Voigt, B., Timmers, A.C.J., Samaj, J., Hlavacka, A., Ueda, T., Preuss, M.L., Nielsen, E., Mathur, J., Emans, N., Stenmark, H., Nakano, A., Baluška, F., and Menzel, D. (2005). Actin-based motility of endosomes is linked to the polar tip growth of root hairs. Eur J Cell Biol **84,** 609-621.

Wang, J., Tong, W., Zhang, X., Chen, L., Yi, Z., Pan, T., Hu, Y., Xiang, L., and Yuan, Z. (2006). Hepatitis C virus non-structural protein NS5A interacts with FKBP38 and inhibits apoptosis in Huh7 hepatoma cells. FEBS Lett **580,** 4392-4400.

Weiergraber, O.H., Eckhoff, A., and Granzin, J. (2006). Crystal structure of a plant immunophilin domain involved in regulation of MDR-type ABC transporters. FEBS Lett **580,** 251-255.

Went, F. (1935). Auxin, the Plant Growth-Hormone. The Botanical Review **1,** 162-182.

Wisniewska, J., Xu, J., Seifertova, D., Brewer, P.B., Ruzicka, K., Blilou, I., Rouquie, D., Benkova, E., Scheres, B., and Friml, J. (2006). Polar PIN localization directs auxin flow in plants. Science **312,** 883.

Woodward, A.W., and Bartel, B. (2005). Auxin: regulation, action, and interaction. Ann Bot **95,** 707-735.

Yamamoto, K., and Kiss, J.Z. (2002). Disruption of the actin cytoskeleton results in the promotion of gravitropism in inflorescence stems and hypocotyls of Arabidopsis. Plant Physiol **128,** 669-681.

Yang, H., and Murphy, A.S. (2009). Functional expression and characterization of Arabidopsis ABCB, AUX 1 and PIN auxin transporters in Schizosaccharomyces pombe. Plant J **59,** 179-191.

Zazimalova, E., Murphy, A.S., Yang, H., Hoyerova, K., and Hosek, P. (2009). Auxin Transporters--Why So Many? Cold Spring Harbor Perspectives in Biology, 1-14.

Acknowledgements

I would like to take this space to acknowledge the people who have helped me get to this point.

First thank you to Professor Enrico Martinoia for the time in the group, and for always being available when problems arose.

Also thank you to Professor Ueli Grossniklaus for agreeing to be on my thesis committee.

A whole mountain of thanks to Dr. Markus Geisler for his excellent supervision, and for always giving me another chance.

Thank you and sympathy for all members of the Geisler lab, past and present, but especially Dr. Aurelien Bailly, Dr. Sina Henrichs, and Vincent Vincenzetti for putting up with me all these years, and all the help and also fun all the time.

In general, thanks to all of the members of the Martinoia group, for good times, commiseration, and timely assistance when necessary.

Especial thanks goes to all my family, for all their support and encouragement, though so far away.

And finally, thank you to my husband, Dr. Awais Khan, without whom I would never ever have made it this far.

H. Valpuri Sovero

Address: Habsburgstr. 20, 8037 Zürich, Switzerland
Tel: +41 43 53 73 085 Mobile: +41 76 446 9268 E-mail: vsovero@access.uzh.ch
Nationality: Finland; US permanent residency

Education:

Date	Degree	University	Major
04/2007 – Current	Doctor of Natural Sciences	University of Zürich	Plant Molecular Physiology "The function of TWISTED DWARF1 in regulating ABCB1-mediated auxin transport"
10/2005 – 03/2007	Master of Science	University of Zürich	Plant Molecular Physiology "Mutagenesis and Deletion of the FK506-binding domain of TWISTED DWARF1"
09/1999 – 03/2004	Bachelor of Science	University of California, San Diego (UCSD) La Jolla, CA	Biochemistry and Cell Biology
10/2002 – 07/2003	Study Abroad	Georg-August University Göttingen, Germany	Biochemistry and Cell Biology
09/1996 – 06/1999	High School Diploma	Davis Senior High School Davis, CA	

Work Experience:

06/2004 – 09/2005 Campbell's Seeds, Davis, CA
Laboratory Technician
- HPLC analysis of carotenoids and capsaicin in vegetables
- Spectrophotometric analysis of lycopene content in tomatoes
- PCR marker analysis for disease resistance in tomato varieties
- Evaluation of bacterial disease of tomato seeds
- DNA and carotenoid extraction from vegetable samples
- Data analysis

05/2001 – 06/2002 UCSD, Department of Biology, San Diego, CA
Laboratory Assistant
- Worked with *Arabidopsis thaliana*
- Planted and harvested seeds
- Prepared leaves and roots for analysis

03/1998 – 08/1999 Agraquest, Davis, CA
Laboratory Assistant
- Assisted with Beet Army and Corn Root Worm, and *Drosophila* colony maintenance
- Chemical inventory

06/1998 – 08/1998 Norddeutsche Pflanzenzucht Hans-Georg Lembke KG, Holtsee, Germany
Summer Assistant
- Worked with *Brassica napus* plants:
- Self pollinated plants in green house
- Harvested seeds and plants from field and greenhouse

Practical Skills:

Biochemistry	HPLC; protein and nucleic acid purification and identification centrifugation, chromatography, and electrophoresis; bioluminescence resonance energy transfer (BRET); immunofluorescence microscopy
Plant Physiology	Measurements of plant growth and response to environmental conditions; Confocal microscopy with fluorescent markers
Molecular Genetics	DNA extraction; PCR; Electrophoresis; restriction; ligation; cloning; site directed mutagenesis; expression of recombinant proteins; sequencing
Cell biology	Yeast and bacterial cell culture; microscopic study of animal and plant cells; transformation of *Arabidopsis*, yeast and bacteria
Computer	Windows and Mac; Data analysis with ImageJ, Prism, Photoshop

Publications:

Bailly A, Sovero V, Geisler M. The TWISTED DWARF's ABC: How Immunophilins Regulate Auxin Transport. *Plant Signaling & Behavior* 2006 1(6): 277-280.

Bailly A, Sovero V, Vincenzetti V, Santelia D, Bartnik D, Koenig BW, Mancuso S, Martinoia E, Geisler M. Modulation of P-glycoproteins by Auxin Transport Inhibitors Is Mediated by Interaction with Immunophilins. *The Journal of Biological Chemistry* 2008 283(31):21817-21826.

Kim JY, Henrichs S, Bailly A, Vincenzetti V, Sovero V, Mancuso S, Pollmann S, Kim D, Geisler M, Nam HG. Identification of an ABCB/P-glycoprotein-specific inhibitor of auxin transport by chemical genomics. *The Journal of Biological Chemistry*. 2010 *In press.*

Conferences:

Oral Presentation: Sovero V, Bailly A, Wang B, Zwiewka M, Mancuso S, Friml J, Geisler M. The NPA-binding protein TWISTED DWARF 1 controls ABCB-mediated auxin transport. ACPD 2009, July 10-14, Prague, Czech Republic.

Poster Presentation: Sovero HV, Bailly A, Vincenzetti V, Mancuso S, Martinoia E, Geisler M. Drug modulation of P-glycoproteins by immunophilins. FESPB 2008, 17-22 August, Tampere, Finland.

Organizing committee and session chair: Plants and People - Mutual Dependence in the 21st Century - PhD Symposium of the Plant Science Center. 6 June, 2008. Zurich, Switzerland.

Teaching Experience:

- Course development and supervision of 1-2 master's students for a three week practical block course: Fall 2007, 2008, 2009
- Supervision of a six week bachelor student project: Spring 2009
- Assistance in bachelor's student lab practical for 30-60 students

Languages:

- English, Finnish – native speaker
- German – Intermediate

Professional affiliation:

- ASPB member